

## INFORMATION TO USERS

This manuscript has been reproduced from the microfilm master. UMI films the text directly from the original or copy submitted. Thus, some thesis and dissertation copies are in typewriter face, while others may be from any type of computer printer.

**The quality of this reproduction is dependent upon the quality of the copy submitted.** Broken or indistinct print, colored or poor quality illustrations and photographs, print bleedthrough, substandard margins, and improper alignment can adversely affect reproduction.

In the unlikely event that the author did not send UMI a complete manuscript and there are missing pages, these will be noted. Also, if unauthorized copyright material had to be removed, a note will indicate the deletion.

Oversize materials (e.g., maps, drawings, charts) are reproduced by sectioning the original, beginning at the upper left-hand corner and continuing from left to right in equal sections with small overlaps. Each original is also photographed in one exposure and is included in reduced form at the back of the book.

Photographs included in the original manuscript have been reproduced xerographically in this copy. Higher quality 6" x 9" black and white photographic prints are available for any photographs or illustrations appearing in this copy for an additional charge. Contact UMI directly to order.

# UMI

A Bell & Howell Information Company  
300 North Zeeb Road, Ann Arbor MI 48106-1346 USA  
313/761-4700 800/521-0600

A

Microstructures of  
Poly(1-Butene) and Poly(Ethylene-*co*-1-Butene)  
Produced by Zirconocene/Methylaluminoxane Catalysis

By  
Jianbin Zhang

A dissertation submitted to the Graduate Faculty in Chemistry in partial fulfillment of the requirements for the degree of Doctor of Philosophy, The City University of New York.

1996

**UMI Number: 9630530**

**Copyright 1996 by  
Zhang, Jianbin**

**All rights reserved.**

---

**UMI Microform 9630530  
Copyright 1996, by UMI Company. All rights reserved.**

**This microform edition is protected against unauthorized  
copying under Title 17, United States Code.**

---

**UMI**  
**300 North Zeeb Road**  
**Ann Arbor, MI 48103**

©1996

Jianbin Zhang

All rights reserved

This manuscript has been read and accepted for the Graduate Faculty in Chemistry in satisfaction of the dissertation requirement for the degree of Doctor of Philosophy.

3/20/96  
date

George Odian  
Chairman of Examining Committee

3/28/96  
date

Robert R. ...  
Executive Officer

George Odian

Dr. Geoge Odian

Howard Haubensack

Dr. Howard Haubensack

Norman Indictor

Dr. Norman Indictor

Supervisory committee

The City University of New York

Abstract  
Microstructures of  
Poly(1-Butene) and Poly(Ethylene-*co*-1-Butene)  
Produced by Zirconocene/Methylaluminumoxane Catalysis  
By: Jianbin Zhang

Adviser: Professor George Odian

Low molecular weight(ca 2000) poly(1-butene) and poly(ethylene-*co*-1-butene) were synthesized at 100 °C and 90 °C respectively using *rac*-(dimethylsilyl)bis(4,5,6,7-tetrahydro-1-indenyl)zirconium dichloride(I) and methylaluminumoxane(MAO) as cocatalyst. The products were characterized by NMR(<sup>1</sup>H and <sup>13</sup>C), size exclusion chromatography(SEC) and vapor pressure osmometry(VPO).

The number-average molecular weight of poly(1-butene) was determined as 1910, 2025 and 2055 by SEC, VPO and NMR, respectively. The poly(1-butene) is 84% isotactic and has high regioselectivity(ca. 95% 1,2-addition). Both saturated and unsaturated end groups were characterized by NMR. Vinylidene and trisubstituted double bonds comprise approximately 67% and 29% , respectively, of the unsaturated end groups with the remainder consisting of vinylene and vinyl double bonds. *n*-Butyl and *sec*-butyl groups constitute the saturated end groups in the approximate ratio 10:1. There is a slight excess of saturated end groups relative to unsaturated end groups. These results are discussed in terms of a reaction mechanism of initiation and propagation with various chain-transfer reactions( $\beta$ -hydride transfer with and without rearrangement, transfer to aluminum, transfer to vinylidene end groups, and  $\beta$ -alkyl transfer).

For poly(ethylene-*co*-1-butene) samples, comonomer composition, triad sequence distribution, and end groups were analyzed by  $^1\text{H}$  and  $^{13}\text{C}$  NMR. The average polymer molecule contains about one double bond and one saturated end group. The unsaturated end groups were formed almost exclusively by transfer from propagating chains containing 1-butene as the terminal unit. At least 98% of the unsaturated end groups are vinylidene and trisubstituted double bonds, which are present in the approximate ratio 3:1. Saturated end groups result from the initiation process and chain transfer to aluminum. Both ethylene and 1-butene are involved in initiation but ethylene more than 1-butene. The product is a random copolymer with very short blocks (no longer than 2-3 monomer units) of both ethylene and 1-butene. The comonomer sequence distributions determined by  $^{13}\text{C}$  NMR were fitted to first-order Markovian statistics, which allowed calculation of the monomer reactivity ratios. The results are discussed in terms of a reaction mechanism consisting of initiation, propagation and chain transfer reactions.

Different poly(1-butene) samples were synthesized using *rac*-(dimethylsilyl)bis(4,5,6,7-tetrahydro-1-indenyl)zirconium dichloride(I)/MAO at different temperatures for different polymerization times and catalyst concentrations. 1-Butene was also polymerized by using *meso*-(dimethylsilyl)bis(4,5,6,7-tetrahydro-1-indenyl)zirconium dichloride(I)/MAO, and cationic zirconocene catalyst system (also called non-coordination anion system) *rac*-(dimethylsilyl)-bis(4,5,6,7-tetrahydro-1-indenyl)zirconium dimethyl/ $\phi\text{NHMe}_2\text{B}(\text{C}_6\text{F}_5)_4$ . The resulting polymers were analyzed by NMR ( $^1\text{H}$  and  $^{13}\text{C}$ ), SEC and IR.

This thesis is dedicated to  
my lovely daughter Wenjun  
my beloved wife Jianqun Zhao

## Acknowledgement

I would like to express my heartfelt thanks to Professor George Odian for his supervising on this research, and for his help and friendship over past five years.

My heartfelt thanks also go to Professor Howard Haubenstock, for his valuable suggestions and friendship, and to Professor Norman Indictor, for his valuable suggestions, friendship and being so generous on his time.

I would like to especially thank Dr. Albert Rossi of Exxon Chemical Co. for supplying various catalysts, poly(1-butene) and poly(ethylene-co-1-butene) samples, and also for his guidance and friendship.

My thanks also go to Dr. Fang Shi for her help when I first entered the research laboratory where I started my Ph.D. thesis.

I am grateful for financial support of this research by the Exxon Chemical Co..

Thanks are also extended to the Chemistry Department of the College of Staten Island for support in the form of teaching assistantships.

Without the support of my family this work could not have been accomplished. To my wife Jianqun, who is also studying for her Ph.D., for giving me so much strength and warmth; to my lovely little daughter Wenjun, who has not fully understood what her Dad is doing every day but is always saying "Dad has work to do, I can play by myself!"; to my parents-in law, who helped us to raise our daughter; to my parents; to my uncle Dr. Henry Wang and aunt Mrs. Anna Wang, who should be credited for helping me to start my Ph.D. program with determination, and also for their support and friendship on many aspects of our life during past five years.

Thank you and God bless you all!

## Contents

	Page
<u>Abstract</u>	iv
<u>Contents</u>	viii
<u>List of Schemes</u>	xii
<u>List of Figures</u>	xiii
<u>List of Tables</u>	xv
<u>1.0 Introduction</u>	1
<u>2.0 Experimental</u>	13
2.1 Polymerization	13
2.1.1 Use of drybox	13
2.1.2 Monomer, solvent, catalyst and cocatalyst preparations	15
2.1.3 Polymerization procedures: pressure reactor	16
2.1.4 Polymer product treatment	23
2.2 NMR analysis	24
2.2.1 NMR sample preparation	24
2.2.2 $^1\text{H}$ and $^{13}\text{C}$ NMR quantitative analysis	25
2.2.3 $^{13}\text{C}$ DEPT NMR analysis	25
2.2.4 $^{13}\text{C}$ - $^1\text{H}$ shift correlated 2D NMR analysis	25
2.3 NMR chemical shift determination	26
2.3.1 $^1\text{H}$ NMR chemical shift	26
2.3.2 $^{13}\text{C}$ NMR chemical shift of double bond	28
2.3.3 $^{13}\text{C}$ NMR chemical shift of saturated carbon	28
2.3.4 $^{13}\text{C}$ NMR chemical shift of different configuration	29
2.4 Molecular weight analysis	34

2.4.1 SEC measurement	34
2.4.2 VPO measurement	34
2.4.3 $^1\text{H}$ and $^{13}\text{C}$ NMR analysis of MW	34
<b><u>3.0 Results and discussion on experimental methods</u></b>	<b>36</b>
3.1 Comparison of polymer sample work-up procedures	36
3.2 Quantitative conditions for NMR analysis	43
3.3 Considerations for $^{13}\text{C}$ NMR signal assignments	45
<b><u>4.0 Results and discussion on microstructure of poly(1-butene)</u></b>	<b>49</b>
4.1 End groups	49
4.1.1 Vinylidene double bonds	49
4.1.2 Trisubstituted double bonds	55
4.1.3 Vinylene double bonds	59
4.1.4 Vinyl double bonds	60
4.1.5 Saturated end groups	60
4.2 Polymer molecular weight	61
4.3 Structure of repeat unit	61
4.4 Discussion	66
<b><u>5.0 Results and discussion on microstructure of poly(ethylene-co-1-butene)</u></b>	<b>82</b>
5.1 Copolymer composition	82
5.2 End groups	82
5.2.1 Vinylidene double bonds	85
5.2.2 Trisubstituted double bonds	88
5.2.3 Vinylene and vinyl double bonds	91
5.2.4 Saturated end groups	91

5.3 Polymer molecular weight	93
5.4 Structure of repeat units	93
5.5 Discussion	95
<u>6.0 Results and discussion on microstructures of poly(1-butene)</u>	
<u>synthesized under different polymerization conditions</u>	120
6.1 Double bond end groups	120
6.1.1 <sup>1</sup> H NMR results	120
6.1.2 <sup>13</sup> C NMR results	123
6.1.3 Discussion in terms of chain transfer reactions	129
6.2 Saturated end groups	129
6.3 Structure of repeat units	131
6.3.1 Stereochemistry	131
6.3.1 Regioselectivity	131
<u>7.0 Appendices</u>	143
1 <sup>1</sup> H NMR of <i>rac</i> -zirconium metallocene catalyst	143
2 <sup>1</sup> H NMR of cocatalyst MAO	146
3 <sup>1</sup> H NMR of catalyst system <i>rac</i> -zirconium metallocene/MAO	149
4 Synthesis of zirconium metallocene catalyst	152
5 Relationships between dyad, triad, tetrad and pentad fractions	154
6 Derivation of comonomer reactivity ratio	157
7 <sup>1</sup> H NMR of <i>meso</i> -zirconium metallocene catalyst	161
8 <sup>1</sup> H NMR of catalyst system <i>meso</i> -zirconium metallocene/MAO	164
9 <sup>13</sup> C NMR of poly(1-butene) synthesized by <i>meso</i> -zirconium metallocene catalyst at 25 °C/60min	167

10 $^{13}\text{C}$ NMR of poly(1-butene) synthesized by <i>meso</i> -zirconium metallocene catalyst at 50 °C/60min	170
11 $^{13}\text{C}$ NMR of poly(1-butene) synthesized by <i>meso</i> -zirconium metallocene catalyst at 80 °C/60min	173
12 $^1\text{H}$ NMR of poly(1-butene) synthesized by cationic zirconium metallocene catalyst at 45 °C/60min	176
13 $^{13}\text{C}$ NMR of poly(1-butene) synthesized by cationic zirconium metallocene catalyst system at 25 °C/60min	178
14 FT Infrared spectrum of poly(1-butene) synthesized by <i>rac</i> -zirconium metallocene catalyst at 80 °C/60min	181
15 FT Infrared spectrum of poly(ethylene- <i>co</i> -1-butene)	183
<u>8.0 References</u>	185

List of Schemes

	Page
Scheme IA Monometallic mechanism of Ziegler-Natta polymerization	5
Scheme IB Bimetallic mechanism of Ziegler-Natta polymerization	6
Scheme II Zirconium metallocene catalyst structure	12
Scheme IIIA Overall picture of pressure reactor and controller	18
Scheme IIIB Pressure reactor bomb top	19
Scheme IIIC Bomb vessel, glass liner and bomb heater	20
Scheme IV Initiation reactions of 1-butene polymerization	74
Scheme V Propagation reactions of 1-butene polymerization	75
Scheme VI Chain transfer reactions of 1-butene polymerization	76
Scheme VII Initiation reactions of ethylene/1-butene copolymerization	110
Scheme VIII Propagation reactions of ethylene/1-butene copolymerization	112
Scheme IX $\beta$ -Hydride transfer reactions of ethylene/1-butene copolymerization	113
Scheme X Other chain transfer reactions of ethylene/1-butene copolymerization	118

## List of Figures

	Page
Figure 1 Observed and simulated spectra of poly(1-butene)	33
Figure 2 $^1\text{H}$ NMR double bond region of crude poly(1-butene)	38
Figure 3 $^1\text{H}$ NMR double bond region of EVAP poly(1-butene)	39
Figure 4 $^1\text{H}$ NMR double bond region of DEASH poly(1-butene)	40
Figure 5 $^1\text{H}$ NMR double bond region of NVM poly(1-butene)	41
Figure 6 $^1\text{H}$ NMR double bond assignments of poly(1-butene)	50
Figure 7 $^{13}\text{C}$ NMR double bond assignments of poly(1-butene)	51
Figure 8 $^{13}\text{C}$ DEPT NMR double bond region of poly(1-butene)	52
Figure 9 $^{13}\text{C}$ NMR single bond region of poly(1-butene) with end group assignments	58
Figure 10 $^{13}\text{C}$ DEPT NMR single bond region of poly(1-butene)	62
Figure 11 $^{13}\text{C}$ - $^1\text{H}$ shift correlated 2D spectrum of poly(1-butene)	63
Figure 12 $^{13}\text{C}$ NMR single bond region of poly(1-butene) with repeat unit assignments	67
Figure 13 $^1\text{H}$ NMR of poly(ethylene- <i>co</i> -1-butene) sample 1	83
Figure 14 $^1\text{H}$ NMR of poly(ethylene- <i>co</i> -1-butene) sample 2	84
Figure 15 $^{13}\text{C}$ NMR double bond region of poly(ethylene- <i>co</i> -1-butene) sample 1	97
Figure 16 $^{13}\text{C}$ DEPT NMR double bond region of poly(ethylene- <i>co</i> -1-butene) sample 1	98
Figure 17 $^{13}\text{C}$ NMR double bond region of poly(ethylene- <i>co</i> -1-butene) sample 2	99

Figure 18 $^{13}\text{C}$ DEPT NMR double bond region of poly(ethylene- <i>co</i> -1-butene) sample 2	100
Figure 19 $^{13}\text{C}$ NMR single bond region of poly(ethylene- <i>co</i> -1-butene) sample 1	101
Figure 20 $^{13}\text{C}$ DEPT NMR single bond region of poly(ethylene- <i>co</i> -1-butene) sample 1	102
Figure 21 $^{13}\text{C}$ NMR single bond region of poly(ethylene- <i>co</i> -1-butene) sample 2	103
Figure 22 $^{13}\text{C}$ DEPT NMR single bond region of poly(ethylene- <i>co</i> -1-butene) sample 2	104
Figure 23 $^1\text{H}$ NMR double bond regions of poly(1-butene) synthesized at different temperature with 60 minutes polymerization time	121
Figure 24 $^1\text{H}$ NMR double bond region of poly(1-butene) synthesized at different temperature with 10 & 1 minutes polymerization time	125
Figure 25 $^{13}\text{C}$ NMR double bond region of poly(1-butene) synthesized at different temperature with 60 minutes polymerization time	127
Figure 26 $^{13}\text{C}$ NMR side chain methylene region(pentad fractions) of poly(1-butene) synthesized at different temperature with 60 minutes polymerization time	132
Figure 27 $^{13}\text{C}$ NMR main chain methylene and methine region (regioselectivity) of poly(1-butene) synthesized at different temperature with 60 minutes polymerization time	140

## List of Tables

	Page
Table 1 $^1\text{H}$ NMR chemical shifts of double Bonds	27
Table 2 Empirical parameters by Grant and Paul	30
Table 3 Calculated $\text{C}_{10}$ methylene side chain chemical shifts and observed chemical shifts of poly(1-butene) by Asakura	31
Table 4 Effects of work-up procedures on double bond contents	42
Table 5 Allylic carbon chemical shifts of olefin model compounds	48
Table 6 Double bond contents of poly(1-butene)	54
Table 7 Assignments of double bond $^{13}\text{C}$ NMR signals	57
Table 8 $^{13}\text{C}$ Chemical shifts for repeat units of poly(1-butene)	64
Table 9 Pentad stereochemistry of poly(1-butene)	68
Table 10 Relative amounts of $\beta$ -hydride transfer reactions for 1-butene polymerization	71
Table 11 Copolymer composition, MW, and double bond composition of ethylene/1-butene copolymers	86
Table 12 $^{13}\text{C}$ NMR end group and repeat unit assignments	89
Table 13 Comonomer distribution statistics of ethylene/1-butene copolymers	96
Table 14 Double bond compositions by $^1\text{H}$ NMR for poly(1-butene) synthesized at different temperature with 60 minutes polymerization time	122
Table 15 Double bond compositions by $^1\text{H}$ NMR for poly(1-butene) synthesized at different temperature with 10 & 1 minutes polymerization time	124

Table 16 $^{13}\text{C}$ NMR double bond compositions for poly(1-butene) synthesized at different temperature with 60 minutes polymerization time	128
Table 17 Ratio of saturated end group 12:14 by $^{13}\text{C}$ NMR for poly(1-butene) synthesized at different temperature with 60 minutes polymerization time	130
Table 18-23 Pentad fractions by $^{13}\text{C}$ NMR for poly(1-butene) synthesized at different temperature with 60 minutes polymerization time	133
Table 24 Percentage of reverse repeat units by $^{13}\text{C}$ NMR for poly(1-butene) synthesized at different temperature with 60 minutes polymerization time	141

## 1.0 Introduction

Polymers of ethylene, propylene, and butenes are the basic building blocks of the polyolefin industry. They are easily available, cheap, reactive, and readily transferable to a wide range of useful products. The discovery of Ziegler-Natta catalysis in 1950s marked a tremendous expansion of the polyolefin industry.

Ziegler -Natta catalysis has proven to be a remarkably versatile technology for the production of polyolefins.<sup>(1-5)</sup> Among them, poly(ethylene) and poly(propylene) now account for about 20-25% of global plastics production. While by far poly(ethylene) is the largest volume poly(olefin), poly(propylene) has become the fastest growing. Current consumption of poly(propylene) alone is estimated to be 16 million tons/year with an average growth of 6-8% per year.<sup>(6)</sup>

Ziegler-Natta catalyst has the capability to yield unbranched and stereospecific polyolefins. The poly(ethylene) produced by this catalyst is linear and has a higher density and more crystalline than prepared by free-radical polymerization. Ziegler-Natta polymerization of propylene can yield an isotactic poly(propylene). About 11 billion pounds of poly(ethylene) and 10 billion pounds of isotactic poly(propylene) are produced each year by this method in the United States. Also about 4 billion pounds of low density poly(ethylene) is synthesized by the copolymerization of ethylene with 1-butene and/or 1-hexene using this catalyst to control level of short branching and crystallinity. Ziegler-Natta polymerization is also important in the commercial polymerization of butadiene and isopropene to elastomers.<sup>(7)</sup>

A Ziegler-Natta Catalyst usually consists of two components: a transition metal compound from group IVB to VIII B and an organometallic compound from group IA to IIIA metal of the periodic table. The transition metal component employed is usually a halide of titanium, vanadium, chromium, molybdenum or zirconium. The second component often consists of an alkyl, aryl or hydride of aluminum, lithium, magnesium or zinc. The best known systems are those derived from  $\text{TiCl}_4$  and  $\text{TiCl}_3$  and an aluminum trialkyl. The catalyst system may be heterogeneous (some titanium-based systems) or soluble (most vanadium-containing systems). The stereoregularity of the polymer can also be altered by the addition of Lewis bases such as amines.

The development of Ziegler-Natta catalysis for olefin polymerization can also be described as having progressed through three generations, from the initial discoveries of Ziegler and Natta in the 1950s through to the supported and highly active catalysts commonly used for poly(ethylene) and poly(propylene) production today.<sup>(8-11)</sup> Isotactic poly(propylene) was first synthesized by Natta in 1954 using a catalyst system consisting of  $\text{TiCl}_3$  and  $\text{Al}(\text{C}_2\text{H}_5)_3$  activator. It was based on Ziegler's catalyst system used for the synthesis of ethylene polymers, but when applied to the polymerization of propylene, resulted in a polymer in which only 30-40% of the resin had the typical characteristics of isotactic poly(propylene). The remaining product was atactic, with poor structural uniformity and a rubbery consistency.

Natta soon realized that the polymer isotacticity was directly connected to the uniformity of the catalyst surface. By employing solid, crystalline  $\text{TiCl}_3$ , in polymerizations with  $\text{Al}(\text{C}_2\text{H}_5)_3$  he obtained a higher percentage of

isotactic product. The high isotacticity (about 90%) permitted a scaled-up industrial process to be developed by Montecatini, which contained a large section for the separation of the undesirable atactic fraction from the isotactic fraction and a section for the removal of the catalyst residues that would affect product quality. This is the first generation of Ziegler-Natta catalyst.

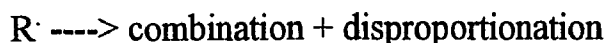
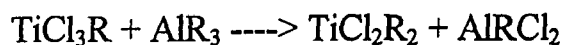
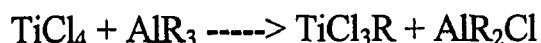
Improvements in both isotacticity and yield were the driving forces for continued research in the new catalyst. The treatment of the  $\text{TiCl}_3$ , first with an electron donor (a Lewis base) and then with  $\text{TiCl}_4$  gave a highly stereospecific catalyst, four to five times more active than the original Natta catalyst system. The discovery and introduction of the electron donor can be regarded as the basis of the second generation catalyst. The improvements in isotacticity and yield, however, were not sufficient to reduce catalyst residues to a level that would enable the deashing process to be eliminated.

Continued research led to a deeper understanding of the catalyst and system and it was soon realized that only a small percentage of the titanium was active. Only those atoms located on the lateral faces and edges and along the crystal defects were found to take part in the polymerization reaction. This led to the realization that much of the catalyst mass acted simply as a support for the active sites, and that significant improvement could be made by depositing the active titanium on a support whose residues, unlike those to  $\text{TiCl}_3$ , would be inert and not detrimental to the properties of the polymer.

This was the third generation catalyst system and the discovery of magnesium chloride in the active form, as an ideal support for the fixation of  $\text{TiCl}_4$  and its derivatives, opened a new era in the field of Ziegler-Natta

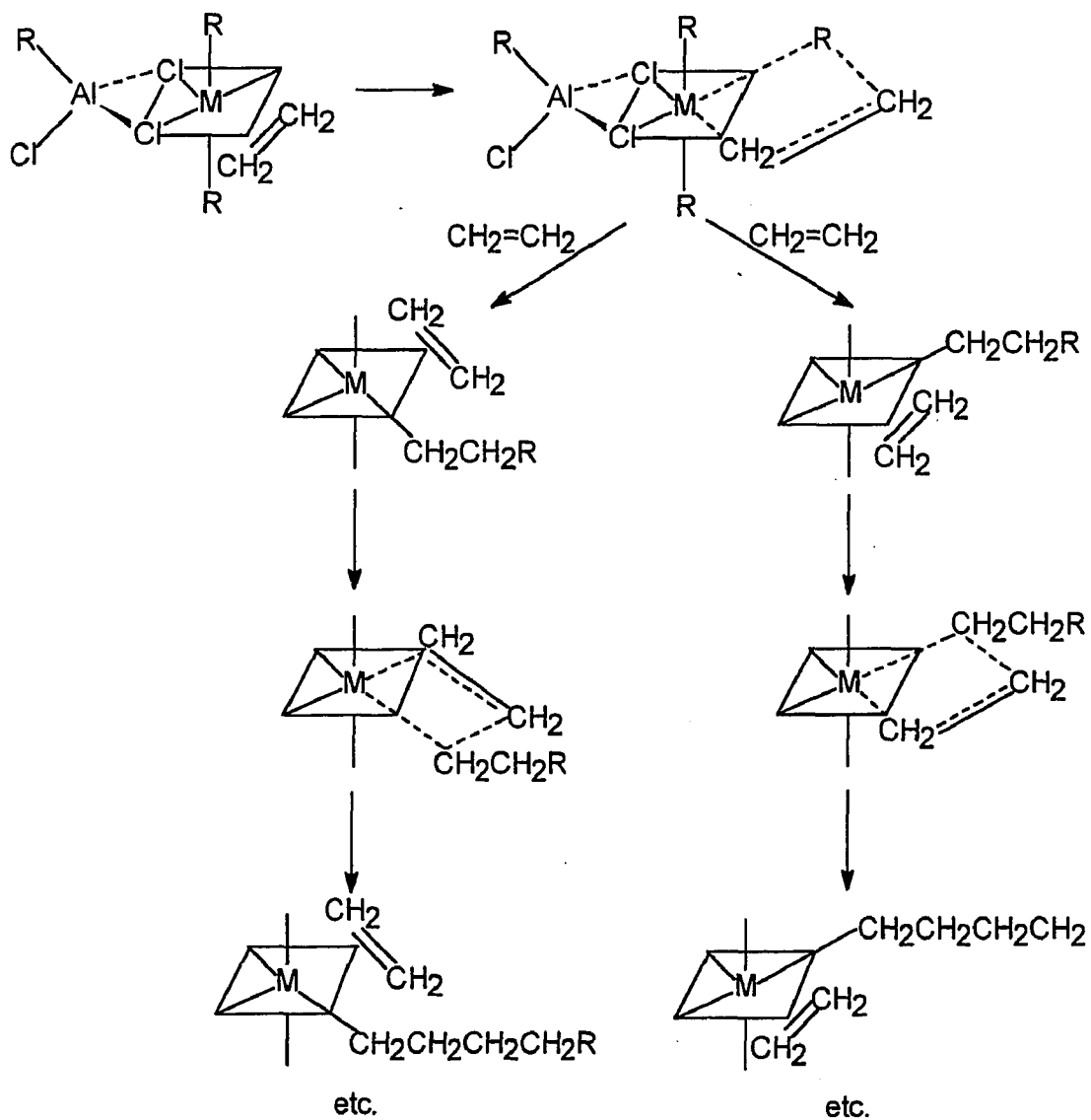
catalyzed polymerization, from both the industrial and scientific points of view. The active polymerization centers could now be dispersed throughout the support, making them all essentially accessible to the monomer. Since all the titanium chloride molecules were now available to take part in the polymerization reaction, fewer were needed. Consequently, the yield of polymer per gram of titanium was so high that no extraction procedures were necessary in order to produce a viable commercial resin. Elimination of the deashing part of the industrial process had obvious economic and environmental advantages and resulted in the explosive growth of polyolefins in the global plastics marketplace.

The nature of Ziegler-Natta catalyst system is still a subject for debate.  $\text{TiCl}_4$  or  $\text{TiCl}_3$  plus  $\text{AlR}_3$  gives rise to very complex heterogeneous initiator systems, the structure of which is still not clear. A critical "aging" period for the catalyst is often needed before it achieves its highest activity, and complex reactions occur during this period, involving alkylation and reduction of the titanium compound by  $\text{AlR}_3$ <sup>(12)</sup>:

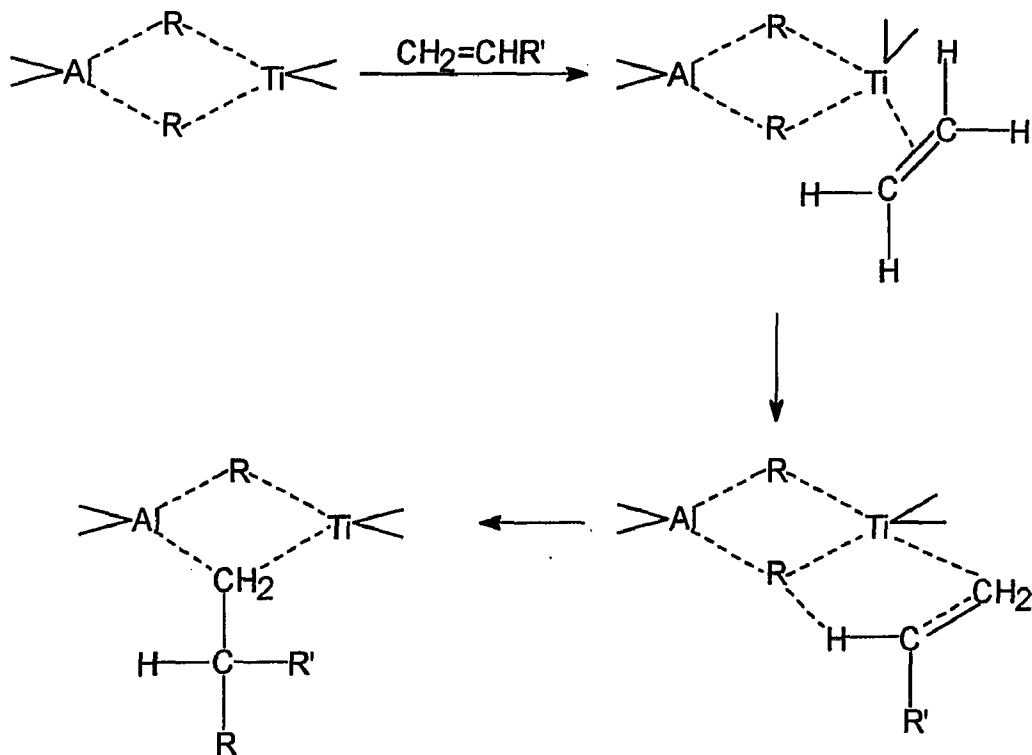


Two polymerization mechanisms have been proposed, one involving coordination of the olefin to a vacant sites on the transition metal known as "monometallic" mechanism and the another suggesting a participation by both

the transition metal and the aluminum atom known as “bimetallic” mechanism. The two mechanisms are described in Schemes IA and IB:



**Scheme IA: Monometallic Mechanism**



Scheme IB: Bimetallic Mechanism

Even though the third generation heterogeneous Ziegler-Natta catalyst has proven to be efficient for olefin polymerization in terms of simple and economic industrial processes, there has been considerable effort to obtain soluble (homogeneous) catalysts that bring about isospecific polymerization. The soluble catalyst has the tremendous advantage over heterogeneous catalyst simply because the polymerization reaction media is homogeneous for soluble catalyst system. A variety of soluble initiators, such as di- $\eta^5$ -cyclopentadienyldiphenyltitanium and tetrabenzylzirconium, are active but aspecific initiators. However, the combination of some of these initiators with methylaluminoxane (oligomeric  $[\text{Al}(\text{CH}_3)\text{-O}]_n$ ) are partially effective for initiating isospecific polymerization.<sup>(13-16)</sup> Isotactic indices as high as 85% were obtained in the polymerization of propylene at  $-45\text{ }^\circ\text{C}$  with di- $\eta^5$ -cyclopentadienyldiphenyltitanium and methylaluminoxane. The polymer has an isotactic stereoblock structure. Methylaluminoxane apparently interacts with the transition-metal compound to form an initiator with considerable tendency to isospecific polymerization. However, polymerization at higher temperature ( $25\text{ }^\circ\text{C}$ ) yields the atactic structure.

Attention turned to chiral analogs of the various initiators to obtain very highly isospecific initiators. Chiral initiators such as  $\eta^5$ -cyclopentadienyl- $\eta^5$ -indenylmethylzirconium chloride are active but are still not exceptionally high in isospecificity.<sup>(17-18)</sup> A major breakthrough occurred with the preparation of rigid chiral metallocene initiators, such as *racemic* 1,1'-ethylenedi- $\eta^5$ -indenylzirconium dichloride, the titanium and hafnium analogs, and the corresponding *racemic* 1,1'-ethylenedi- $\eta^5$ -4,5,6,7-tetrahydroindenyl compounds.<sup>(19-24)</sup> Isotactic indices of greater than 90% are

easily achieved in the polymerization of propylene and other  $\alpha$ -olefins by this type of rigid chiral metallocenes together with methylaluminoxane. Isotactic indices of 98-99% have been obtained in a number of polymerizations. These initiators are about as highly isospecific as the best of the heterogeneous Ziegler-Natta initiators.

In order to get highly isospecific polymerization, both chirality and molecular rigidity are needed for the homogeneous catalyst. The rigidity of this catalyst molecule is due to the  $\text{CH}_2\text{CH}_2$  bridge (or  $\text{Si}(\text{CH}_3)_2$  bridge) between indene ligands (two rings) and the complexation with methylaluminoxane which increases its rigidity. Chirality is due to the relationship of the two indene structures. Methylaluminoxane has two roles: one is to alkylate Zr-Cl bond, another is to increase the rigidity of metallocene by complexation. The unique aspects of soluble metallocene catalyst lie in the following facts: first, it is the only known soluble catalyst which can produce high linear poly(ethylene) and isotactic poly(propylene); second, very narrow molecular weight distributions can be obtained, usually with  $M_w/M_n$  being below 2-3 ( $M_w/M_n$  for heterogeneous Z-N polymerization is usually in the range of 5-20); third, higher catalyst activity may be achieved; fourth, the broader flexibility of electronic and steric variations in the cyclopentadienyl type ligands allows greater maneuvering in the design of catalyst systems which govern the polyinsertion reaction leading to regio- and stereoregular polyolefins. All these unique aspects make soluble metallocene catalyst very important and promising as the fourth generation Ziegler-Natta catalyst in industrial polymerization of olefins.

The recent literature contains many papers related to homogeneous metallocene catalysts. Both bridged and unbridged metallocene catalysts, e.g., ethylenebis(indenyl)zirconium dichloride and bis(cyclopentadienyl)zirconium dichloride in the presence of methylaluminoxane(MAO),  $[\text{Al}(\text{CH}_3)_2\text{O}]_n$ , have been studied for the homogeneous polymerization of  $\alpha$ -olefins such as propene and 1-butene.<sup>(16, 20, 25)</sup> These catalysts are single-site catalysts which show high activity coupled with high stereospecificity(usually isospecific) and narrow molecular weight distributions.<sup>(22)</sup> The mechanism for formation of unsaturated end groups during polymerizations with these catalysts is not well-established., probably because the reaction is very sensitive to monomer, catalyst, cocatalyst, temperature, and other reaction conditions.

$\beta$ -Hydride transfer,  $\beta$ -alkyl transfer, and chain transfer to aluminum have been reported as the molecular weight limiting reactions in propene polymerization, but the relative importance of the three reactions is sensitive to the specific system. Catalyst identity does not appear to be important in the temperature range of 0-80 °C unless the catalyst is sterically hindered. Polymerization proceeds exclusively by  $\beta$ -hydride transfer using catalysts such as  $\text{Cp}_2\text{ZrCl}_2$  and  $\text{Cp}_2\text{HfCl}_2$  (Cp=cyclopentadienyl) and  $\text{CH}_2\text{CH}_2$  and  $\text{Si}(\text{CH}_3)_2$  bridged  $\text{Ind}_2\text{ZrCl}_2$  and  $(\text{H}_4\text{Ind})_2\text{ZrCl}_2$  [Ind=1-indenyl,  $\text{H}_4\text{Ind}$ =4,5,6,7-tetrahydro-1-indenyl].<sup>(19-20, 26-27)</sup> At lower temperatures and/or with more sterically hindered catalysts,  $\beta$ -alkyl transfer and/or chain transfer to aluminum become important. For example, polymerization with  $(\text{CH}_3)_5\text{CpCpZrCl}_2$  proceeds with 80%  $\beta$ -hydride transfer and 20% chain transfer to aluminum at 50 °C, while only chain transfer to aluminum occurs at -30 °C.<sup>(16)</sup> Polymerization with  $[(\text{CH}_3)_5\text{Cp}]_2\text{ZrCl}_2$  proceeds with 91%  $\beta$ -

methyl transfer, 8%  $\beta$ -hydride transfer, and 1% chain transfer to aluminum at 50 °C, while chain transfer to aluminum occurs exclusively at -40 °C.<sup>(26)</sup>

Polymerization by cationic zirconocenes, also called non-coordinating anion zirconocenes, such as  $[(\text{CH}_3)_5\text{Cp}]_5\text{ZrR}^+\text{Z}^-$ , where Z is a stable anion such as  $\text{B}\phi_4^-$ , proceeds almost exclusively by  $\beta$ -methyl transfer at 0 °C.<sup>(28-29)</sup>

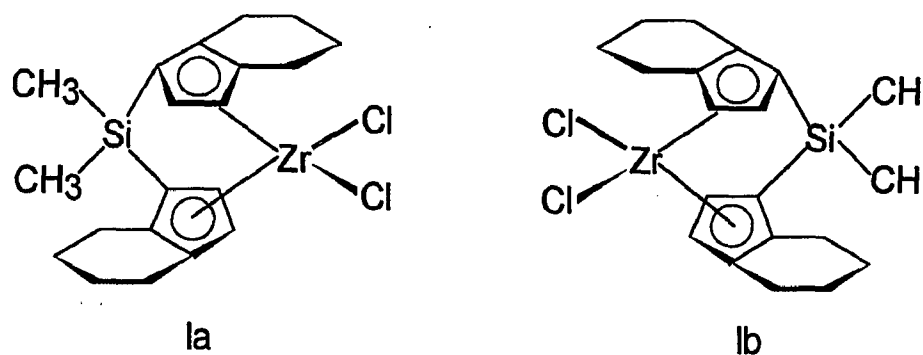
Much less is available in the literature on mechanisms for formation of unsaturated end groups for 1-butene polymerization.  $\beta$ -Hydride transfer is the exclusive reaction for  $\text{Cp}_2\text{ZrCl}_2$  at 0 °C.<sup>(26)</sup> Chain transfer to aluminum becomes important for polymerization by  $[(\text{CH}_3)_5\text{Cp}]_5\text{ZrCl}_2$ . The ratio of chain transfer to aluminum to  $\beta$ -hydride transfer increases from 1:3 to 2:1 as the polymerization temperature decreases from 50 to 0 °C.<sup>(26)</sup> Chain transfer to aluminum is the exclusive reaction for  $\text{CH}_2\text{CH}_2$  bridged  $\text{Ind}_2\text{Ti}(\text{CH}_3)_2$  at -45 °C.<sup>(30)</sup>  $\beta$ -Hydride transfer, but exclusively after reverse addition of monomer (all other  $\beta$ -hydride transfer discussed above occur after normal propagation), is the only transfer reaction for polymerization of by  $\text{CH}_2\text{CH}_2$  bridged  $\text{Ind}_2\text{ZrCl}_2$  at 30 °C.<sup>(31)</sup> There are few other reports of transfer reactions in  $\alpha$ -olefin polymerizations except for the report of chain transfer to aluminum as the exclusive reaction in 1,5-hexadiene cyclopolymerization by  $\text{Cp}_2\text{ZrCl}_2$  at -25 °C.<sup>(32)</sup>

The studies of this thesis on polymerization of 1-butene catalyzed by *rac*-dimethylsilyl( $\text{H}_4\text{Ind}$ ) $_2\text{ZrCl}_2$  (I) in the presence of methylaluminoxane (MAO) were focused on the chain transfer reactions which control molecular weight of poly(1-butene), and stereo- and regio-selectivity of the polyinsertion reactions of 1-butene monomer.  $^1\text{H}$  and  $^{13}\text{C}$  NMR were used

for analysis of end groups formed by chain transfer reactions and analysis of repeat units leading to information about stereo- and regio-selectivity.

Most documented studies of the microstructure of ethylene copolymers have focused mostly on comonomer sequence distribution.<sup>(33-41)</sup> The structural studies have indicated that polymer molecular weight is controlled by various chain transfer reactions, mostly  $\beta$ -hydride transfer but also  $\beta$ -alkyl transfer and chain transfer to aluminum.<sup>(42-43)</sup> A better understanding of polymerization mechanism requires the polymer sequence distribution, which gives information on the propagation step, and also the polymer end groups, which give information on the initiation and termination steps. Elucidation of the polymer end groups includes the end groups that are saturated and unsaturated (and what type of double bond) and also the sequence of monomer units at the end groups (e.g., EE, BB, BE, or EB).

The studies of this thesis on copolymerization of ethylene with 1-butene by *rac*-dimethylsilyl( $H_4Ind$ )<sub>2</sub>ZrCl<sub>2</sub> (I) in the presence of methylaluminoxane (MAO) were carried out on the microstructure of poly(ethylene-co-1-butene) including both end groups and monomer sequence distribution. Again, <sup>1</sup>H and <sup>13</sup>C NMR were employed as the major tools for structural analysis. Also the copolymer samples were analyzed by both SEC and VPO which were also used in poly(1-butene) sample studies.



*rac*-dimethylsilyl(H<sub>4</sub>Ind)<sub>2</sub>ZrCl<sub>2</sub>

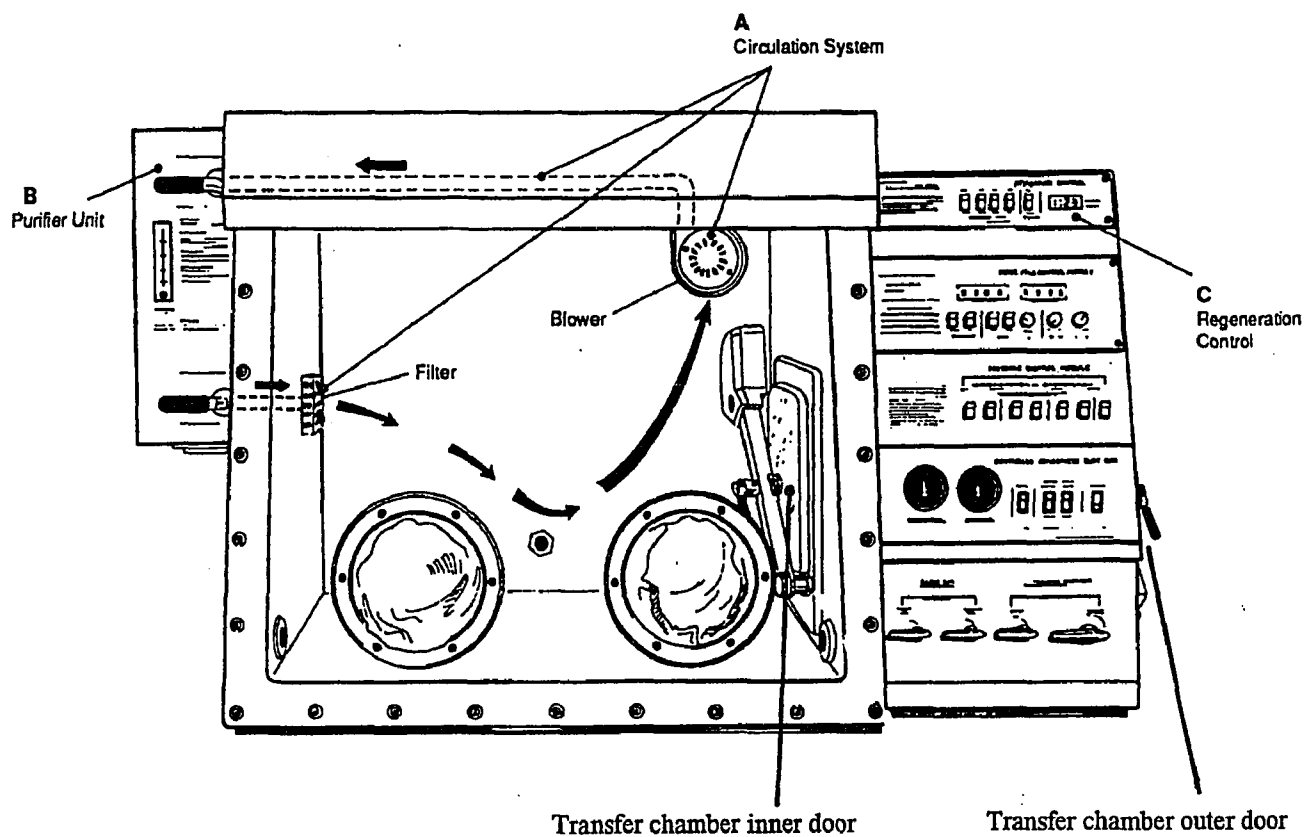
Scheme II Zirconium metallocene catalyst

## 2.0 Experimental

### 2.1 Polymerization

#### 2.1.1 Use of drybox

A drybox shown in the picture below, model 50800, equipped with atomspure gas purifier from Labconco Co., was used throughout our entire experimental period:



Description of Atmospure Systems

The procedures for using the drybox consists of the following steps:

(1) Establishing inert gas environments

The inert gas environment is achieved by alternately purging and filling the drybox with purified nitrogen gas. A high capacity gas purifier (purchased from Supelco, Inc.) is installed between drybox and gas tank to further remove both oxygen and moisture from nitrogen gas before nitrogen goes into drybox. Inside the drybox there is a circulation system(A) which constantly circulates the nitrogen gas in the drybox through a purifier unit(B) which contains copper catalyst to remove oxygen and moisture from nitrogen in the drybox by reacting with oxygen and moisture.

After the inert gas environment is established inside the drybox, the appropriate operating pressure is obtained. The operating pressure range for our drybox is adjusted between 0.4 and 3.0 inches water column to always maintain a slightly positive pressure compared to the atmosphere no matter if the drybox is in use or not.

(2) Transfer from laboratory into drybox

Make sure the inner chamber door is closed. Place material into the transfer chamber and close the outer transfer chamber door. Set transfer chamber purge/fill cycle to three times and perform the purge/fill operation automatically. After three cycles are completed, open the inner chamber door to position material inside drybox to complete transfer. Latch both inner and outer transfer chamber doors.

(3) Transfer from drybox outward to laboratory

Make sure the outer chamber door is closed. Place material into the transfer chamber and close the inner door. Open the outer transfer chamber

door to remove material from the transfer chamber and close the outer transfer chamber door and latch both inner and outer transfer chamber doors. Perform the transfer chamber purge/fill cycles three times.

### 2.1.2 Monomer, solvent, catalyst and cocatalyst preparation

Polymer samples analyzed in this work came from two sources. One was polymerization in our laboratories using a Parr reactor. The other was samples supplied by Dr. Albert Rossi of Exxon Chemical Co..

#### (1) Monomer purification

In our 1-butene polymerization, 1-butene, 98.5% in isobutane, was obtained from MG Industry and purified by going through 4Å molecular sieves and subsequently charged into a 100 ml steel pipet by cooling the pipet in a dry ice/acetone bath.

In Exxon's 1-butene polymerization and ethylene/1-butene copolymerization, 1-butene was put through  $\text{Al}_2\text{O}_3$  to remove polar impurities and subsequently put through 4Å molecular sieves. Polymerization-grade ethylene was purified by going through 4Å molecular sieves.

#### (2) Solvent purification

Anhydrous toluene(99.8%) was obtained from Aldrich Chemical Co. in a septum capped bottle, and has b.p. of 110.6 °C and m.p. of -93 °C. The water content of this toluene is less than 0.005% and the content of evaporating residue is less than 0.0005%. The density of the toluene is 0.865 g/ml.

The anhydrous toluene was placed into drybox for at least 12 hours before use. The dried 4A molecular sieves was put into drybox immediately after being removed from furnace set at 240 °C.(4Å molecular sieves was

heated in the furnace at 240 °C for at least 2 days.) After the molecular sieves was cooled for 5-10 min inside drybox, it was added to anhydrous toluene, and the toluene bottle was capped tightly and stored for at least overnight before use. The toluene bottle was never taken out of drybox before all the toluene was used up.

### (3) Catalyst preparation

Zirconocene catalyst I, obtained from Exxon Chemical Co. and synthesized according to the literature procedure<sup>(44-45)</sup>, was dissolved in anhydrous toluene (treated with 4Å molecular sieves as described in (2)) pre-treated with small amount of MAO spike solution. The <sup>1</sup>H NMR of zirconocene catalyst I was taken on Varian 200 MHz spectrometer using Deuterated benzene (C<sub>6</sub>D<sub>6</sub>) as solvent at room temperature and shown in appendix 1.

### (4) Cocatalyst methylaluminoxane (MAO)

Cocatalyst MAO was obtained as a 10 wt-% in toluene contained in a small metal tank from Albemarle Co. and used without further purification. The MAO tank was stored in the drybox for at least one day before use. The tank was never taken out of the drybox before MAO was used up.

A MAO washing solution was prepared by adding 1 ml 10% MAO to 200 ml anhydrous toluene. A MAO spike solution was prepared by adding 10 ml 10% MAO to 100 ml anhydrous toluene.

## 2.1.3 Polymerization procedure

### (1) 1-Butene polymerization in our pressure reactor

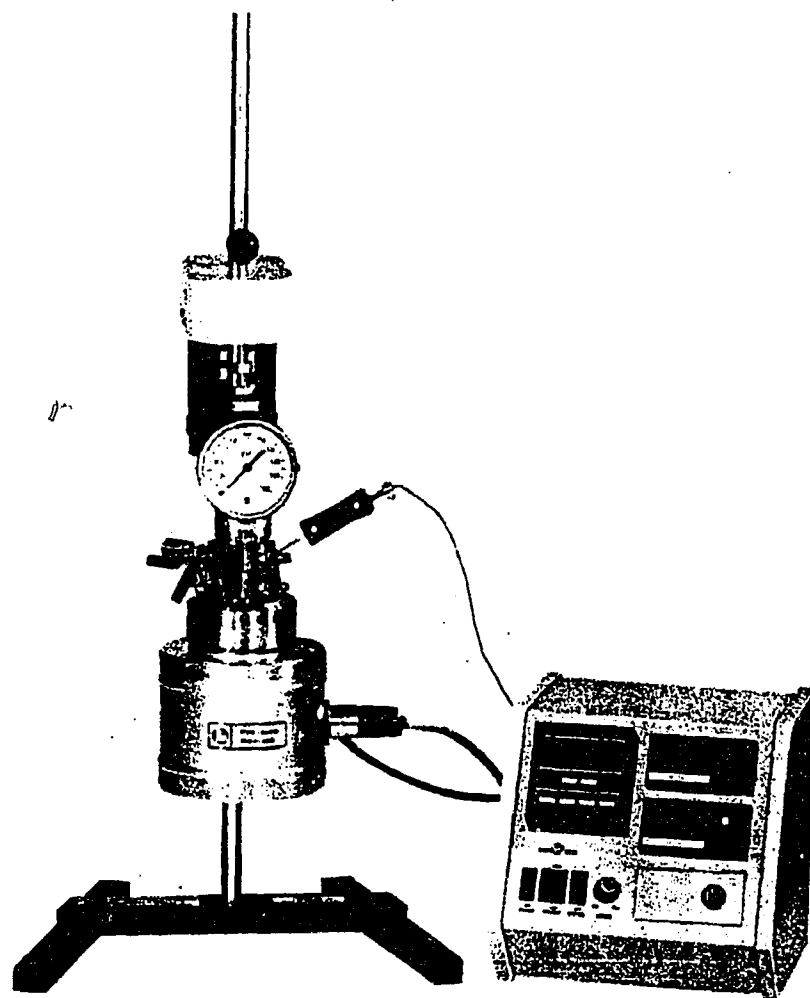
#### (a) Description of the pressure reactor

1-Butene polymerization was carried out in a 100 ml Series 4561 mini reactor with 4842 controller obtained from Parr Instrument Co. as shown on page 18. The pressure reactor comprises of three parts: bomb, heater and temperature controller. The bomb is consisted of bomb top and vessel, and the bomb top is illustrated on page 19.

The bomb top is consisted of following fittings: pressure gage(1) having a range of 0 to 2000 psi for use at working pressures up to 1400 psig; safety rupture disc(2); gas inlet valve(3) for charging gas(monomer) into the reactor; liquid sampling valve(4) for withdrawing samples from the reactor under pressure; gas release valve(5) for withdrawing gas samples or for releasing pressure from the reactor; stirrer drive system(6); leak detector nipple(7); water cooling channel(8); thermocouple(9); dip tube(10) extending to the bottom of the reactor for introducing the incoming gas below the surface of the liquid in the reactor; stirring shaft(11) for efficiently mixing the reaction liquid in the reactor.

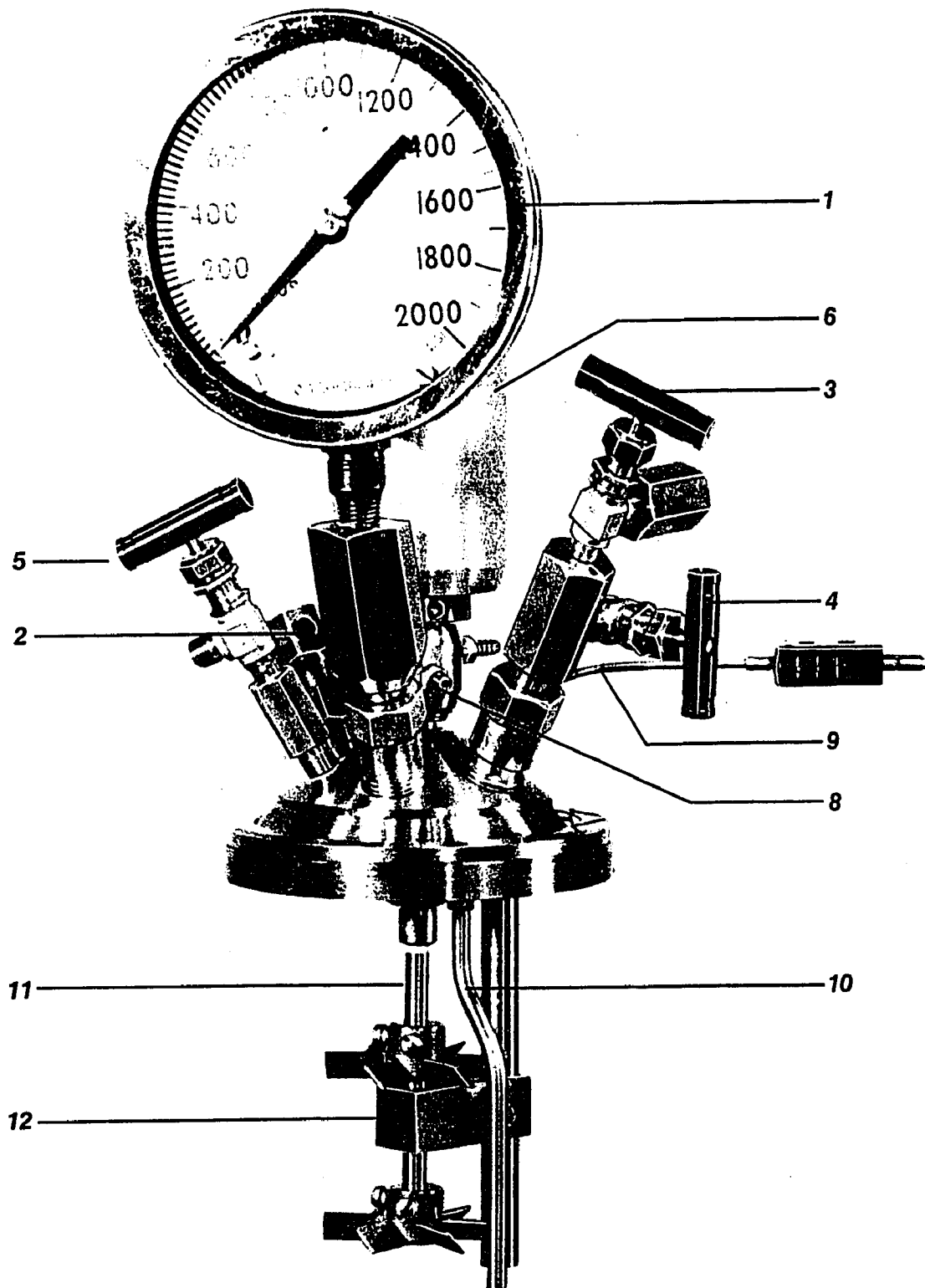
The bomb vessel is consisted of stainless steel vessel and glass liner, which are shown on page 20. The glass liner(removable, open top, beaker type) will fit into the stainless steel vessel to prevent the contact between liquid reactants and the stainless steel vessel. The reaction will generally carried out in the glass liner.

The heater has the fabric mantle inside which fits exactly the size of the bomb vessel. After the reactor bomb is charged with desired reactants and assembled properly, the bomb vessel will be fit into the heater which is attached onto the bomb support shown on page 20.

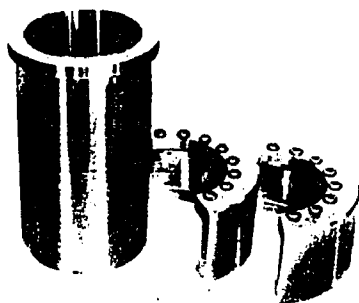


4561 Mini Reactor with 4842 Controller

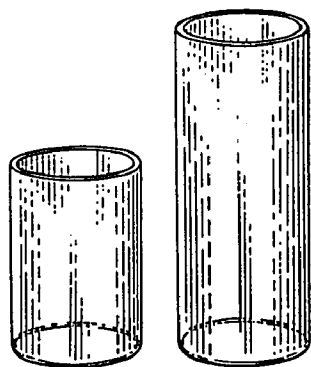
Scheme IIIA  
4561 Mini Reactor with 4842 controller



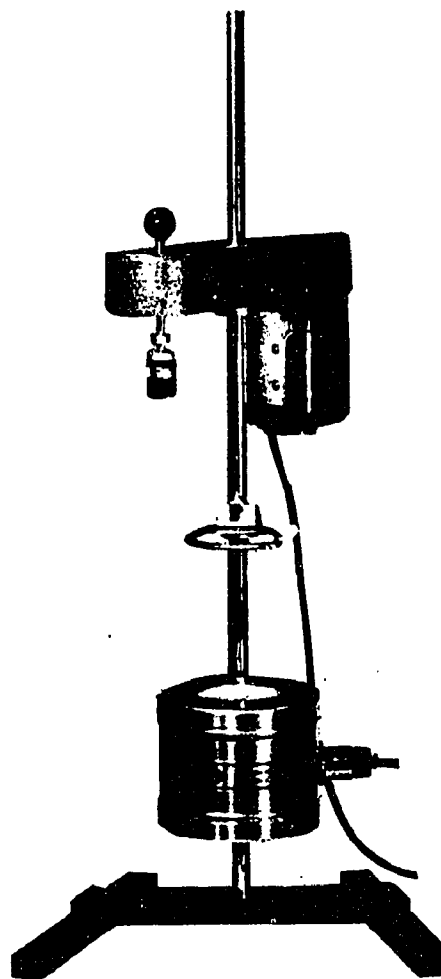
Scheme IIIB  
Bomb top of the pressure reactor



Bomb vessel



Glass liner



Bomb Support and Heater

Scheme IIC  
Bomb vessel, glass liner and heater with support

The heater is connected to a 4842 controller (shown on page 20) which has a microprocessor based control module. It has an operating temperature range of 0-600 °C and the system accuracy of +/- 2 °C. It also provides the control of stirring speed of the reactor.

(b) Polymerization

The stainless steel bomb, glass liner and 100ml pipet were dried in oven at 140 °C for 4 h and then put into drybox while still hot. The top of the reactor was also dried by assembled with another bomb vessel and heated up to 140 °C for 4 h, and then the top was put into drybox while still hot. All parts were stored overnight in the drybox.

The 100ml pipet (shown on page 20) was closed and taken out of drybox, and then weighed. The pipet was connected to the monomer source and put into a dry ice/acetone bath to be cooled efficiently. The valves were opened to charge monomer into pipet. After certain time of charging monomer into pipet, all valves were closed, and the pipet was disconnected from monomer source. The pipet was weighed and extra monomer was vented to obtain desired amount of monomer inside the pipet. Finally the charged pipet was put back into the drybox.

The bomb vessel, glass liner and top of reactor were washed with MAO washing solution twice before charging reagents. The glass liner inside the bomb vessel was first charged with 30 ml toluene, followed by addition of desired amount of spike solution and 10% MAO solution, then after more than 2 min added desired amount of zirconocene catalyst solution. The overall zirconocene catalyst concentration in the reactor is  $7.1 \cdot 10^{-6}$  M with a MAO:Zr ratio of 1000:1. The top of reactor was closed onto the bomb vessel

and tightened, and then the pipet filled with desired amount of 1-butene monomer was attached to the reactor. All above operations were carried out in the drybox. The reactor was taken out of the drybox and settled into the heater programmed by 4842 controller. The reactor was heated to the desired temperature while stirring at 250 rpm. Polymerization was started by opening the pipet valve to add monomer to the bomb.

(2) 1-Butene polymerization and ethylene/1-butene copolymerization carried out at Exxon Chemical Co.

1-Butene polymerization and ethylene/1-butene Copolymerization were also carried out at Exxon Chemical Co., using a continuous flow reactor at 90 °C with about 20 bar pressure. The reactor was charged with catalyst and cocatalyst mixture at catalyst concentration of  $7.1 \cdot 10^{-6}$  M with MAO:Zr ratio of 1000:1 for 1-butene polymerization. The resulting poly(1-butene) was analyzed and discussed in Section 4.0 of the thesis.

For ethylene/1-butene copolymerization, the reactor was charged with catalyst and cocatalyst mixture at catalyst concentration of  $3.6 \cdot 10^{-6}$  M with MAO:Zr molar ratio of 500:1 and 1000:1 for samples 1 and 2, respectively. The feed into the reactor contained 4.3 M 1-butene in butane with ethylene:1-butene molar ratios of 1:4.76 and 1:1.15 for samples 1 and 2, respectively. Aliquots of the reaction mixture were analyzed by gas chromatography to determine the conversions of ethylene and 1-butene. Ethylene conversions were 98.1 and 99.7%, respectively, and 1-butene conversions were 43.5 and 69.1% respectively, for samples 1 and 2. Gas chromatographic analysis of the reaction mixture showed the ethylene:1-butene molar ratio to be 1:72 and 1:56, respectively, for samples 1 and 2. Therefore, the effective ethylene:1-

butene molar ratio in the reaction mixture at steady-state was much richer in 1-butene than the feed composition because the greater conversion of ethylene compared to 1-butene, a consequence of the higher reactivity of ethylene relative to 1-butene. The two copolymer samples were analyzed and discussed in Section 5.0 of the thesis.

#### 2.1.4 Polymer product treatment

##### (1) Our 1-butene polymerization

After measured polymerization time, the whole reactor was disconnected from the heater and controller, and opened. The reaction mixture was immediately quenched with 25 ml of 1% NaOH solution and transferred into a 125 ml separatory funnel, and subsequently washed with 3 portions of 25ml distilled water. The organic layer was transferred to a 50ml round bottom flask and volatile materials were removed using a rotavapor.

##### (2) Exxon's 1-butene polymerization and ethylene/1-butene copolymerization

Polymer and/or copolymer samples were obtained by quenching aliquots of the exiting reaction mixture with aqueous NaOH solution. The organic layer was separated and then washed with water several times. The organic layer was then heated at 140 °C for 2-3 min to drive off water. Volatile materials were removed using a rotavapor.

##### (3) Polymer sample work-up procedures

The polymer sample obtained after rotary evaporation, referred as crude, contains some toluene. Three procedures (EVAP, DEASH, NVM) were used to remove the toluene:

*EVAP*: The crude sample was spread on a flat glass surface to form a thin film and placed in a vacuum oven (<1 torr) for two days either at room

temperature or 45 °C. The two EVAP procedures are referred to as EVAP/RT and EVAP/45, respectively.

*DEASH*: Aqueous ammonia (2%) was added to a solution of the crude sample (2g) dissolved in cyclopentane (50ml) and the mixture vigorously stirred at room temperature for two hours. The organic layer was separated, washed three times with distilled water, and then filtered. Most of the cyclopentane was evaporated off in a rotary evaporater at 45 °C and then the sample evacuated in a vacuum oven (<1 torr) for two days either at room temperature or at 45 °C. The two deash procedures are referred to as DEASH/RT and DEASH/45, respectively. In a variation of the above procedures, the organic layer was dried after washing with distilled water by treating with Na<sub>2</sub>SO<sub>4</sub> for two hours followed by filtration, and then the solvent evaporated. NMR analysis showed no difference between dried and undried samples.

*NVM*: The crude sample was placed in a vacuum oven, the vacuum lowered to ca. 1 torr, and then the temperature raised to and subsequently held at 125 °C for two hours.

After the studies of polymer sample work-up procedures(Section 3.1), the polymer sample work-up procedure *EVAP/45* was chosen as standard polymer work-up procedure for all polymer and/or copolymer samples.

## 2.2 NMR Analysis

### 2.2.1 NMR sample preparation

Polymer samples were dissolved in CDCl<sub>3</sub> to form a 10% (wt/vol) solution for <sup>1</sup>H NMR measurements, and TMS was added to the solution as internal reference. For <sup>13</sup>C NMR measurements, a 20% (wt/vol) was made

by dissolving polymer samples in  $\text{CDCl}_3$  with 25 mg/ml  $\text{Cr}(\text{AcAc})_3$  added, and TMS as internal reference.

### 2.2.2 $^1\text{H}$ and $^{13}\text{C}$ NMR quantitative analysis

$^1\text{H}$  and  $^{13}\text{C}$  NMR spectra of Exxon's poly(1-butene) samples (analyzed in Section 4.0) were obtained on a JEOL 400 MHz spectrometer.  $^1\text{H}$  NMR spectra of copolymer samples (analyzed in Section 5.0) and our poly(1-butene) samples (analyzed in Section 6.0) were obtained on a Varian 500 MHz spectrometer;  $^{13}\text{C}$  NMR spectra were obtained on a Varian 300 MHz spectrometer. The conditions used for quantitative  $^1\text{H}$  NMR were 40 °C, 30 ° pulse angle, 3 s delay between pulses, and 500 scans. The conditions used for quantitative  $^{13}\text{C}$  NMR were 40 °C, 90 ° pulse angle, inverse gated decoupling with 3 s delay between pulses, and 12000-50000 scans depending on polymer molecular weight (the higher the polymer weight, the more scans). For both  $^1\text{H}$  and  $^{13}\text{C}$  NMR, it was verified that 3 s delay was sufficient for quantitative results by performing NMR experiments with 10 s delay on polymer sample, and by performing NMR experiments with model alkene compounds.

### 2.2.3 $^{13}\text{C}$ DEPT NMR analysis

$^{13}\text{C}$  DEPT (distortionless enhancement by polarization transfer) NMR with 135 °  $^1\text{H}$  pulse was run under the same conditions as the quantitative  $^{13}\text{C}$  NMR. The resulting spectrum shows positive signals for 1° and 3° carbons, negative signals for 2° carbons, and no signals for 4° carbons, compared to quantitative  $^{13}\text{C}$  NMR spectrum of sample polymer sample.

### 2.2.4 $^{13}\text{C}$ - $^1\text{H}$ shift-correlated 2D NMR analysis

$^{13}\text{C}$ - $^1\text{H}$  shift correlated 2D NMR was run under the same conditions for quantitative  $^{13}\text{C}$  NMR.  $^{13}\text{C}$  spectral data was obtained with a SW=60 ppm in 2K data point. A total of 256 spectra were used to provide the equivalent of 2.5 ppm sweep width in the  $^1\text{H}$  NMR frequency dimension. NS=64 for each  $^{13}\text{C}$  NMR spectrum. The processed 2D NMR spectrum yielded correlation “peaks” between carbons and protons bonded directly to each other. There was a limited utility to this experiment since most of the proton signals attached to saturated carbons are insufficiently separated from each other. The one exception was the allylic proton signals which were well separated from other saturated proton signals. Analysis of the  $^{13}\text{C}$ - $^1\text{H}$  shift correlated 2D NMR spectrum yielded assignments for the allylic carbons.

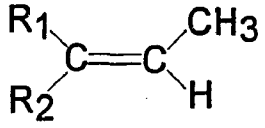
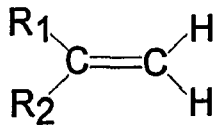
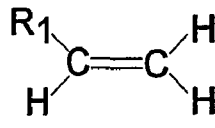
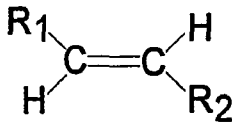
### 2.3 NMR Chemical shift determination

#### 2.3.1 $^1\text{H}$ NMR chemical shift

$^1\text{H}$  NMR chemical shifts of saturated protons appear between 0.5-2.5 ppm range, depending on the chemical environments around protons. Usually methyl protons appear between 0.5-0.9 ppm, methylene and methine protons appear between 0.9-2.0 ppm.

$^1\text{H}$  NMR chemical shifts of double bond protons usually appear between 4.0-6.0 ppm range. The studies on model alkene compounds provide a detailed chemical shift placements of different types of double bond protons. The terminologies used for double bond types are: vinyl for  $\text{CH}_2=\text{CHR}$ , vinylidene for  $\text{CH}_2=\text{CR}_1\text{R}_2$ , vinylene for  $\text{R}_1\text{CH}=\text{CHR}_2$ , trisubstituted for  $\text{R}_1\text{CH}=\text{CR}_2\text{R}_3$ , and tetrasubstituted for  $\text{R}_1\text{R}_2\text{C}=\text{CR}_3\text{R}_4$ . Table 1 shows the detailed chemical shift range for different types of double bond protons.

Table 1  $^1\text{H}$  Chemical Shifts of Double Bonds

<u>Structure</u>	<u><math>^1\text{H}</math> Chemical Shift</u>	<u>Multiplicity*</u>
 $\begin{array}{c} \text{R}_1 \quad \text{CH}_3 \\ \diagdown \quad / \\ \text{C} = \text{C} \\ / \quad \diagdown \\ \text{R}_2 \quad \text{H} \end{array}$	5.18 ppm	quartet <sup>(1)</sup>
 $\begin{array}{c} \text{R}_1 \quad \text{H} \\ \diagdown \quad / \\ \text{C} = \text{C} \\ / \quad \diagdown \\ \text{R}_2 \quad \text{H} \end{array}$	4.88, 4.66 ppm	doublet <sup>(2)</sup>
 $\begin{array}{c} \text{R}_1 \quad \text{H} \\ \diagdown \quad / \\ \text{C} = \text{C} \\ / \quad \diagdown \\ \text{H} \quad \text{H} \end{array}$	5.88, 4.92 ppm	triplet, doublet <sup>(3)</sup>
 $\begin{array}{c} \text{R}_1 \quad \text{H} \\ \diagdown \quad / \\ \text{C} = \text{C} \\ / \quad \diagdown \\ \text{H} \quad \text{R}_2 \end{array}$	5.39 ppm	doublets <sup>(4)</sup>

(1) If considering only splitting by germinal  $-\text{CH}_3$  protons; the multiplicity is complicated if also considering the splitting by  $\text{R}_1$  and  $\text{R}_2$ .

(2) Singlets if  $\text{R}_1 = \text{R}_2$ ; each single peak can also be split by  $\text{R}_1$  and  $\text{R}_2$ .

(3) The triplet and doublet can also be split into more complicated patterns if considering  $\text{R}_1$ .

(4) The doublet may also be split by  $\text{R}_1$  and  $\text{R}_2$ .

\* The multiplicity shown in the Table is caused only by double bond protons, the splitting by  $\text{R}_1$  and  $\text{R}_2$  alkyl protons can usually be neglected.

### 2.3.2 $^{13}\text{C}$ NMR chemical shift of double bond

The double bond carbon atoms of alkenes substituted only by alkyl groups show absorption in the range of about 105-155 ppm downfield from TMS. In general, the terminal  $=\text{CH}_2$  group absorbs upfield from an internal  $=\text{CH}-$  group, and cis  $-\text{CH}=\text{CH}-$  signals are upfield from those of corresponding trans groups. Calculations of approximate chemical shifts for double bond carbons can be made with following equation:<sup>(46-47)</sup>

$$\delta(\text{K}) = 123.3 + \sum A_{\text{KJ}}(\text{R}_\text{J}) + \sum A_{\text{KJ}'}(\text{R}_{\text{J}'})$$

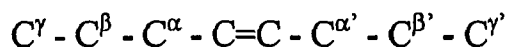
where  $\delta(\text{K})$  = chemical shift of carbon K

$\text{R}_\text{J}$  = substituent at position J

$\text{R}_{\text{J}'}$  = substituent at position J' across double bond

$A_{\text{KJ}}, A_{\text{KJ}'}$  = substituent parameters

Substituent parameters are given below:



$$\alpha = 10.6 \quad \beta = 7.2 \quad \gamma = -1.5$$

$$\alpha' = -7.9 \quad \beta' = -1.8 \quad \gamma' = 1.5$$

$$\alpha, \alpha' (\text{trans}) = 0 \quad \alpha, \alpha' (\text{cis}) = -1.1$$

$$\alpha, \alpha = -4.8 \quad \alpha', \alpha' = 2.5 \quad \beta, \beta = -2.3 \quad \gamma, \gamma = -0.85$$

Model compounds<sup>(48)</sup> are used to verify the calculations and assignments.

### 2.3.3 $^{13}\text{C}$ NMR chemical shift of saturated carbon

The saturated carbon atoms of alkanes (linear and branched) substituted only by alkyl groups show absorption in the range of about 0-50 ppm downfield from TMS except methane (-2.3 ppm from TMS). Calculations of

chemical shifts for saturated carbons can be made with following equation:<sup>(46-47)</sup>

$$\delta_C(k) = -2.97 + \sum n_{kl} A_l$$

where:  $\delta_C(K)$  is the carbon chemical shift value of the kth carbon atom,  $n_{kl}$  is the number of carbon atoms in the lth position relative to the kth carbon atom, and  $A_{kl}$  is the additive chemical shift parameter assigned to the lth carbon atom.

The empirical parameters are given by Grant and Paul<sup>(49)</sup> in Table 2. Model compounds<sup>(48)</sup> are used to verify the calculations and assignments.

#### 2.3.4 $^{13}\text{C}$ NMR chemical shift of different configurations

The Grant and Paul parameters can be used to calculate only the  $^{13}\text{C}$  NMR chemical shifts without stereospecific concern. In order to distinguish different stereospecific carbons, the so called  $\gamma$ -effect and Suter-Flory rotational isomeric model have to be taken into account as corrective terms in the calculations. Asakura et al<sup>(50-51)</sup> calculated chemical shifts for diastereomers of 2,4,6,8,10,12,14,16,18-nonaethylnonadecane (NEND), in which the methylene  $\text{C}_9$  and methine  $\text{C}_{10}$  of the backbone chain and methylene  $\text{C}_{10}$  and methyl  $\text{C}_{10}$  of the side chain serve as models of  $\underline{\text{C}}\text{H}_2$  (backbone),  $\underline{\text{C}}\text{H}$ ,  $\underline{\text{C}}\text{H}_2$  (side chain), and  $\underline{\text{C}}\text{H}_3$  of poly(1-butene), respectively. The  $\gamma$ -effect and Suter-Flory rotational isomeric model were used in their calculations and the calculated results agree well with actual chemical shifts obtained from model compounds and poly(1-butene) samples. Table 3 summarizes chemical shifts calculated for the  $\text{C}_{10}$  methylene side chain carbons of model NEND and those observed for the methylene side chain carbons of isotactic poly(1-butene).

Table 2 Empirical parameters by Grant and Paul

Carbon position	$A_1$	Corrective term	Coefficient (ppm)
$\alpha$	9.09	1°(3°)	-1.12
$\beta$	9.40	1°(4°)	-3.37
$\gamma$	-2.49	2°(3°)	-2.50
$\delta$	0.31	2°(4°)	-7.23
$\varepsilon$	0.11	3°(2°)	-3.65
		3°(3°)	-9.47
		4°(1°)	-1.50
		4°(2°)	-8.36

Table 3 Calculated and Observed  
Methylene Side Chain Carbon Chemical Shifts

Stereoisomer	Calcd <sup>a</sup>	NEND	PB
		obsd	obsd
m(mmmm)m	0.0	0.0	0.0
m(mmmm)r	0.0		
r(mmmm)r	-0.103		
m(mmmr)m	-0.159		
m(mmmr)r	-0.159		
r(mmmr)m	-0.258	-0.209	-0.19
r(mmmm)r	-0.261		
r(rmmr)r	-0.328		
m(rmmr)r	-0.416	-0.387	-0.39
m(rmmr)m	-0.416		
m(mmrm)m	-0.528		
m(mmrm)r	-0.528		
r(mmrm)r	-0.547	-0.557	-0.54
r(mmrm)m	-0.623		
r(rmrr)m	-0.575		
r(rmrr)r	-0.655		
m(rmrr)r	-0.655	-0.637	-0.61
m(rmrr)m	-0.655		
r(mrmr)r	-0.702		
m(mrmr)r	-0.789		
m(mrmr)m	-0.789	-0.769	-0.80 <sup>b</sup>
r(mrmr)m	-0.795		

Table 3(continued)

m(rrrr)m	-0.835		
m(rrrr)r	-0.914	-0.888	-0.99
r(rrrr)r	-0.914		
r(mrrr)m	-0.972		
r(mrrrr)r	-1.053		
m(mrrr)r	-1.053	-1.034	-1.09
m(mrrr)m	-1.058		
r(mrrm)r	-1.115		
m(mrrm)r	-1.115	-1.145	-1.23
m(mrrm)m	-1.206		

<sup>a</sup> Pentad chemical shifts were obtained by averaging over the heptad peaks.

<sup>b</sup>This peak is broad.

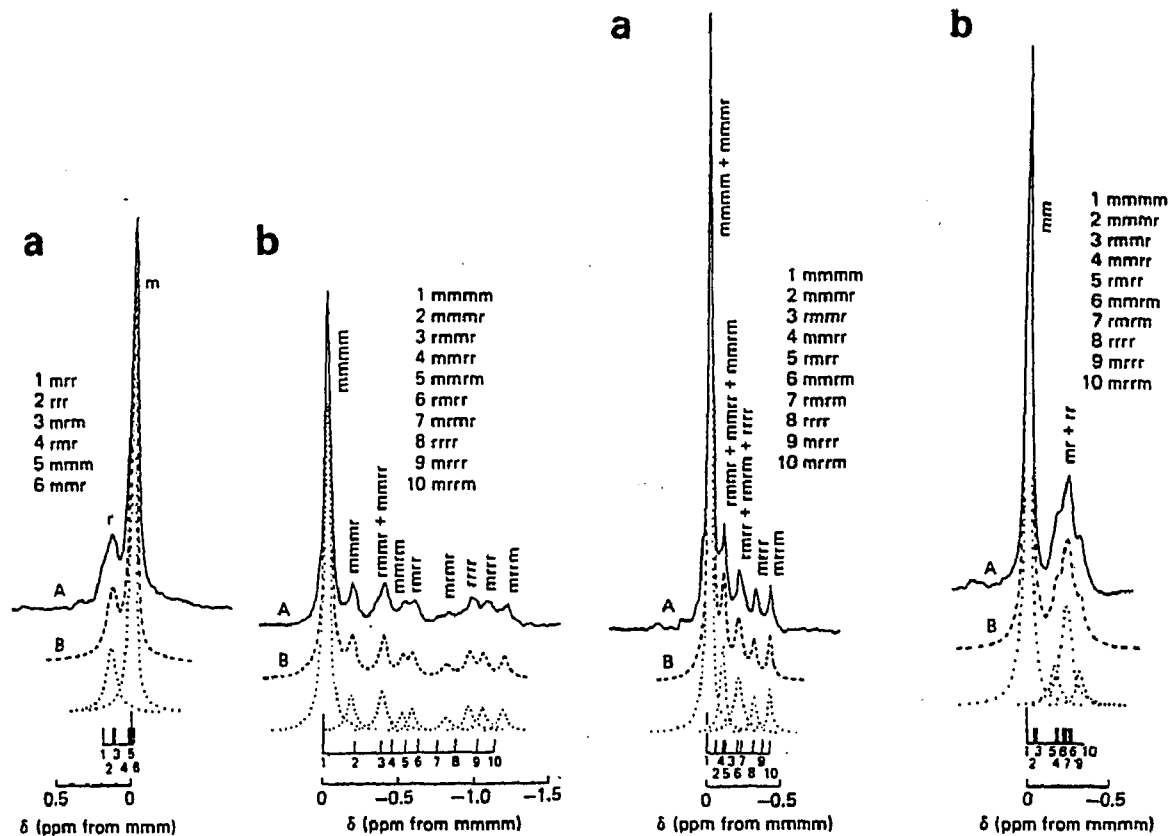


Figure 1  $^{13}\text{C}$  n.m.r. spectra of methylene carbon of the backbone (a) and the side chain (b) of PB: A, observed spectrum; B, simulated spectra assuming Lorentzian. The stick spectrum calculated theoretically is also included<sup>a</sup>

Figure 2  $^{13}\text{C}$  n.m.r. spectra of methyl carbon of the side chain (a) and methine carbon of the backbone chain (b) of PB: A, observed spectrum; B, simulated spectra assuming Lorentzian. The stick spectrum calculated theoretically is also included

Table 1 Analysis of  $^{13}\text{C}$  n.m.r. data of poly(1-butene). Dyad: m 0.753, r 0.247; triad: mm 0.669, mr 0.188, rr 0.143

Pentad	Observed	Bernoulli trial <sup>a</sup>	Error	First-order Markov <sup>b</sup>	Error	Second-order Markov <sup>c</sup>	Error	Bicatalytic sites model <sup>d</sup>	Error
m m m m m	0.583	0.321	0.262	0.514	0.069	0.580	0.003	0.585	-0.002
m m m m r	0.079	0.211	-0.132	0.145	-0.066	0.097	-0.018	0.079	0.000
m m m r r	0.007	0.035	-0.028	0.007	0.000	0.004	-0.003	0.019	-0.012
m m r m m	0.036	0.211	-0.175	0.065	-0.029	0.038	-0.002	0.032	0.004
m m r r r	0.078	0.069	0.009	0.099	-0.021	0.070	0.008	0.085	-0.007
m r m m m	0.032	0.069	-0.037	0.009	0.023	0.027	0.005	0.038	-0.006
m r m m r	0.042	0.023	0.019	0.065	-0.023	0.050	-0.008	0.046	-0.004
m r m r m	0.043	0.035	0.008	0.022	0.021	0.028	0.015	0.042	0.001
m r r r r	0.045	0.023	0.022	0.068	-0.023	0.069	-0.024	0.046	-0.001
r r r r r	0.055	0.004	0.051	0.052	0.003	0.043	0.012	0.054	0.001
$s^e$			0.117		0.037		0.013		0.005

<sup>a</sup>  $4mrrr/(mr)^2 = 10.9$ ,  $P_m = 0.753$

<sup>b</sup>  $P(m/r) = 0.123$ ,  $P(r/m) = 0.359$

<sup>c</sup>  $P_{mm}/m = 0.931$ ,  $P_{mr}/m = 0.362$ ,  $P_{rm}/m = 0.553$ ,  $P_{rr}/m = 0.441$

<sup>d</sup>  $\alpha = 0.041$ ,  $\sigma = 0.453$ ,  $\omega = 0.705$

<sup>e</sup> Standard deviation

Figure 1 Observed and simulated spectra of poly(1-butene)

Of the four carbon atoms in poly(1-butene) repeat unit, the side chain methylene is most sensitive to the tacticity variations of the polymer chain with the side chain methyl carbon being second sensitive. The backbone methylene and methine carbon atoms can also tell the tacticity variations in some extent. Figure 1 illustrates the observed and simulated  $^{13}\text{C}$  NMR spectra of poly(1-butene) obtained by Asakura et al.

## 2.4 Molecular weight analysis

### 2.4.1 SEC measurement

Molecular weight analysis by size exclusion chromatography (SEC) was performed at 40 °C using a Water 150C GPC instrument, THF as the mobile phase, a set of four ultrastyrigel columns ( $10^6$ ,  $10^5$ ,  $10^4$  and  $10^3$  Angstroms) as the stationary phase. The running conditions are flow rate 1ml/min, 2 hrs initial delay, 5 min delay between each sample injection, 60 min running time for each sample, 100 ul and 200 ul injection volumes for standard and polymer samples respectively. Narrow molecular weight polystyrene samples were used as calibration standards.

### 2.4.2 VPO measurement

Vapor pressure osmometry (VPO) was performed using a Jupiter instrument with toluene as solvent at 50 °C. A set of succrose octaacetate solutions with different concentrations were used to calibrate the VPO instrument.

### 2.4.3 $^1\text{H}$ and $^{13}\text{C}$ NMR analysis of molecular weight

In  $^1\text{H}$  NMR spectra, olefin proton signals appear between 4.0-6.0 ppm, and aliphatic proton signals appear between 0.5-2.0 ppm. It is assumed that each polymer chain contains only one unsaturated(double bond) end group,

and there is no tetrasubstituted double bond as end group (for  $^1\text{H}$  analysis). A comparison of the aliphatic to olefin areas in the proton spectrum gives a measure of the number-average molecular weight. The calculation assumes that each carbon on the chain can be represented as a  $\text{CH}_2$  unit, with a molecular weight of 14 units. The mass of the extra proton on the methyl groups of the butene monomers balances the methine group to which the branch is attached. Therefore, the molecular weight can be expressed as:

$$M_n = \{(\text{aliphatic area}) / [(2)(\text{area of one proton})]\} (14.027) + 26.028$$

where:  $(\text{area of one proton}) = (1/2)[(\text{area of } \text{CH}_2=\text{C}<) + (\text{area of } -\text{CH}=\text{CH}-) + (2/3)(\text{area of } \text{CH}_2=\text{CH}-) + (2)(\text{area of } -\text{CH}=\text{C}<)]$

Further corrections can be made for the contribution of aliphatic protons on the olefin end groups made in the upfield region of the spectrum. But these are insignificant above molecular weight of 2000. In our molecular weight analysis by  $^1\text{H}$  NMR, the effects of aliphatic protons on molecular weight were taken into account.

In  $^{13}\text{C}$  NMR spectra, olefin carbon signals appear between 105-155 ppm, and aliphatic carbon signals appear between 0-50 ppm. Based on the assumption that each polymer chain contains only one unsaturated (double bond) end group, the number average molecular weight can also be calculated from a comparison of the aliphatic and olefin areas in  $^{13}\text{C}$  NMR spectrum. Since all but two carbons are aliphatic, the molecular weight can be expressed in the terms of the number of methylene units:

$$M_n = [(\text{aliphatic area}) / (\text{olefin area})] (14.027) + 26.038$$

### 3.0 Results and Discussion on Experimental Methods

#### 3.1 Comparison of polymer sample work-up procedures

Three work-up procedures, EVAP, DEASH and NVM were evaluated by  $^1\text{H}$  NMR analysis of the double bond content. The vinylene, trisubstituted, vinyl, and vinylidene double bond contents were obtained from the proton signals at 5.50-5.33, 5.33-5.10, 5.10-4.80, and 4.80-4.60 ppm, respectively. Figures 2-5 show the 400 MHz  $^1\text{H}$  NMR spectra in the double bond region for the Crude, Evap, Deash, and NVM samples, respectively. Table 4 shows the results as the area for each of the double bonds relative to the signal area for all single bond protons (0.4-2.5 ppm) where the latter is set at 100. Table 4 also shows calculations for the total double bond signal area relative to the single bond signal area and the percent composition of the four double bond types. These calculations involve two corrections in order to place counting of the four different double bonds on an equivalent basis. First, only the  $\text{CH}_2$ =signal area of the vinyl ( $\text{CH}_2\text{CHR}$ ) double bond is used. Second, the signal area for the trisubstituted double bond proton is multiplied by two.

The most significant results of the comparison of work-up procedures are the differences in vinylidene content. About 20% of the vinylidene content of the crude sample, probably a volatile oligomer fraction, is lost through the Evap and Deash procedures. An additional 10% lowering of the vinylidene content is observed when the NVM procedure is compared to the Evap and Deash procedures. This probably occurs through thermal polymerization of double bond end groups at high temperature (125 °C) of the NVM procedure. There is no significant difference between the Evap and

Deash procedures. There is also no significant difference between evaporation of solvent at room temperature and 45 °C.

It is easy to read too much into the results in Table 4. For example, the % vinyl double bond looks to be decreased by the Evap and Deash procedures. However, the signal areas for any of the double bond protons are probably not more accurate than plus or minus 0.005-0.01 area units relative to 100 units for the single bond proton region. This relative error is seen when one looks at some of the duplicate NMR analyses in Table 4 or by visual comparison of the small signal area regions in Figures 2-5. Within this limit of 0.005-0.01 area units there are no changes in the vinylene, trisubstituted, and vinyl double bond contents when the crude sample is subjected to the Evap, Deash, and NVM work-up procedures. This analytical limit means that changes of 25-50 % in the vinylene and vinyl contents and changes of 5-10% in the trisubstituted content are not detectable using  $^1\text{H}$  NMR analysis.

After the comparison of different polymer sample treatment procedures, we have chosen the EVAP/45 procedure as the standard procedure for work-up of all crude polymer samples prior to any analysis, because this sample treatment procedure guarantees the complete removal of solvent and very low molecular weight components contained in polymer samples. All the work described in this thesis was performed on polymer samples processed by the EVAP/45 procedure.

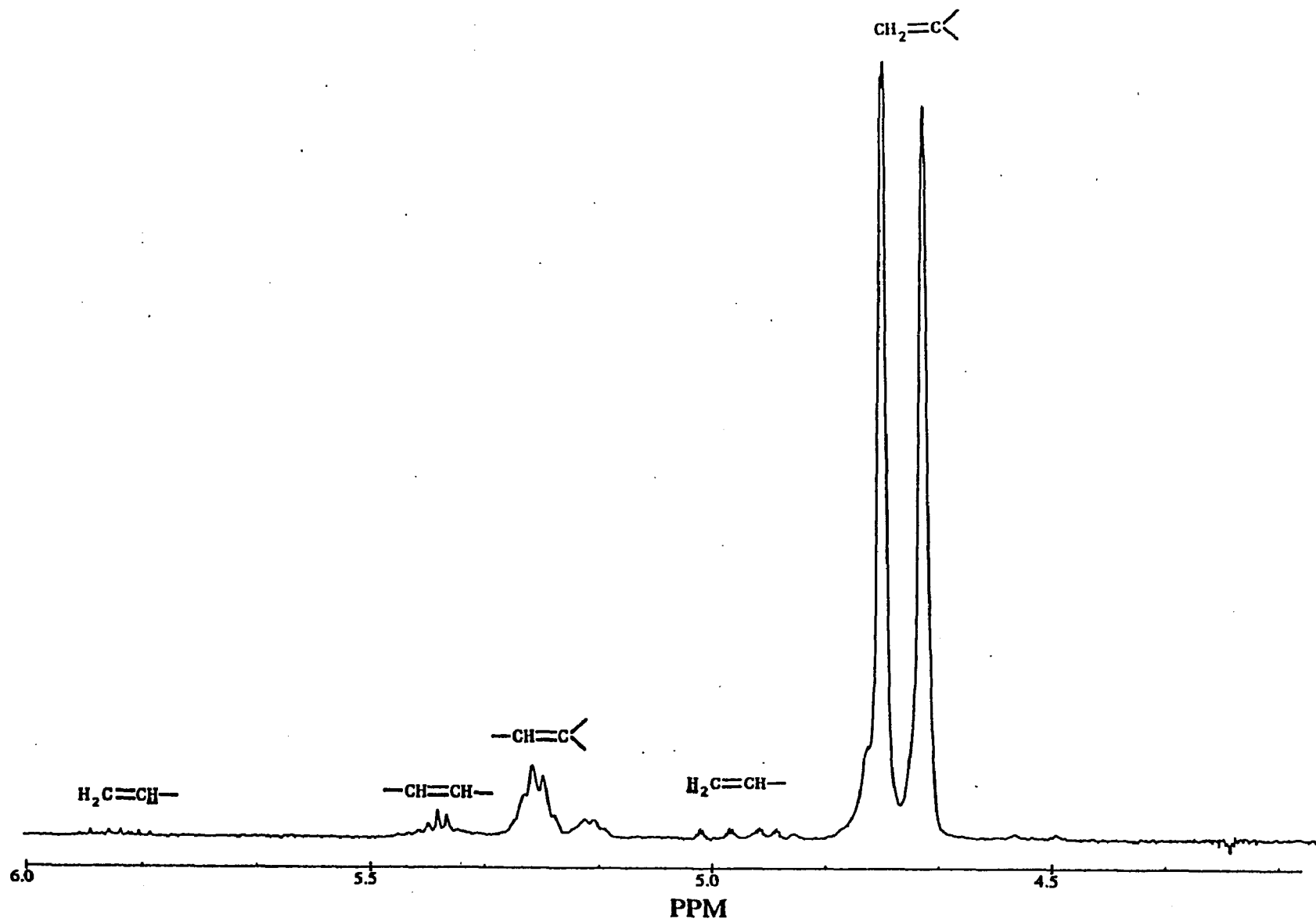


Figure 2  $^1\text{H}$  NMR double bond region of crude poly(1-butene)

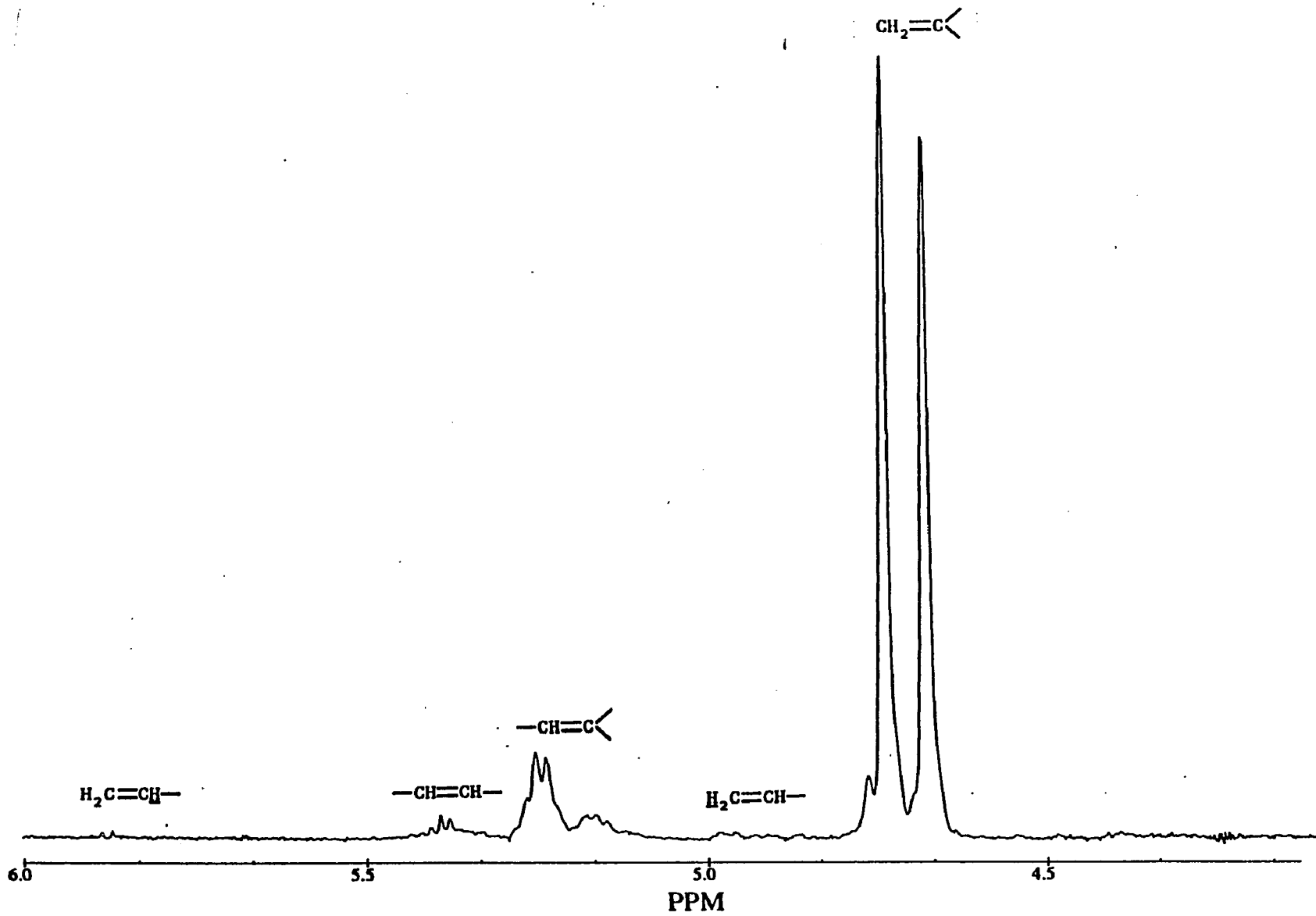


Figure 3  $^1\text{H}$  NMR double bond region of EVAP poly(1-butene)

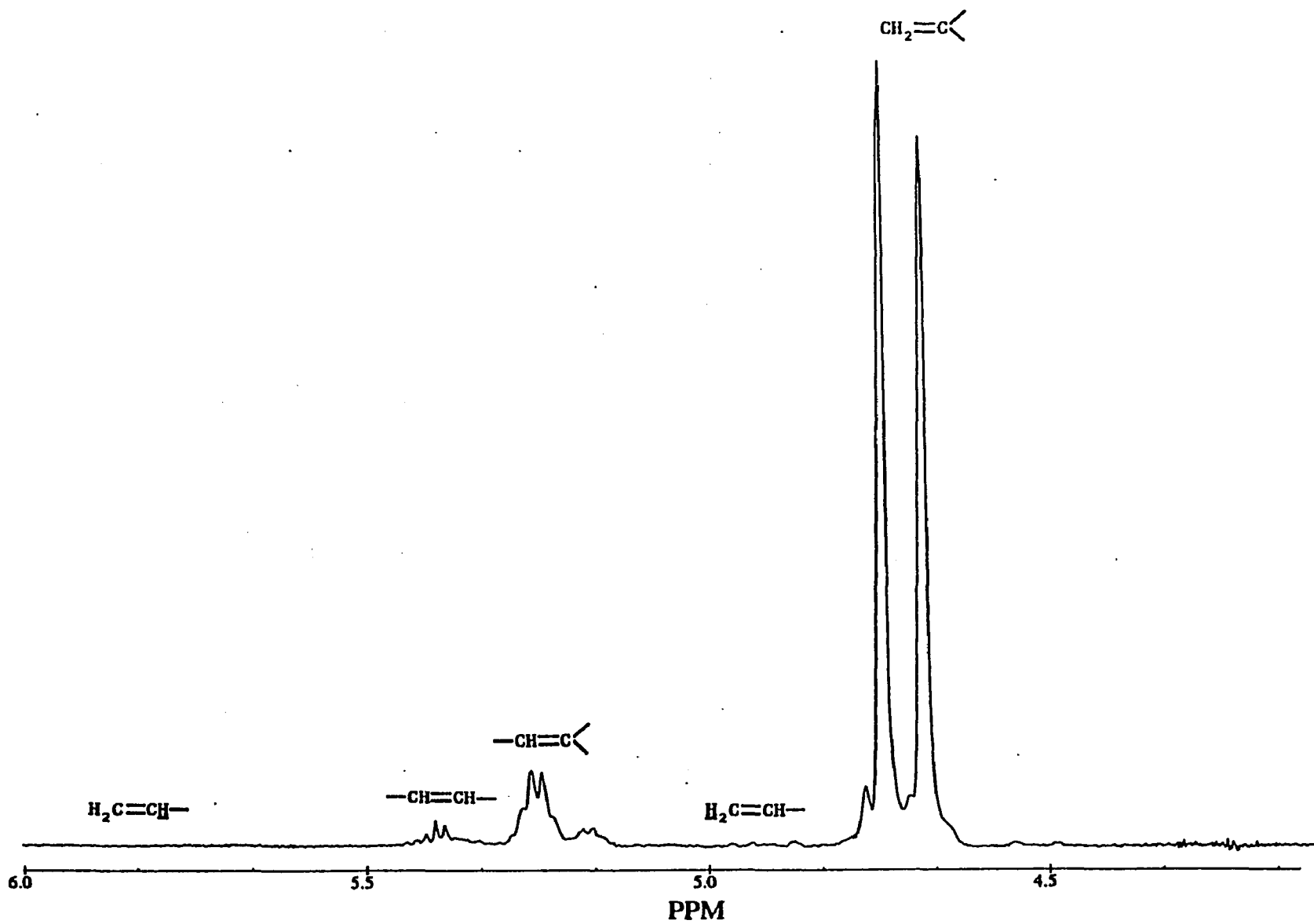


Figure 4  $^1\text{H}$  NMR double bond region of DEASH poly(1-butene)

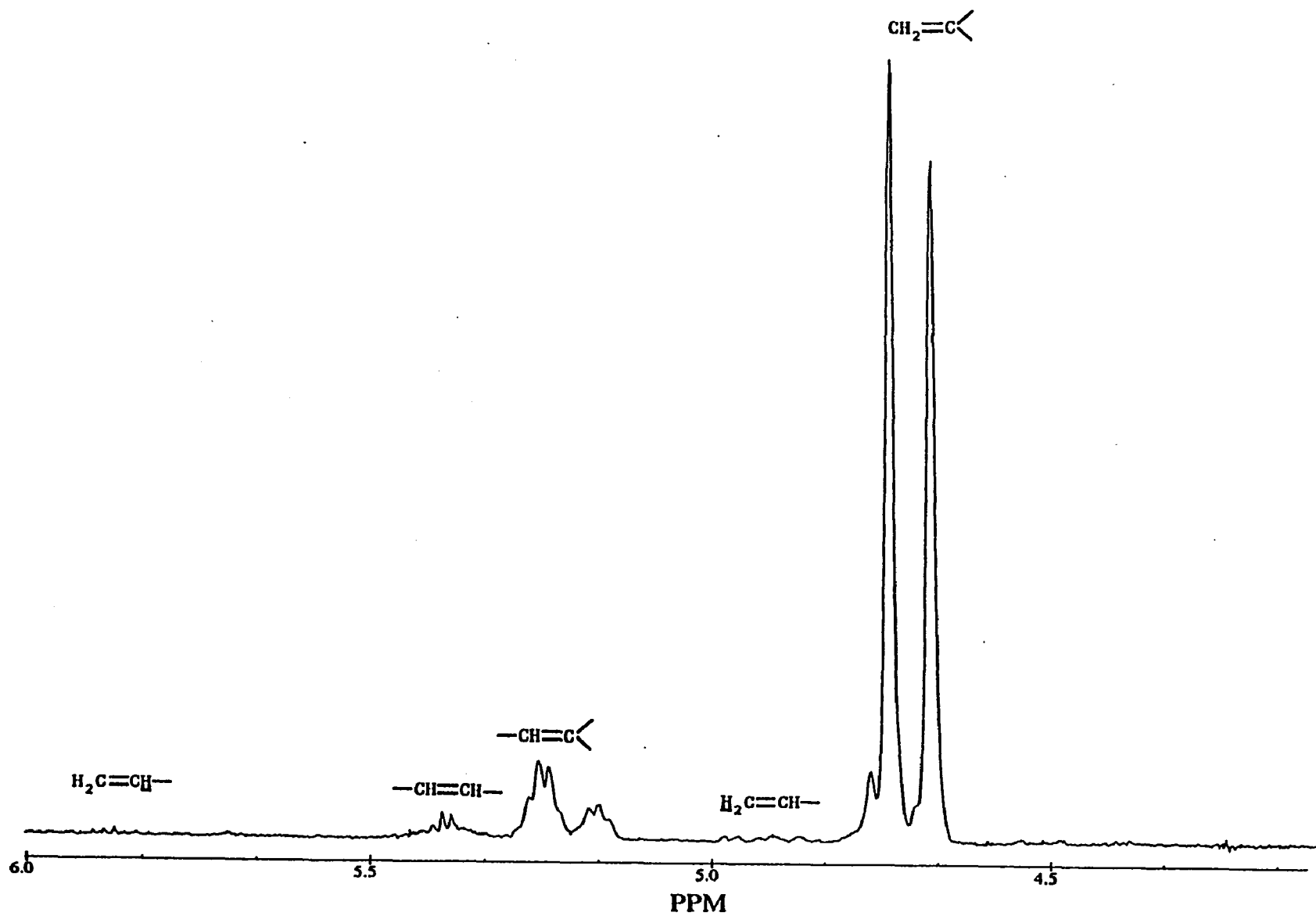


Figure 5  $^1\text{H}$  NMR double bond region of NVM poly(1-butene)

Table 4 Effect of Work-Up Procedures on Double bond  
Content of Poly(1-butene)

Signal Areas and Relative Percentages of Double Bonds From $^1\text{H}$ NMR					
	$\text{R}_1\text{CH}=\text{CHR}_2$	$\text{R}_1\text{CH}=\text{CR}_2\text{R}_3$	$\text{CH}_2=\text{CHR}$	$\text{CH}_2=\text{CR}_1\text{R}_2$	Total C=C
$\delta(\text{ppm})$	5.50-5.33	5.33-5.10	5.10-4.80	4.80-4.60	
Crude	0.016 <sup>a</sup> (2.1) <sup>b</sup>	0.070 (18.4)	0.014 (1.8)	0.59 (77.7)	0.76
Crude	0.018 (2.3)	0.082 (21.0)	0.010 (1.3)	0.59 (75.4)	0.78
Crude	0.020 (2.6)	0.083 (21.4)	0.010 (1.3)	0.58 (74.7)	0.78
EVAP/RT	0.016 (2.5)	0.077 (24.3)	0.0060 (0.9)	0.46 (72.3)	0.64
EVAP/45	0.018 (2.8)	0.087 (26.9)	0.0040 (0.6)	0.45 (69.7)	0.65
EVAP/45	0.022 (3.3)	0.087 (26.0)	0.0020 (0.3)	0.47 (70.4)	0.67
Deash/RT	0.022 (3.2)	0.090 (26.2)	0.0040 (0.6)	0.48 (70.0)	0.69
Deash/45	0.022 (3.2)	0.090 (26.2)	0.0050 (0.7)	0.48 (70.0)	0.69
Deash/45	0.020 (2.8)	0.087 (24.7)	0.011 (1.6)	0.50 (70.9)	0.71
NVM	0.020 (3.1)	0.090 (28.1)	0.020 (3.1)	0.42 (65.6)	0.64
NVM	0.021 (3.3)	0.087 (27.8)	0.012 (1.9)	0.42 (67.0)	0.63

<sup>a</sup> Double bond proton signal areas are relative to single bond proton area(0.4-2.5) set at 100. <sup>b</sup> Numbers in parentheses are the percentages of different double bonds relative to total of all double bonds.

### 3.2 Quantitative conditions for NMR analysis

The quantitative conditions for  $^1\text{H}$  NMR analysis were determined by our studies on both model olefin compounds and poly(1-butene). The sample and running conditions for  $^1\text{H}$  NMR acquisition listed in the experimental section satisfy our quantitation requirements if a good uniformity of magnetic field (which gives very symmetric peak and TMS line width of less than 1.0 Hz) is achieved and line broadening of 0.3 is applied.

There are a number of considerations that must be addressed when acquiring quantitative  $^{13}\text{C}$  NMR spectra. These include different spin-lattice relaxation time and unequal Nuclear Overhauser Enhancements (NOE) of different types of carbons, line widths, spectral overlap.<sup>(52-54)</sup>

It is well known that for  $90^\circ$  pulse angles, a pulse delay of  $5T_1$  is needed to ensure that 99% of rf excited nuclei will be fully relaxed between pulses. Such pulse delay is essential to obtain reliable quantitative results. Some of the carbon nuclei in poly( $\alpha$ -olefin) can be as long as 10 seconds, and this would result in extraordinary long spectral acquiring time if pulse delay of  $5T_1$  has to be met. In order to obtain quantitative  $^{13}\text{C}$  NMR spectra in reasonable period of time without sacrificing S/N ratio by using lower than  $90^\circ$  pulse angles, paramagnetic relaxation reagent  $\text{Cr}(\text{AcAc})_3$  was added to shorten the carbon  $T_1$ . Previous studies recommended the addition of 15 mg/ml  $\text{Cr}(\text{AcAc})_3$  to 20%(wt/vol) NMR polymer sample solution. Nuclear Overhauser Effects can arise from energy transfer from the proton nuclear spin reservoir to the  $^{13}\text{C}$  nuclear spin reservoir during proton heteronuclear spin decoupling. It is possible for the NOE to vary among various types of polymer carbons, particularly for protonated versus nonprotonated carbons in

systems having restricted molecular mobilities. The gated proton decoupling method, which suppresses NOE, was used to preclude the possibility of differences in NOE contributions to ensure the quantitative  $^{13}\text{C}$  NMR spectral acquisition. We studied the effects of adding  $\text{Cr}(\text{AcAc})_3$  and NOE by comparing the spectra obtained with different pulse delay time(1-10 seconds) and found out that a 3 second pulse delay is good enough to obtain quantitative  $^{13}\text{C}$  NMR spectra on our polymer samples with gated proton decoupling employed. Both poly(1-butene) and model olefin compounds were used in these spectral comparison studies.

Linewidth is usually related to the sample concentration, the uniformity of the magnetic field, and also the amount of paramagnetic relaxation reagent added to NMR sample. The previous studies showed that the linewidth at half height for the methylene carbon signal of poly(ethylene) is 1.0-2.0 Hz at about 20%(wt/vol) concentration. With a good uniformity of the magnetic field(good shimming) and 15 mg/ml  $\text{Cr}(\text{AcAc})_3$  added to 20%(wt/vol) NMR sample solution, the usual line width is 3.0-4.0 Hz at half height. Our studies on the consistency of signal areas for both model olefin compounds and poly(1-butene) sample indicate that in order to obtain the best quantitative signal areas, a line broadening of 3 should be applied to the FID before the Fourier transform is performed to increase the signal-to-noise ratio. When there is severe signal overlapping in the spectrum, a line broadening of 1 or less is applied in order to minimize the overlapping. For severe overlapped signals in which each signal area has to be sought out separately, deconvolution of overlapping signals by curve fitting is performed.

### 3.3 Considerations for $^{13}\text{C}$ NMR signal assignments

It is very obvious that  $^1\text{H}$  NMR signals of poly( $\alpha$ -olefins) are insufficiently resolved for analysis of saturated end groups, stereochemistry and regioselectivity due to the narrow span of  $^1\text{H}$  NMR spectra (0-2.5 ppm for saturated end groups, and 4.0-6.0 ppm for unsaturated double bond carbons). Only  $^{13}\text{C}$  NMR spectra have wide enough span (0-50 ppm for saturated carbons, and 100-160 ppm for unsaturated double bond carbons) to make the data useful for analysis of saturated end groups, stereochemistry, and regioselectivity. Analysis of unsaturated end groups used both  $^1\text{H}$  and  $^{13}\text{C}$  NMR data. The  $^1\text{H}$  NMR signal assignments are based mainly on spectra of model olefin compounds (Table 1). The  $^{13}\text{C}$  NMR signals assignments are more complicated and require many considerations. Here are the list of considerations taken for assignments of  $^{13}\text{C}$  NMR spectra of both poly(1-butene) and poly(ethylene-co-1-butene):

1. Qualitative and quantitative consistency is needed between  $^1\text{H}$  and  $^{13}\text{C}$  NMR signal assignments. For example, if a pair of signals in  $^1\text{H}$  NMR spectrum is assigned to as a vinylidene double bond end group, there must be a pair of signals in  $^{13}\text{C}$  NMR spectrum of the polymer sample which should be assigned to the same vinylidene double bond end group. In addition to the above qualitative consistency, the content of this vinylidene double bond end group obtained by both  $^1\text{H}$  and  $^{13}\text{C}$  NMR spectral analysis should be equal to each other, e.g., to also satisfy quantitative consistency.

2. Internal consistency is needed in the  $^{13}\text{C}$  NMR signal assignments, e.g., the two carbons of the same one double bond must have reasonably

equal signal areas, also the two carbons of the same repeat unit must have reasonably equal signal areas.

3. The assignments need to correlate with the DEPT  $^{13}\text{C}$  NMR spectrum, e.g, if a signal is assigned to as a methylene carbon in  $^{13}\text{C}$  NMR spectrum, the signal at the same chemical shift in  $^{13}\text{C}$  DEPT NMR( $135^\circ$   $^1\text{H}$  pulse) must appear to be a methylene type of signal by pointing downwards.

4. The observed  $^{13}\text{C}$  NMR signal chemical shifts assigned to a double bond end group were compared to calculated chemical shifts for a wide variety of double bond carbons.<sup>(46-47)</sup> Signal assignments were considered acceptable if the difference between calculated and observed chemical shifts was no greater than 2-3 ppm.

5. The observed  $^{13}\text{C}$  NMR signal chemical shifts assigned to a repeat unit had to be compared to calculated chemical shifts for a wide variety of repeat unit carbons.<sup>(46-47)</sup> The same were also done for the assignments of saturated end groups. Again assignments were considered acceptable if the difference between calculated and observed chemical shifts was less than 2-3 ppm.

6. The assignments of repeat units for poly(ethylene-*co*-1-butene) had to be confirmed by comparing the  $^{13}\text{C}$  NMR signals for different but related monomer sequences. Also the assignments had to be consistent with the signal area changes dominated by monomer composition changes in copolymers, e.g, if sample #1 has more 1-butene coporated in copolymer than sample #2, the signal assigned to BBB sequence must appear in higher intensity in  $^{13}\text{C}$  NMR spectrum of sample #1 than in that of sample #2.

7. The assignments of double bond carbon signals were aided by correlation with signal assignments for single bond carbons  $\alpha$ - and  $\beta$ - to the double bond. However, data from the single bond region is inherently limited compared to that from the double bond region because the single bond region has more signals, signals for saturated end groups and repeat units in addition to single bond carbons near double bonds. The presence of so many signals, some poorly resolved from others, makes signal assignments less fruitful. Chemical shift values for carbons near double bond were calculated using the Grant and Paul parameters followed by correction for the double bond substituent. Examination for various model compounds<sup>(48)</sup> showed a 3-4 ppm correction for 2° and 3° allylic carbons  $\alpha$ - to a double bond with about a 10 ppm correction for 4° allylic carbons. Smaller corrections were observed for single bond carbons  $\beta$ - to a double bond. In Table 5 are given calculated chemical shifts using Grant and Paul parameters<sup>(49)</sup> and actual signal chemical shifts for allylic carbons of some model compounds.<sup>(48)</sup>

Table 5. Chemical shifts for olefin model compounds

$\delta$ (calculated)	$\delta$ (found)
$\begin{array}{c} 43.1 \\ \text{CH}_2=\text{C}-\text{CH}_2-\text{CH}-\text{CH}_3 \\   \quad   \\ \text{CH}_3 \quad \text{CH}_3 \\ 19.1 \end{array}$	$\begin{array}{c} 48.0 \\ \text{CH}_2=\text{C}-\text{CH}_2-\text{CH}-\text{CH}_3 \\   \quad   \\ \text{CH}_3 \quad \text{CH}_3 \\ 22.2 \end{array}$
$\begin{array}{c} 54.6 \\ \text{CH}_2=\text{C}-\text{CH}-\text{CH}_2-\text{CH}_3 \\   \quad   \\ \text{CH}_3 \quad \text{CH}_2 \\ 17.2 \quad   \\ \quad \quad \text{CH}_3 \end{array}$	$\begin{array}{c} 51.4 \\ \text{CH}_2=\text{C}-\text{CH}-\text{CH}_2-\text{CH}_3 \\   \quad   \\ \text{CH}_3 \quad \text{CH}_2 \\ 18.1 \quad   \\ \quad \quad \text{CH}_3 \end{array}$
$\begin{array}{c} 23.5 \\ \text{CH}_2=\text{C}-\text{C}-\text{CH}_2-\text{CH}_3 \\   \quad   \quad   \\ \text{CH}_3 \quad \text{CH}_3 \quad \text{CH}_3 \\ 14.1 \quad \swarrow 31.2 \\ \quad \quad \searrow 50.2 \end{array}$	$\begin{array}{c} 26.9 \\ \text{CH}_2=\text{C}-\text{C}-\text{CH}_2-\text{CH}_3 \\   \quad   \quad   \\ \text{CH}_3 \quad \text{CH}_3 \quad \text{CH}_3 \\ 19.4 \quad \swarrow 33.5 \\ \quad \quad \searrow 39.2 \end{array}$
$\begin{array}{c} 9.8 \\ \text{CH}_2-\text{CH}=\text{C}-\text{CH}_2-\text{CH}_2-\text{CH}_3 \\   \\ \text{CH}_3 \\ 16.9 \end{array}$	$\begin{array}{c} 13.3 \\ \text{CH}_2-\text{CH}=\text{C}-\text{CH}_2-\text{CH}_2-\text{CH}_3 \\   \\ \text{CH}_3 \\ 23.4 \quad (\text{cis}) \end{array}$
	$\begin{array}{c} 13.3 \\ \text{CH}_2-\text{CH}=\text{C}-\text{CH}_2-\text{CH}_2-\text{CH}_3 \\   \\ \text{CH}_3 \\ 15.5 \quad (\text{trans}) \end{array}$
$\begin{array}{c} 19.9 \\ \text{CH}_3-\text{CH}_2-\text{CH}=\text{C}-\text{CH}_2-\text{CH}_3 \\   \\ \text{CH}_3 \\ 16.9 \end{array}$	$\begin{array}{c} 21.2 \\ \text{CH}_3-\text{CH}_2-\text{CH}=\text{C}-\text{CH}_2-\text{CH}_3 \\   \\ \text{CH}_3 \\ 22.9 \quad (\text{cis}) \end{array}$
	$\begin{array}{c} 21.3 \\ \text{CH}_3-\text{CH}_2-\text{CH}=\text{C}-\text{CH}_2-\text{CH}_3 \\   \\ \text{CH}_3 \\ 15.7 \quad (\text{trans}) \end{array}$

## 4.0 Results and Discussion on Microstructure of Poly(1-Butene)

### 4.1 Results on end groups

Most studies of end groups in metallocene-catalyzed polymerizations of  $\alpha$ -olefins have been carried out on relatively high molecular weight samples, and this placed major limits on end group analysis. End group analysis was considerably enhanced by working with a low molecular weight poly(1-butene). The poly(1-butene) was obtained by polymerization of neat 1-butene at 100 °C using  $7.1 \cdot 10^{-6}$  M dimethylsilyl-bridged  $(H_4Ind)_2ZrCl_2$  with a MAO:Zr ratio of 1000:1. The poly(1-butene) produced under these conditions contains a much wider range of double bond types than previously reported for  $\alpha$ -olefin polymerizations. Figure 6 shows the 400 MHz  $^1H$  NMR of the poly(1-butene) sample. The double bond region contains proton signals for vinylene, trisubstituted, vinyl, and vinylidene double bonds at 5.50-5.30, 5.30-5.10, 5.10-4.80, and 4.80-4.60 ppm,<sup>(46)</sup> respectively. Structural details on the various double bonds were obtained from  $^{13}C$  NMR shown in Figure 7. There are eighteen different signals, i.e., nine different double bonds detected by  $^{13}C$  NMR spectrum. Figure 8 shows the double bond region of  $^{13}C$  DEPT NMR spectrum of poly(1-butene).

#### 4.1.1 Vinylidene double bonds

The major unsaturated end groups are vinylidene revealed by both  $^1H$  and  $^{13}C$  NMR analysis.  $^1H$  and  $^{13}C$  NMR indicate 69.7% and 66.7% vinylidene, shown in Table 6 respectively.

$^1H$  NMR indicates two different vinylidene double bonds. The major vinylidene signal is a pair of doublets at 4.74 and 4.68 ppm (the splitting of each signal into doublet is barely visible). The minor vinylidene double bond

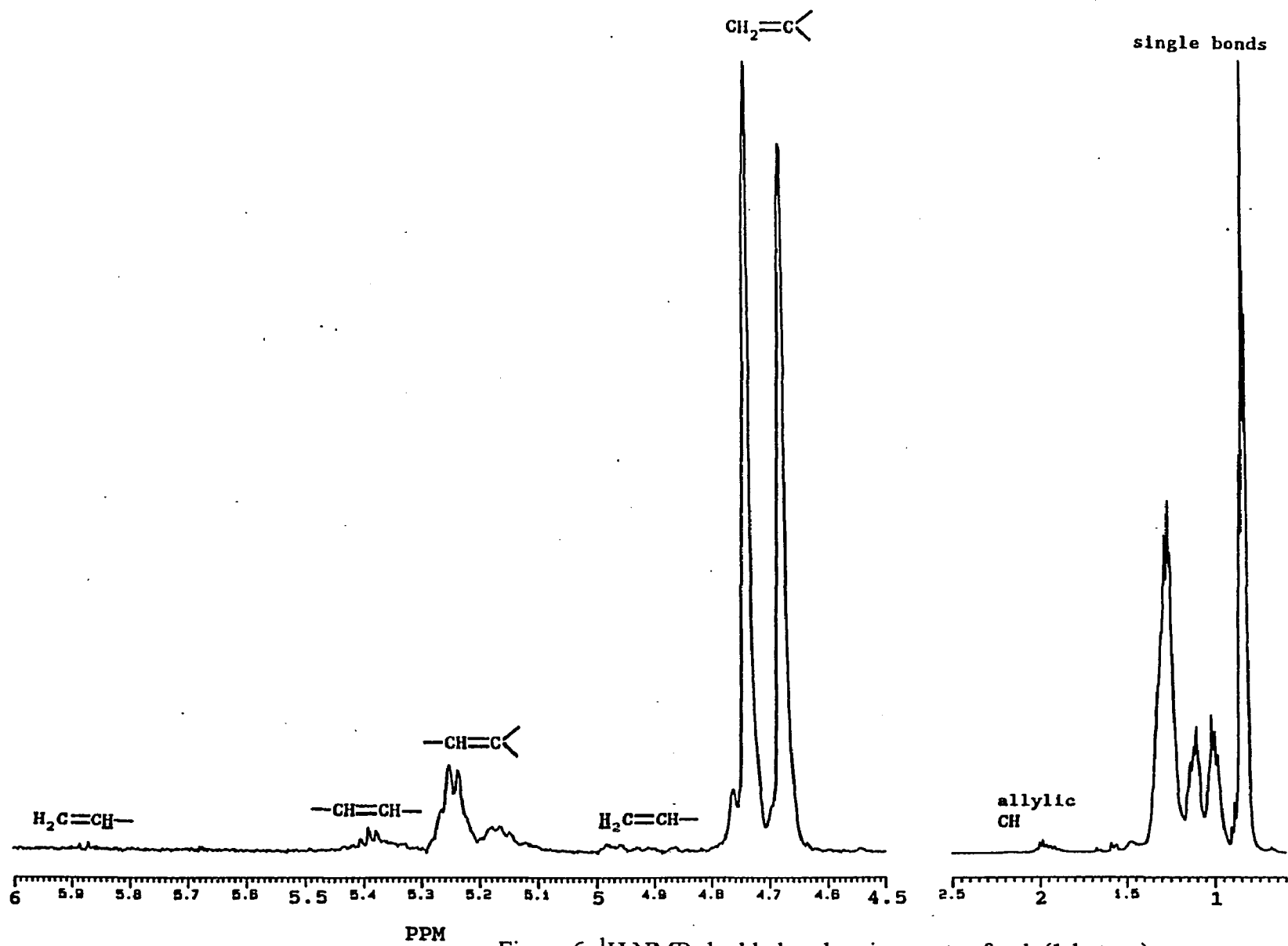


Figure 6  $^1\text{H}$  NMR double bond assignments of poly(1-butene)

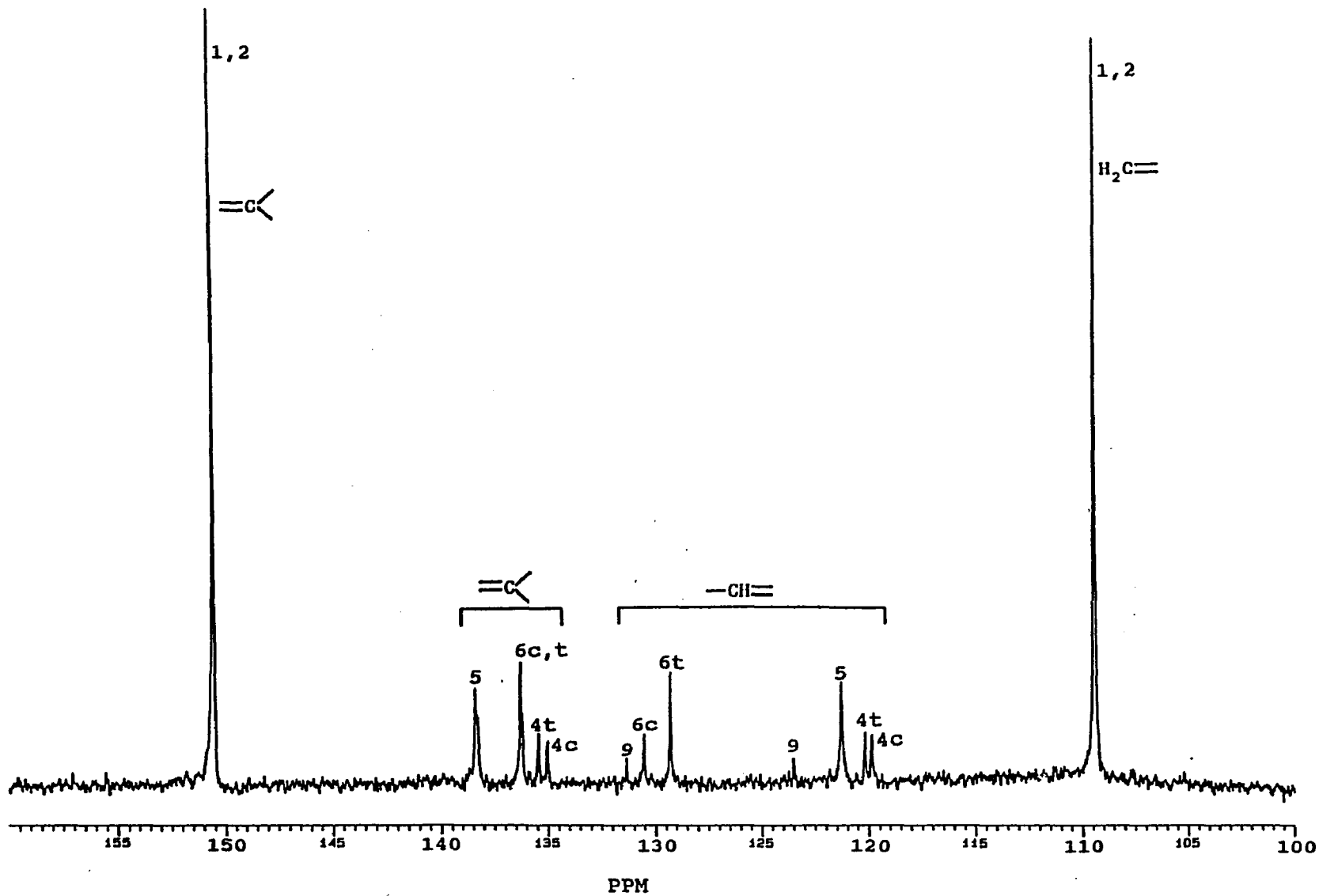


Figure 7  $^{13}\text{C}$  NMR double bond assignments of poly(1-butene)

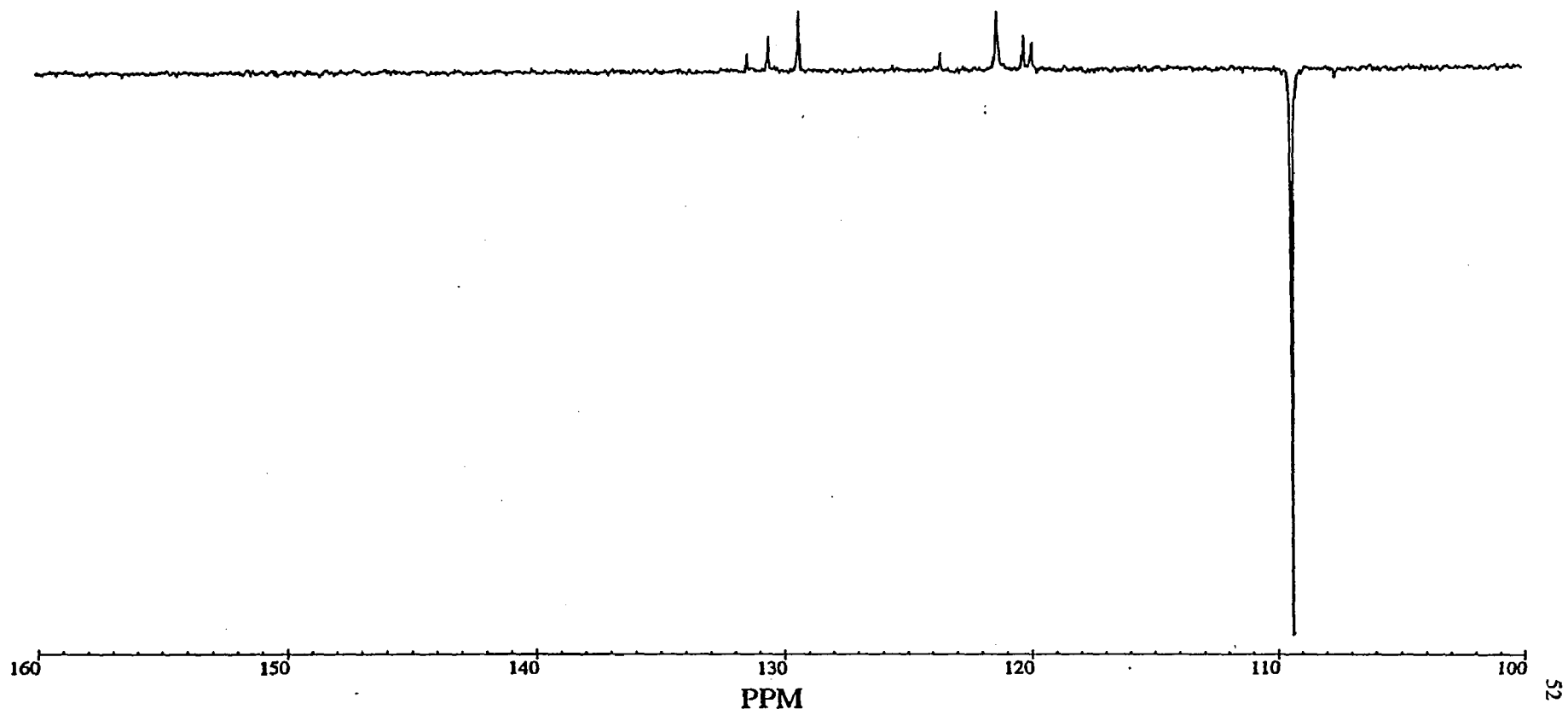
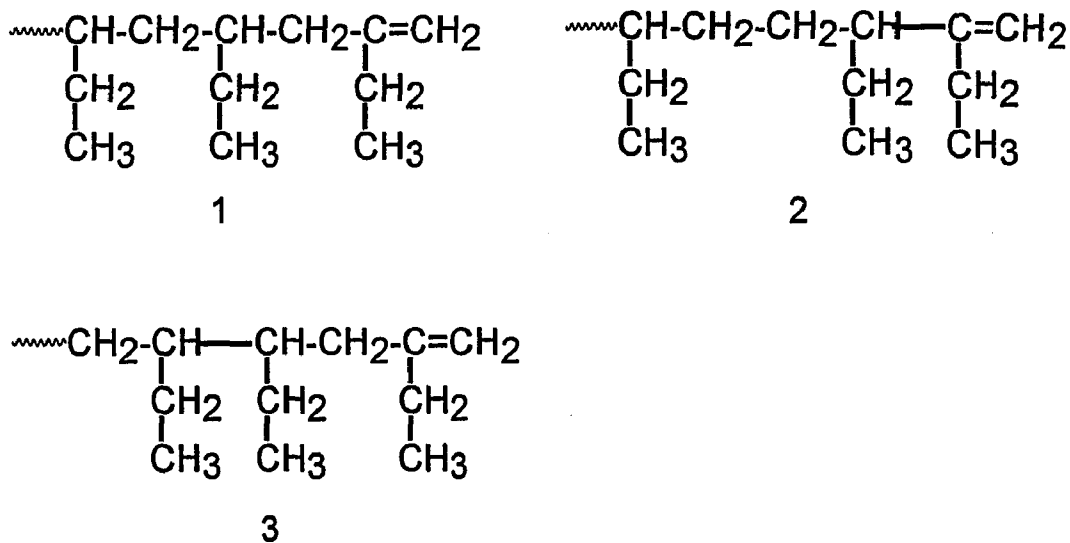


Figure 8  $^{13}\text{C}$  DEPT NMR double bond region of poly(1-butene)

signal, only partially resolved from the major vinylidene signal, is at slightly lower field- see the signal at 4.76 ppm in Figure 6. The minor vinylidene  $^1\text{H}$  NMR signal area is 3-5% of the major vinylidene signal area. That major vinylidene signal was assigned to double bond end group **1** while the minor vinylidene signal was assigned to double bond **2** and/or **3** based on mechanistic considerations( see below). **2** and **3** differ from **1** in having reverse placement of the penultimate and pen-penultimate unit, respectively.



The  $^{13}\text{C}$  NMR results verify **1** as the major double bond end group. The pair of signals at 150.5 and 109.4 ppm (Figure 7), the largest  $^{13}\text{C}$  NMR signals in the double bond region, are close to the chemical shift values (148.0 and 109.4 ppm,, respectively) calculated for **1** and the DEPT  $^{13}\text{C}$  NMR spectrum (Figure 8) shows the carbons to be  $4^\circ$  and  $2^\circ$  carbons, respectively. The  $^{13}\text{C}$  NMR single bond region supports the assignment of **1** as noted by signals at 33.7, 41.6, 28.6, and 12.4 ppm for the carbons of the penultimate unit (Figure 9). The calculated side chain and in chain allylic

Table 6 Double Bond Contents in Poly(1-butene)

Type of double bond	Percent by NMR*	
	<sup>1</sup> H	<sup>13</sup> C
H <sub>2</sub> C=CR <sub>1</sub> R <sub>2</sub>	69.7	66.7
R <sub>1</sub> CH=CR <sub>2</sub> R <sub>3</sub>	26.9	31.7
R <sub>1</sub> CH=CHR <sub>2</sub>	2.8	1.6
H <sub>2</sub> C=CHR	0.6	---

\*All percentages are within +/-5% experimental errors.

carbon chemical shift values for double bond end group 1 are 25.1 and 36.5 ppm, respectively. Considering the difference between calculated chemical shift values and actual chemical shift values for vinylidene double bond model compound, a 3-4 ppm correction should be added to the above calculated chemical shift values for 1 to make the estimated actual chemical shift values 28.1-29.1 and 39.5-40.5 ppm, respectively. Further verification for 1 came from the  $^1\text{H}$ - $^{13}\text{C}$  shift correlated 2D NMR spectrum (Figure 11) which showed crosspeaks between side chain and in chain allylic carbon signals at 28.6 and 41.6 ppm, respectively, and allylic protons at 2 ppm. No signal was observed in the  $^{13}\text{C}$  NMR for minor vinylidene end groups 2 and 3. We assume that signals for the minor vinylidene end groups are buried under the signals for the major vinylidene end groups, indicating that the major and minor vinylidene double bond end groups have very nearly the same chemical shift values. The calculated chemical shift values for the double bond carbons of 3 are exactly the same as for 1. Double bond end group 2 has very close but not exactly the same calculated chemical shift values.

#### 4.1.2 Trisubstituted double bonds

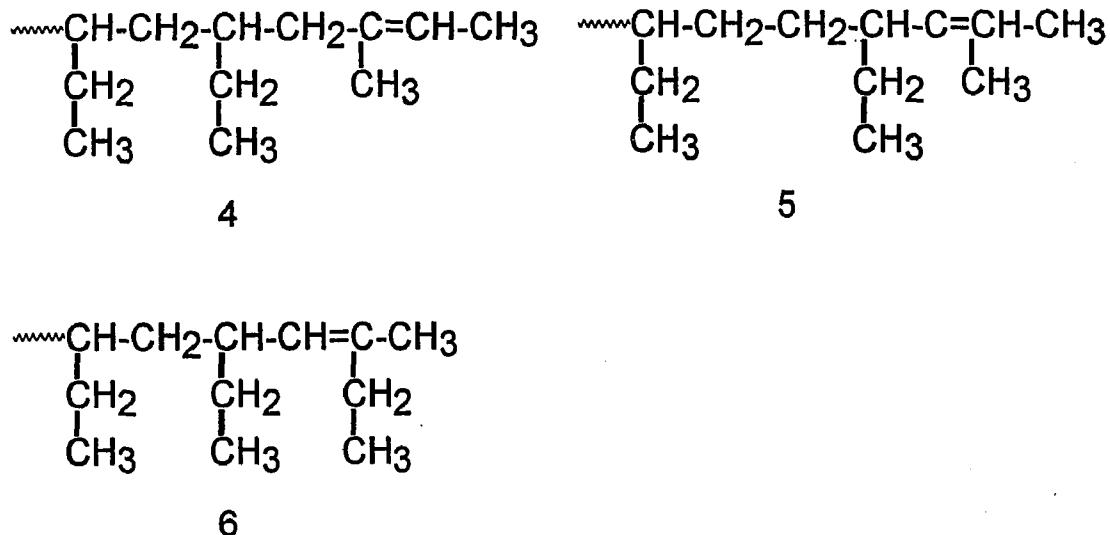
Trisubstituted double bonds are the next most abundant double bonds, 26.9% and 31.7% respectively, by  $^1\text{H}$  and  $^{13}\text{C}$  NMR (Table 6). The  $^1\text{H}$  NMR is quite complex in the region of 5.30-5.10 ppm for trisubstituted double bond protons, indicating the presence of more than one type of trisubstituted double bond. This is verified by the  $^{13}\text{C}$  NMR double bond region which shows the presence of at least five different trisubstituted double bonds. Two different sets of trisubstituted double bonds are compatible with the  $^{13}\text{C}$  NMR data:

- (1) Trisubstituted double bond end groups.

(2) Internal trisubstituted double bonds.

4, 5, and 6 are the trisubstituted double bond end groups compatible with the calculated  $^{13}\text{C}$  chemical shift values and the results of DEPT  $^{13}\text{C}$  NMR spectrum (for both single and double bond carbons). Specific signal assignments are shown in Table 7 and Figure 7 and 9.

4, 5, and 6 can each exist as cis and trans isomers but only five sets of signals are observed. The five sets of signals are assigned to a combination of 5 and cis and trans isomers of 4 and 6. The signal assigned to 5 may be for a combination of the cis and trans isomers or only the trans isomer (with signals for the cis isomer not observed due to low concentration).



The  $^{13}\text{C}$  NMR data is also compatible with the presence of internal trisubstituted doubles 7 and 8 (internal trisubstituted double bonds are located "inside" the polymer chain, not at the end of the polymer chain.). Signal assignments for 7 and 8 are shown in parentheses in Table 7. but are not noted in Figure 7. Both 7 and 8 can exist as cis and trans isomers, which

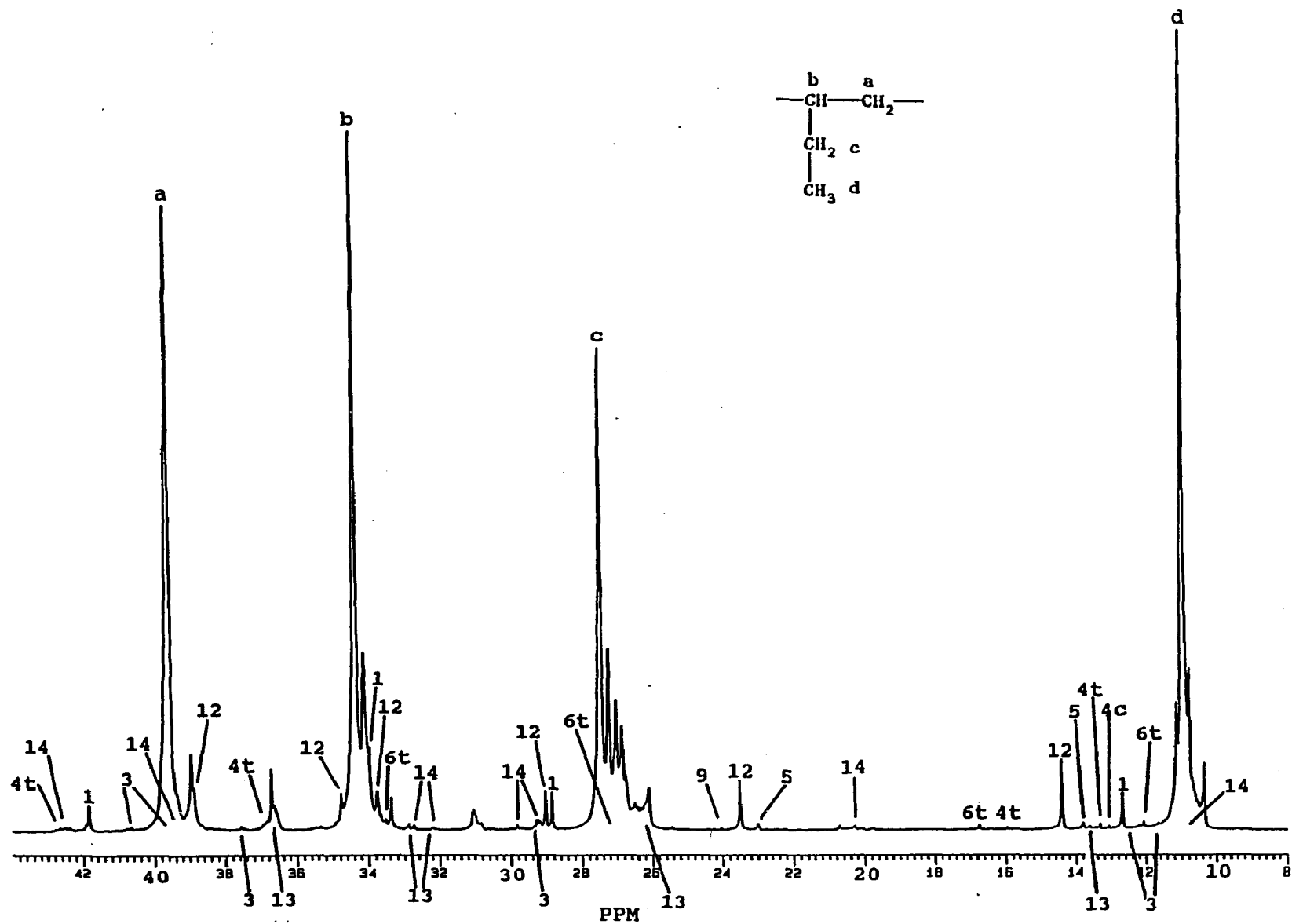
Table 7 Assignments of Double Bond  $^{13}\text{C}$  NMR Signals

$\delta(\text{ppm})$	Number Signals <sup>a</sup>	Carbon Type	Signal Area <sup>b</sup>	Assignments <sup>c</sup>
150.5	1	4 <sup>o</sup> (>C=)	100	1, 2, 3
138.3	3	4 <sup>o</sup> (>C=)	27.0	5
136.3	2	4 <sup>o</sup> (>C=)	21.5	6 <sub>t</sub>
135.5	1	4 <sup>o</sup> (>C=)	6.9	4 <sub>t</sub>
135.0	1	4 <sup>o</sup> (>C=)	4.5	4 <sub>c</sub>
131.3	1	3 <sup>o</sup> (-CH=)	2.5	9 or 10
130.5	1	3 <sup>o</sup> (-CH=)	8.2	6 <sub>c</sub>
129.3	1	3 <sup>o</sup> (-CH=)	13.5	6 <sub>t</sub>
123.5	1	3 <sup>o</sup> (-CH=)	2.6	9 or 10
121.3	1	3 <sup>o</sup> (-CH=)	16.7	5
120.2	1	3 <sup>o</sup> (-CH=)	6.0	4 <sub>t</sub>
119.9	1	3 <sup>o</sup> (-CH=)	7.1	4 <sub>c</sub>
109.4	1	2 <sup>o</sup> (H <sub>2</sub> C=)	98.9	1, 2, 3

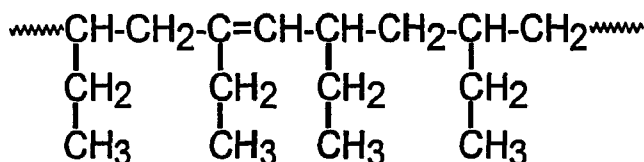
<sup>a</sup> Number of signals at that chemical shift

<sup>b</sup> Based on 100 for the signal at 150.5 ppm

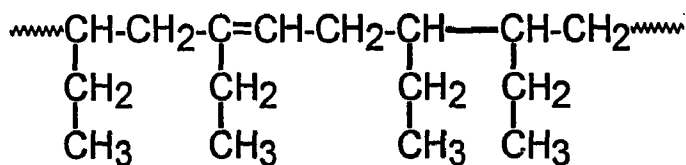
<sup>c</sup> c and t refer to cis and trans isomers



means that four of the five sets of trisubstituted double bond signals can be accounted for by internal trisubstituted double bonds. The broadest interpretation of the trisubstituted double bond region is the presence of 7 and 8 in addition to 4, 5, and 6, with *cis* and *trans* isomers of any one of these units being unresolved from each other.



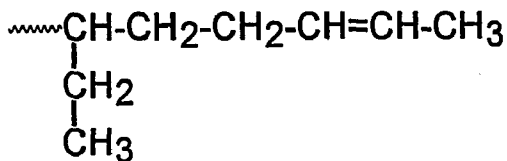
7



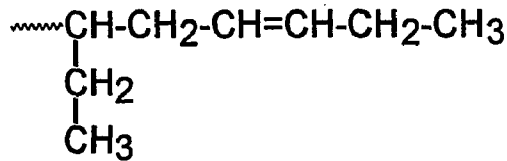
8

#### 4.1.3 Vinylene double bonds

Both  $^1\text{H}$  and  $^{13}\text{C}$  NMR indicate a small amount (2.8% and 1.6%, respectively) of vinylene end groups (Table 6). The best fit between calculated and observed  $^{13}\text{C}$  chemical shift values assigns this small pair of signals as vinylene double bond end group 9. Vinylene double bond end group 10 cannot be ruled out as an alternate to 9 although the calculated chemical shift values do not fit as well.



9



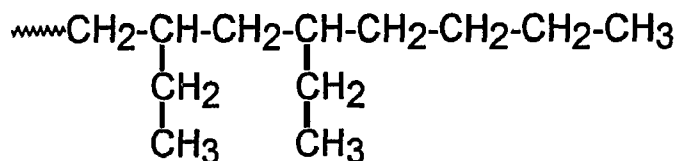
10

#### 4.1.4 Vinyl double bonds

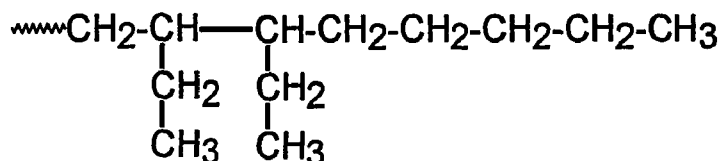
A very small amount (0.6%) of vinyl double bonds are observed by  $^1\text{H}$  NMR but not by  $^{13}\text{C}$  NMR (Table 6). The absence of vinyl signals in the  $^{13}\text{C}$  NMR is compatible with their low concentration. There is no analytical basis for assigning any specific structure for the vinyl double bond.

#### 4.1.5 Saturated end groups

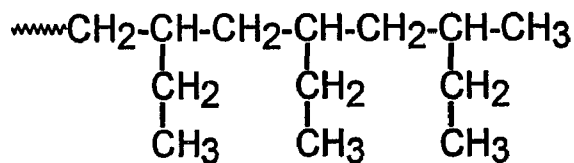
Figure 9 shows the  $^{13}\text{C}$  NMR assignments for saturated end groups, based on comparison between calculated chemical shift values and signal chemical shift values, correlations between signal areas, and the  $^{13}\text{C}$  NMR DPET spectrum shown in Figure 10.



12



13



14

The major saturated end group is **12**, referred to as a n-butyl saturated end group. **13** and **14** are minor saturated end groups. **13**, also a n-butyl saturated end group, differs from **12** in having a reverse placement of the penultimate unit. **14** is referred to as a s-butyl saturated end group. The relative amounts of the saturated end groups are in the approximate ratio of **12:13:14=18:3:2**.

#### 4.2 Results on polymer molecular weight

There was good agreement among SEC, NMR and VPO measurements of the number-average molecular weight of the poly(1-butene) sample. SEC yielded  $M_n=1910$ .  $M_n$  values of 2090 and 2020 were calculated from the  $^1\text{H}$  and  $^{13}\text{C}$  NMR data respectively, assuming an average of one double bond per polymer molecule, by comparison of the double bond and single bond region signal areas. VPO yielded  $M_n=2025$ , indicating that the assumption of one double bond per polymer molecule is valid within experimental error.

The polymer molecular weight distribution is very narrow. SEC yielded  $M_w/M_n=1.88$ , indicative of the single site nature of the zirconocene catalyst. Heterogeneous Ziegler-Natta type catalysts are multi-site and yield broader molecular weight distribution, usually with  $M_w/M_n>5$ .

#### 4.3 Results on structure of repeat unit

Analysis of the repeat unit structure involved simultaneous analysis of regioselectivity and stereoregularity. Chemical shift values for various repeat unit sequences of normal (or 1,2- or primary) and reverse (or 2,1- or secondary) insertions were calculated by Grant and Paul parameters<sup>(49)</sup> and the results are shown in Table 8.

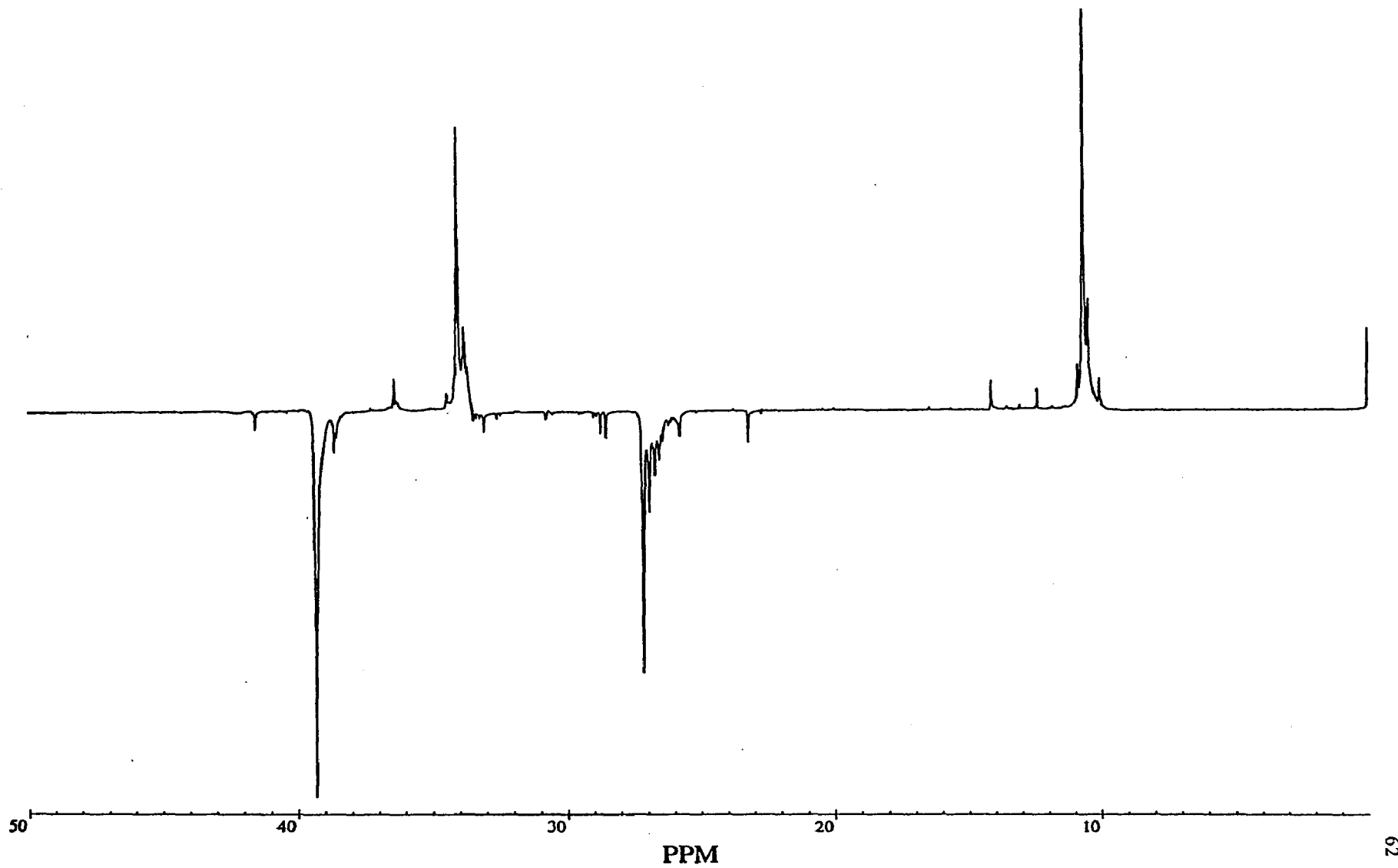


Figure 10  $^{13}\text{C}$  DEPT NMR single bond region of poly(1-butene)

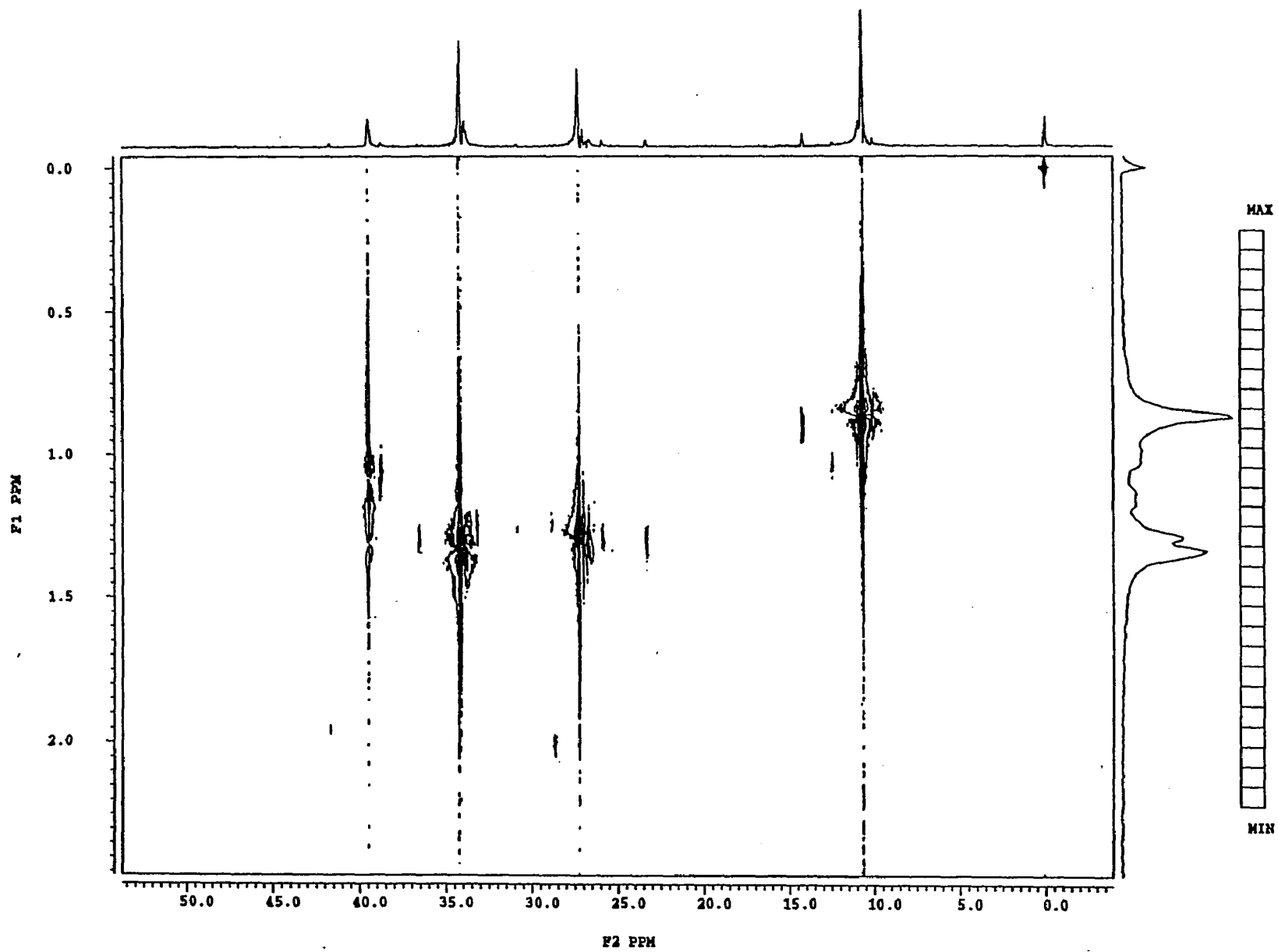


Figure 11  $^{13}\text{C}$ - $^1\text{H}$  shift correlated 2D spectrum of poly(1-butene)

Table 8  $^{13}\text{C}$  Chemical shift calculations of repeat units

<b>BBBBB</b>	$  \begin{array}{ccccccc}  & & 39.5 & 33.3 & & & \\  & &   &   & & & \\  \sim\text{CH}_2 & -\text{CH} & -\text{CH}_2 & -\text{CH} & -\text{CH}_2 & -\text{CH} & \sim \\  &   & &   & &   & \\  & \text{CH}_2 & 28.2 & \text{CH}_2 & & \text{CH}_2 & \\  &   & &   & &   & \\  & \text{CH}_3 & 11.6 & \text{CH}_3 & & \text{CH}_3 &   \end{array}  $
<b>BBBBB</b>	$  \begin{array}{ccccccc}  & & 36.9 & 36.5 & 39.3 & 30.1 & 32.9 & 35.9 & \\  & &   &   &   &   &   &   & \\  \sim\text{CH}_2 & -\text{CH} & - & \text{CH} & -\text{CH}_2 & -\text{CH}_2 & -\text{CH} & \sim \\  &   & &   & &   & &   & \\  & \text{CH}_2 & 25.6 & \text{CH}_2 & 25.4 & \text{CH}_2 & 27.9 & \text{CH}_2 & \\  &   & &   & &   & &   & \\  & \text{CH}_3 & 11.7 & \text{CH}_3 & 11.8 & \text{CH}_3 & 11.5 & \text{CH}_3 &   \end{array}  $
<b>BBBBBB</b>	$  \begin{array}{ccccccccccc}  & & & 35.8 & 32.6 & 32.7 & 36.1 & 36.7 & 36.7 & & 36.9 & 37.0 & \\  & & &   &   &   &   &   &   & &   &   & \\  \sim\text{CH} & -\text{CH}_2 & - & \text{CH} & -\text{CH}_2 & -\text{CH}_2 & -\text{CH} & -\text{CH}_2 & -\text{CH} & - & \text{CH} & -\text{CH}_2 & -\text{CH} & -\text{CH}_2 & \sim \\  &   & &   & &   & &   & &   &   &   & &   & \\  & \text{CH}_2 & & \text{CH}_2 & & 28.0 & \text{CH}_2 & 25.7 & \text{CH}_2 & & \text{CH}_2 & 25.7 & \text{CH}_2 & & \text{CH}_2 & \\  &   & &   & &   & &   & &   &   &   & &   & \\  & \text{CH}_3 & & \text{CH}_3 & & 11.5 & \text{CH}_3 & 11.9 & \text{CH}_3 & & \text{CH}_3 & 11.9 & \text{CH}_3 & & \text{CH}_3 &   \end{array}  $
<b>BBBBBBB</b>	$  \begin{array}{ccccccccccc}  & & & 32.9 & 30.0 & 39.0 & & 39.1 & 30.3 & 30.5 & 39.5 & & 36.5 & 36.9 & \\  & & &   &   &   & &   &   &   &   & &   &   & \\  \sim\text{CH} & -\text{CH}_2 & -\text{CH}_2 & -\text{CH} & - & \text{CH} & -\text{CH}_2 & -\text{CH}_2 & -\text{CH} & - & \text{CH} & -\text{CH}_2 & -\text{CH} & -\text{CH}_2 & \sim \\  &   & &   & &   & &   & &   &   & &   &   & \\  & \text{CH}_2 & & 25.3 & \text{CH}_2 & & \text{CH}_2 & 25.3 & 25.4 & \text{CH}_2 & & \text{CH}_2 & 25.6 & \text{CH}_2 & \\  &   & &   & &   & &   & &   &   & &   &   & \\  & \text{CH}_3 & & 11.8 & \text{CH}_3 & & \text{CH}_3 & 11.8 & 11.8 & \text{CH}_3 & & \text{CH}_3 & 11.9 & \text{CH}_3 &   \end{array}  $

The calculations of chemical shift values on different stereo-placements of poly(1-butene) repeat units by Asakura and coworkers<sup>(50-51)</sup> were used for elucidation of different stereochemical arrangements of repeat units for our poly(1-butene) sample. Figure 12 shows the assignment of signals for repeat unit regioselectivity and stereoregularity. Of the four signals for the repeat unit of poly(1-butene), the signal for the side chain CH<sub>2</sub> carbon is the most sensitive to stereochemistry while the signal for the backbone CH<sub>2</sub> carbon is the least sensitive. There is a spread of about 1 ppm among the various pentad arrangements for the side chain CH<sub>2</sub> carbon signal and only a spread of 0.2 ppm for backbone CH<sub>2</sub> carbon signal. The side chain CH<sub>2</sub> carbon signal was used for stereochemical analysis. The stereoisomeric pentad fractions are shown in Table 9. The meso and racemic dyad fractions were calculated as 0.84 and 0.16, respectively, i.e., the poly(1-butene) is 84% isotactic. The relationships between dyad, triad, tetrad and pentad used to obtain poly(1-butene) isotacticity was listed in Appendix 8.3.

B and B refer to normal and reverse insertions of 1-butene monomers, respectively. Small amounts of isolated reverse repeat units(BBBBB) are observed, but there is no evidence of reverse units being near each other, neither adjacent reverse units (BBBBB) nor two reverse units separated by one normal unit (BBBBB). Most of the signals for BBBBB are poorly resolved from other signals and this limits quantification of the extent of reverse repeat units and, to some extent, confidence in these assignments. We estimate between 0.5 and 2 reverse repeat units per polymer molecular, not counting the end groups. Overall, this means that the average polymer

molecule has a degree of polymerization of 36, contains two end groups and 34 repeat units, of which 0.5-2 are reverse repeat units.

#### 4.4 Discussion

Proposed initiation, propagation, and chain transfer reactions are described in Scheme IV, V, and VI, respectively. The various equations are simplified by showing only one of the ligands of Zr or Al. It is assumed that MAO alkylates the zirconium chloride ligands to form the initial polymerization sites- zirconium-methyl sites (shown as  $\text{CH}_3\text{Zr}$  in eq 1). Most polymer chains are subsequently initiated by zirconium-hydride sites (shown as  $\text{ZrH}$  in eq 2) formed by various  $\beta$ -hydride transfer reactions (Scheme VI). The two initiation reactions result in propagation (eqs 3, 4) to yield polymer with s-butyl (14) and n-butyl (12 and 13) end groups. 13, not shown in eq 4, differs from 12 only in having reverse placement of the first monomer unit added.

Propagation involves insertion of 1-butene into zirconium-carbon sites with almost exclusively normal addition (1,2-addition) coupled with isospecificity. The major unsaturated end group (vinylidene end group 1) is formed by  $\beta$ -hydride transfer from normal propagating sites (17) (eq 5). Vinylidene end group 2 is formed by  $\beta$ -hydride transfer from propagating sites (19) in which the penultimate unit is reversed (eq 9). Vinylidene end group 3 which may be present is formed by  $\beta$ -hydride transfer from propagating sites in which the pen-penultimate unit is reversed. The amounts of vinylidene end groups 2 plus 3 are no more than 3-5% of the total vinylidene end group content.

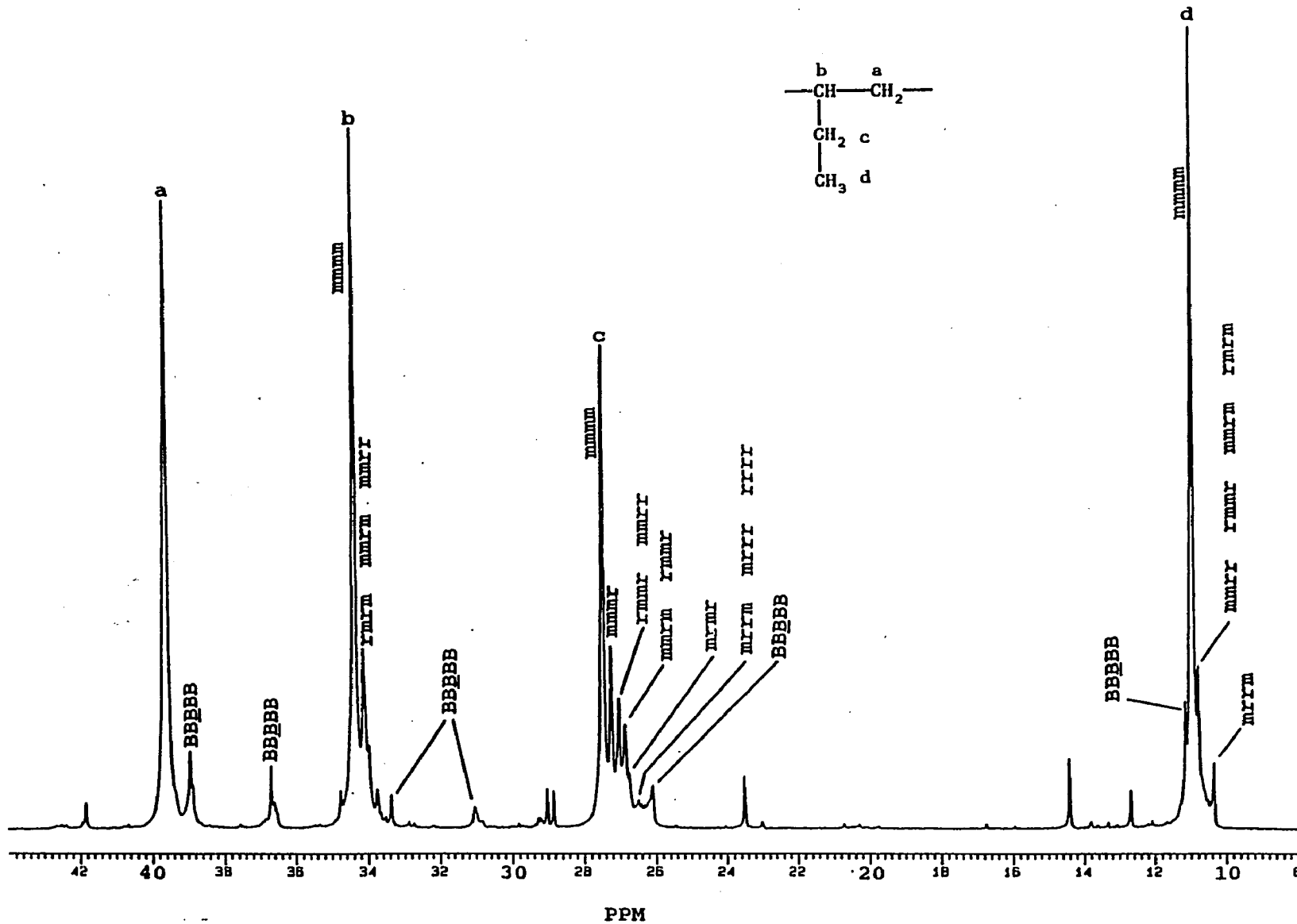


Figure 12  $^{13}\text{C}$  NMR single bond region of poly(1-butene) with repeat unit assignments

Table 9 Pentad Stereochemistry of Poly(1-butene)

Pentad	$\delta$ (ppm)	Fraction
mmmm	27.1	0.581
mmmr	26.9	0.192
mmrr	26.7	0.109
mmrm		
rmrr	26.6	0.080
mrmm	26.4	0.024
rrrr	26.1	0.014
mrrr		
mrrm		

Rearrangement of propagating site **17** to **18** followed by  $\beta$ -hydride transfer from *b* and *c*, respectively, yields trisubstituted double bond end groups **4** and **6** (eqs 7, 8) (Transfer from *a* yields end group **1**). Similarly, rearrangement of propagating site **19** to **20** followed by  $\beta$ -hydride transfer from *b* and *c*, respectively, yields trisubstituted double bond end group **5** and tetrasubstituted double bond end group **11** (eqs 11, 12) (Transfer from **2** yield end group **2**). The formation of trisubstituted double bond end groups in metallocene-initiated polymerization of  $\alpha$ -olefins was first reported in Exxon's patent application for copolymerization of ethylene with  $\alpha$ -olefins<sup>(55)</sup> and more recently by others for the polymerization of 1-hexene.<sup>(56)</sup>

Vinylene end groups (**9**, **10**) are formed by  $\beta$ -hydride transfer from propagating sites (**21**) in which the last unit is reversed (eqs 13, 14). This was reported to be the only chain transfer reaction in the polymerization of 1-butene by ethylene- $\text{Ind}_2\text{ZrCl}_2$  at 30 °C.<sup>(31)</sup>

Transfer to aluminum results in *s*-butyl end groups. Each act of transfer to aluminum (eq 15) results in aluminum-terminated polymer **22** and zirconium-methyl sites. One *s*-butyl end group is formed when zirconium-methyl initiates polymerization (eq 1). The other *s*-butyl end group is formed at the end of the polymerization process when **22** is hydrolyzed. (Transfer to aluminum may involve transfer to aluminum-methyl bonds in MAO as well as transfer to the residual trimethylaluminum present in MAO.)

The formation of internal trisubstituted double bonds **7** and **8** (if present) involves transfer to vinylidene end groups to form propagating center **23** (eq 17). Subsequent propagation of **23** yields **7** and **8** (eqs 18, 19).

The very small amount (<1%) of vinyl end groups is probably formed by  $\beta$ -hydride transfer (eq 20).

The relative amounts of the various  $\beta$ -hydride transfer reactions are shown in Table 10. The relative amounts of **1**, **2**, and **3** were obtained from the  $^1\text{H}$  NMR which showed the minor vinylidene end group signals to be no more than 5% of the major vinylidene end group signal (5% up limit was verified by performing curve fitting on these signals). All other values were obtained from  $^{13}\text{C}$  NMR signal areas (Table 6). (This analysis assumes that the trisubstituted double bonds are end groups, not internal double bonds.)

The amounts of chain transfer to aluminum relative to  $\beta$ -hydride transfer reactions was obtained from the relative amounts of the three saturated end groups (**12:13:14**=18:3:2). **12** and **13** (n-butyl) result from initiation via  $\beta$ -hydride transfer. s-Butyl end groups **14** are formed via three routes:

- (1) The very first act (i.e., at the beginning of polymerization) of initiation by zirconium-methyl sites (eq 1 followed by eq 3).
- (2) Chain transfer to aluminum (eq 16).
- (3) Chain transfer to vinylidene end groups (eq 17).

Note that the s-butyl end group **14** in eq 3 appears to be different from the s-butyl end groups **14** in eqs 16 and 17, but they are not different end groups. The apparent difference arises because **14** in eq 3 is an end group at the initiation end of the polymer chain while **14** in eqs 16 and 17 are end groups at the terminal end of the polymer chain.

Chain transfer to aluminum results in two s-butyl end groups per transfer. If chain transfer to aluminum and chain transfer to vinylidene end

Table 10 Relative Amounts of  $\beta$ -Hydride Transfer Reactions

End group	Equation number <sup>a</sup>	Percent <sup>b</sup>
Vinylidene		
1	5	60
2	9	3
3	5	
Trisubstituted		
4	7	8
5	11	13
6	8	14
Vinylene		
9	13	2
10	14	

<sup>a</sup> Chain transfer reactions in Scheme V

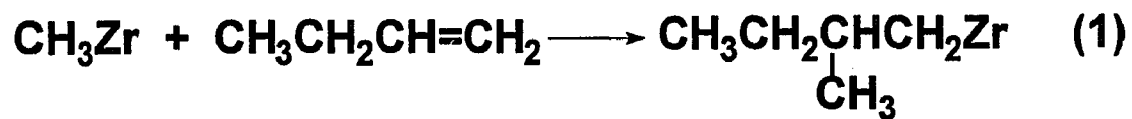
<sup>b</sup> All percentages are within +/-5% experimental errors

groups are unimportant, the ratio of n-butyl:s-butyl should be close to the catalytic efficiency of the polymerization process since one n-butyl end group is formed for each  $\beta$ -hydride transfer while one s-butyl end group is formed for each Zr atom initially present. The experimentally determined catalytic efficiency for this polymerization is 33,000 moles polymer per mole Zr. However, the ratio of n-butyl:s-butyl is far smaller, being about 10, which indicates the occurrence of a significant amount of chain transfer to aluminum and/or chain transfer to vinylidene end groups.

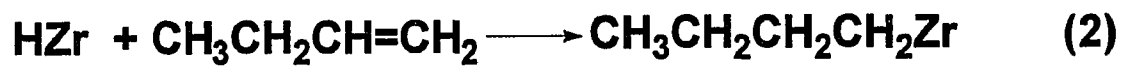
The n-butyl:s-butyl ratio of 10 indicates about 5% chain transfer to aluminum or 10% chain transfer to vinylidene end groups. (The difference between 5% and 10% for the two transfers results from the fact that chain transfer to aluminum yields twice the number of s-butyl end groups as chain transfer to vinylidene end groups.). The overall result is that the ratio of saturated:unsaturated end groups is not one, but greater than one. Some of the polymer molecules, 5% or 10% depending on whether chain transfer to aluminum or chain transfer to vinylidene is important, have two saturated end groups and no double bond end groups. We expect a saturated:unsaturated ratio of about 1.1 based on the n-butyl:s-butyl ratio of 10. Direct evaluation of the saturated:unsaturated ratio from the  $^{13}\text{C}$  NMR signal areas for the various double bond end groups and saturated end groups gives a ratio of 1.3. The difference between 1.1 and 1.3 is probably not experimentally significant. Each ratio is the ratio of the summations of several small signals.

Calculations from the catalytic efficiency, saturated:unsaturated end group ratio and the n-butyl:s-butyl end group ratio show that the amount of s-butyl formed by the very first act (i.e., at the beginning of polymerization) of

initiation by zirconium-methyl sites (eq 1 followed by eq 3) is negligible (< 0.2%). Essentially all of the s-butyl is formed by some combination of chain transfer to aluminum and chain transfer to vinylidene. The relative extent of chain transfer to aluminum relative to chain transfer to vinylidene is unclear. Calculations show that chain transfer to vinylidene alone can account for the s-butyl content while chain transfer to aluminum alone cannot account for the s-butyl content. The amount of MAO (and trimethylaluminum) present in the polymerization system is such that it can account for no more than 60% of the s-butyl content.

**Scheme IV****Initiation Reactions**

15

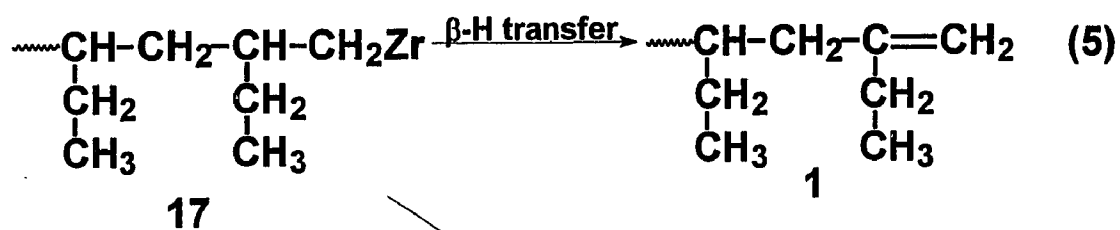


16

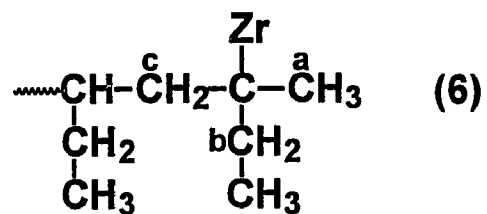


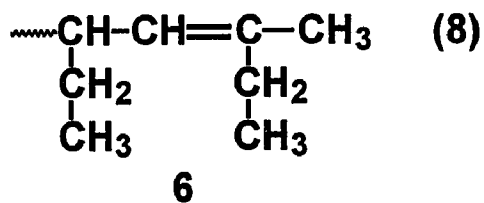
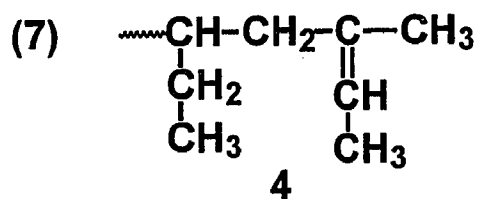
## Scheme VI

## Chain Transfer Reactions

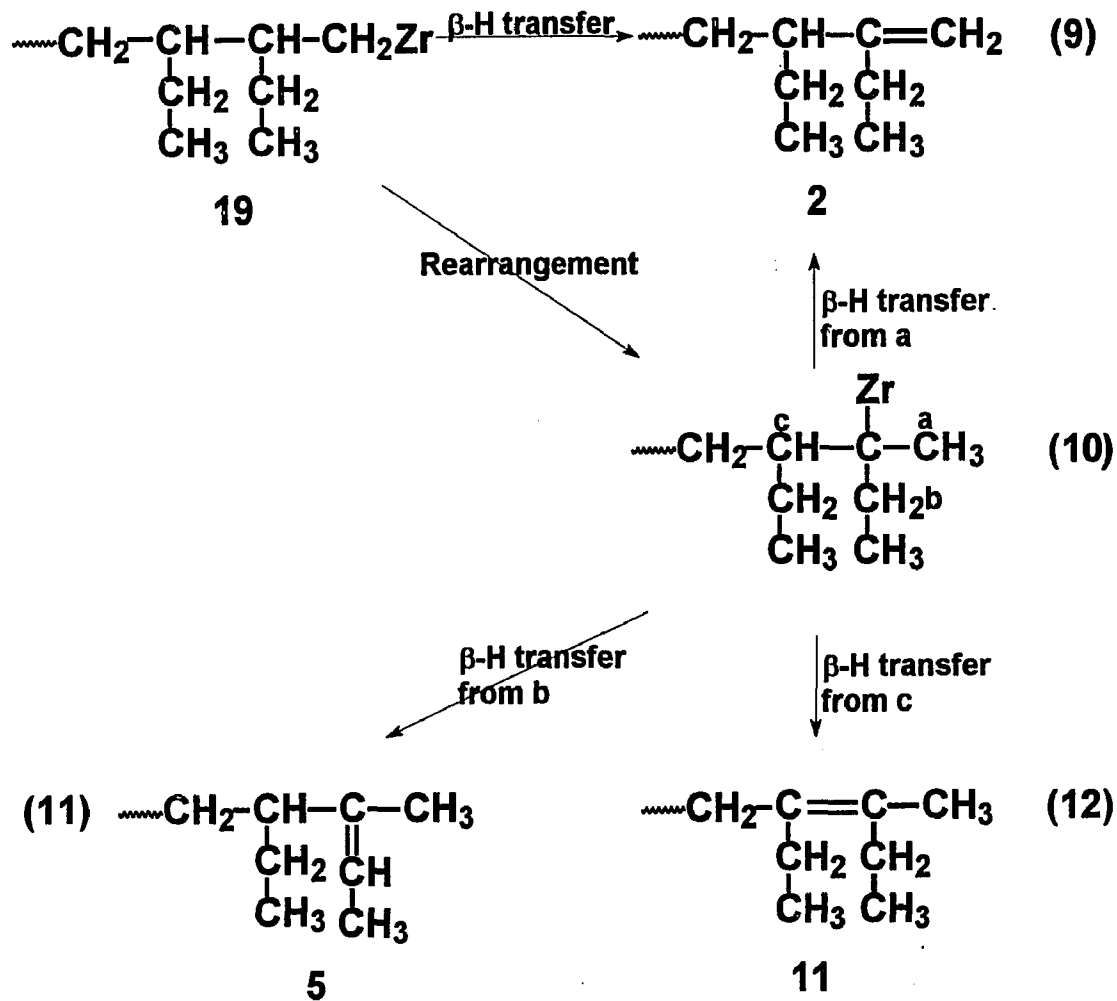


Rearrangement

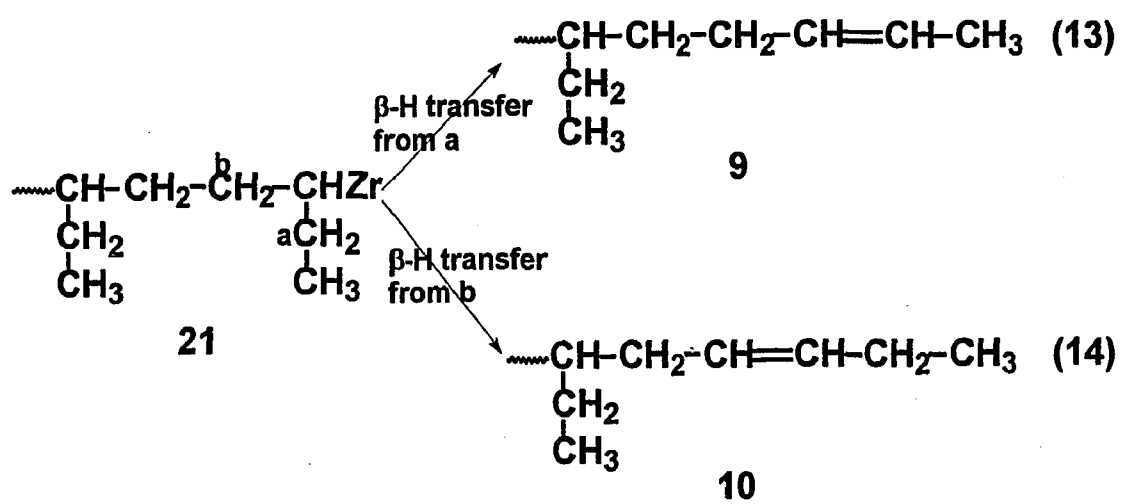
 $\uparrow$   
 $\beta\text{-H transfer}$   
 from a

 $\beta\text{-H transfer}$   
 from b

 $\downarrow$   
 $\beta\text{-H transfer}$   
 from c


## Scheme VI (continued)

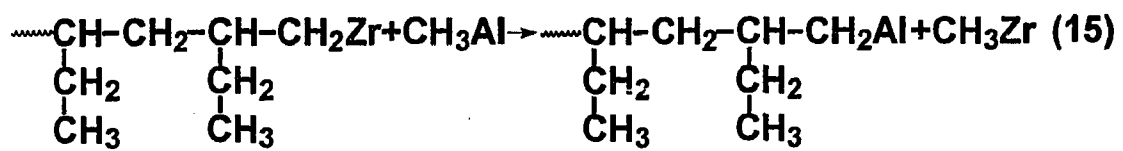


## Scheme VI (continued)



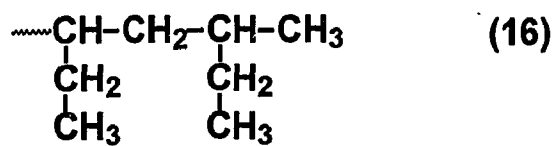
## Scheme VI (continued)

## Transfer to Aluminum



17

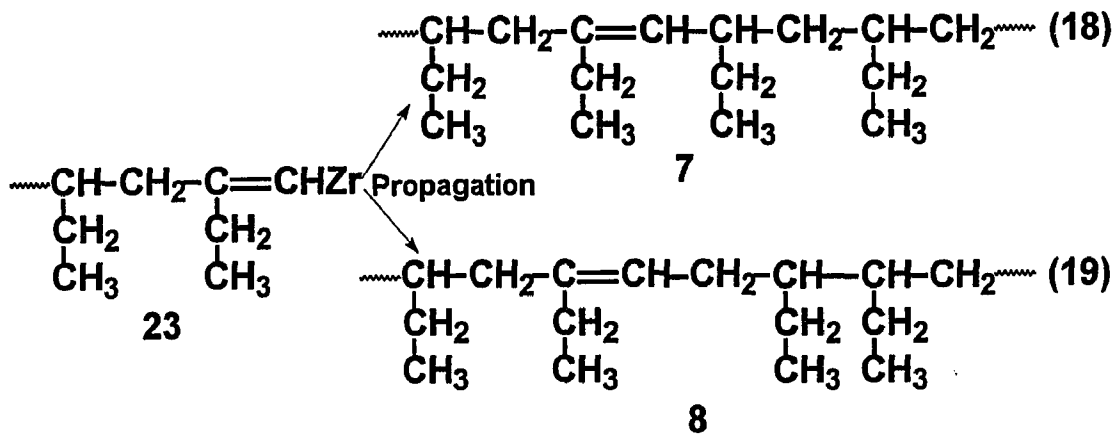
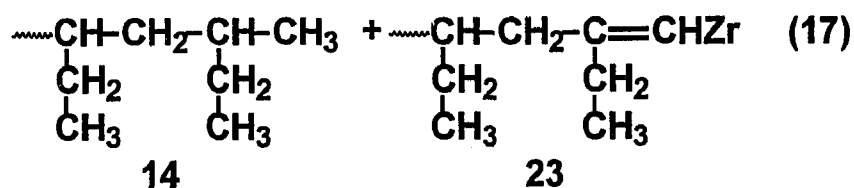
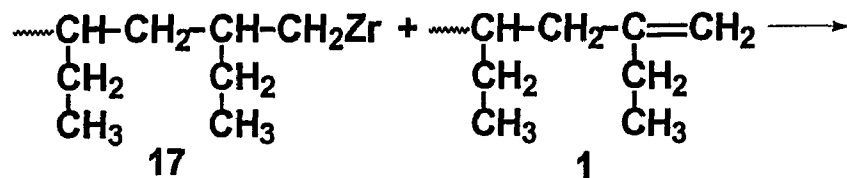
22



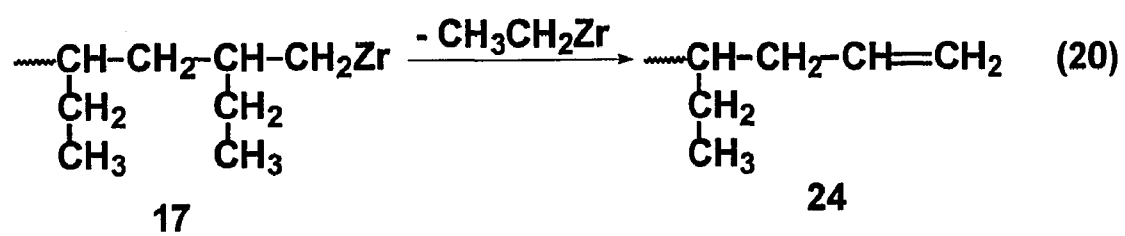
14

## Scheme VI (continued)

## Transfer to Vinylidene End group



## Scheme VI (continued)

 $\beta$ -Alkyl Transfer

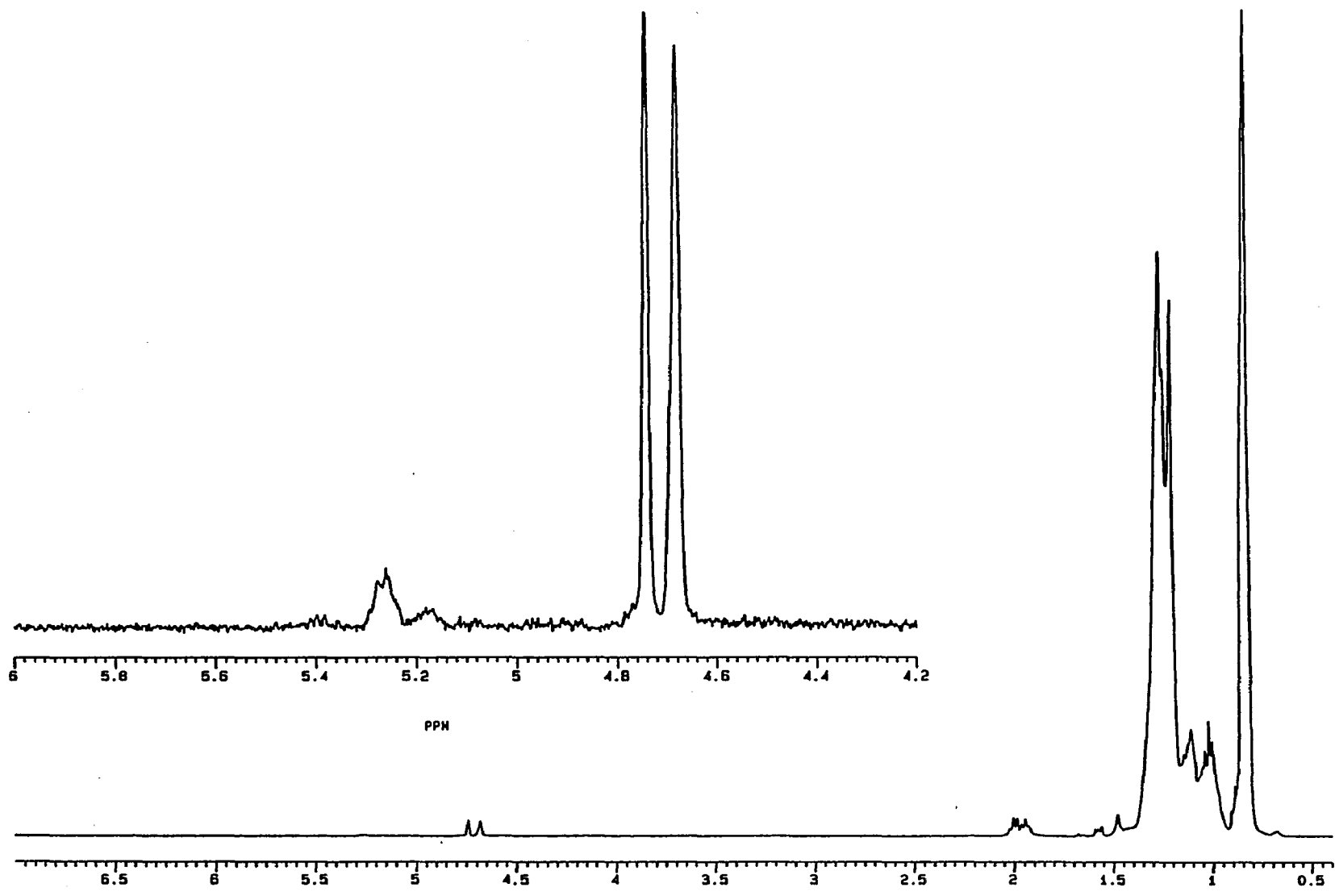
## 5.0 Results and Discussion on Microstructure of Poly(ethylene-co-1-butene)

### 5.1 Results on copolymer composition

Figures 13-14 illustrate the  $^1\text{H}$  NMR spectra of poly(ethylene-co-1-butene) samples 1 and 2. Figures 15-18 illustrate the  $^{13}\text{C}$  NMR and  $^{13}\text{C}$  DEPT spectra of double bond region, and Figures 19-22 illustrate the  $^{13}\text{C}$  NMR and  $^{13}\text{C}$  DEPT spectra of single bond region for two copolymer samples, respectively. The methyl signals of the 1-butene units, 0.95 and 11 ppm upfield from TMS, respectively, in  $^1\text{H}$  and  $^{13}\text{C}$  NMR spectra, are well separated from other signals and their integration relative to all other signals yielded the copolymer composition shown in Table 11. The results from  $^1\text{H}$  and  $^{13}\text{C}$  NMR were in good agreement, 32.4 vs. 34.8 mol-% ethylene for sample a and 56.2 vs. 58.3 mol-% ethylene for sample 2. In good agreement with NMR results, the copolymer composition calculated from the overall conversions of ethylene and 1-butene were 32.6 and 55.6 mol-% ethylene for samples 1 and 2, respectively.

### 5.2 Results on end groups

End group analysis was facilitated in this study by the use of very low molecular weight (ca. 2000) polymers coupled with large number of NMR acquisitions. Signals for vinylene, trisubstituted, vinyl, and vinylidene double bonds are expected in the  $^1\text{H}$  NMR spectrum at 5.50-5.30, 5.30-5.10, 5.10-4.80 and 4.80-4.60 ppm, respectively.<sup>(46)</sup> The results from the  $^1\text{H}$  NMR analysis shown in Figures 13 and 14 show that vinylidene is the major double bond end group. Also there is a significant amount of trisubstituted double bond end group (Table 11). Vinylidene and trisubstituted double bonds are in the approximate ratio of 3:1. Vinyl and vinylene double bond end groups



PPM Figure 13  $^1\text{H}$  NMR of poly(ethylene-co-1-butene) sample 1

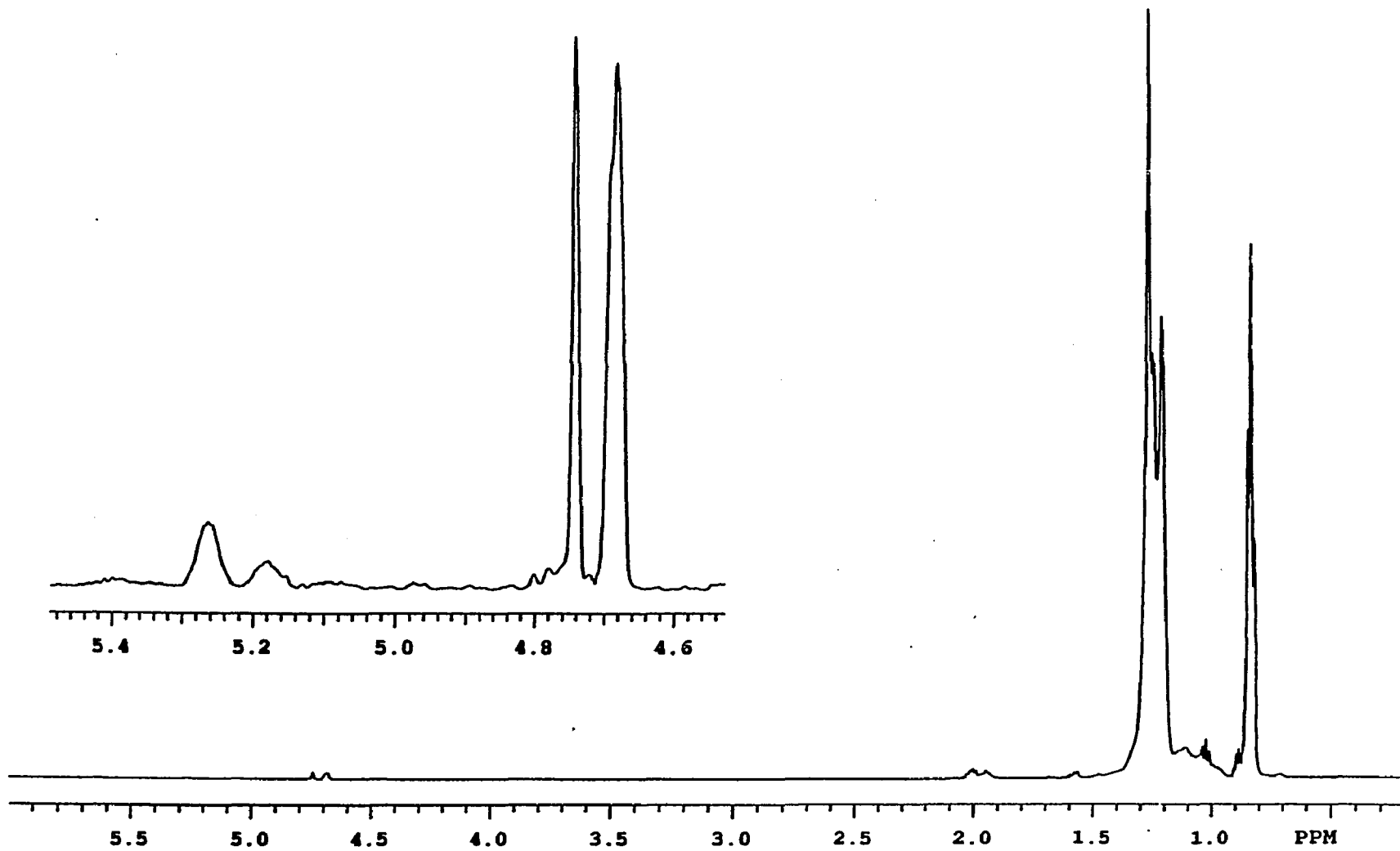
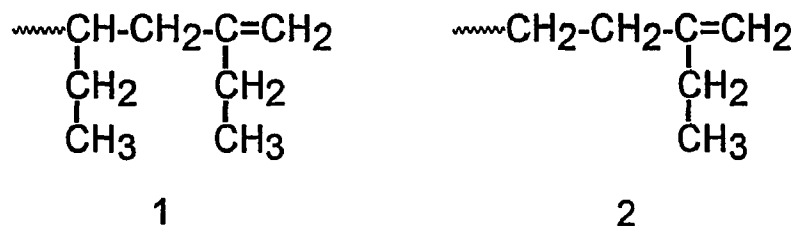


Figure 14  $^1\text{H}$  NMR of poly(ethylene-co-1-butene) sample 2

appear to be present in trace amounts (<1%).

### 5.2.1 Vinylidene double bonds

The major vinylidene  $^1\text{H}$  NMR signals were identified as a doublet at 4.74 and 4.68 ppm. The ratio of the signal area at 4.68 ppm compared to that at 4.74 ppm was smaller for sample 1, which had the lower ethylene content, than for sample 2. The NMR signals correspond to the two vinylidene end groups 1 and 2:



1 and 2 have terminal 1-butene units and the penultimate unit is 1-butene for 1 but ethylene for 2. The geminal vinylidene protons of 2 are very similar and one signal at 4.68 ppm is found. The two geminal vinylidene protons of 1 are more different in ppm than those of 2 and this results in separate signals at 4.74 and 4.68 ppm. Copolymer sample 1, containing less ethylene than sample 2, has a lower content of 2 and this resulted in a smaller signal area at 4.68 ppm. The ratio of 1:2 is 5.9:1 and 2.1:1 for copolymer samples 1 and 2, respectively.

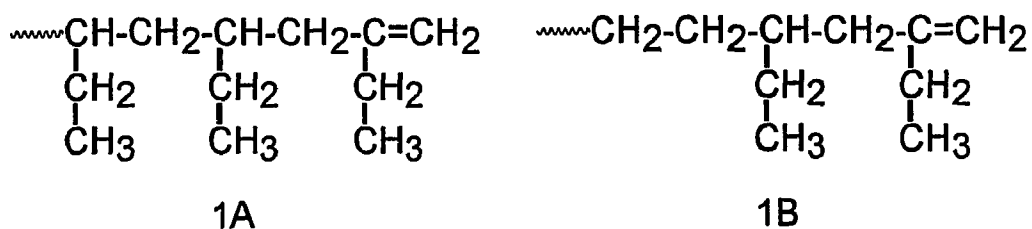
The  $^{13}\text{C}$  NMR results verified the assignments for vinylidene end groups 1 and 2 (Figures 15 & 17, Table 12). The pair of signals at 150.2 and 109.1 ppm are assigned to structure 1, which has calculated chemical shift values of 150.3 and 107.9 ppm. The pair of signals at 151.5 and 107.4 ppm is assigned to structure 2, which has calculated chemical shift values of 150.3 and 107.9 ppm. These assignments are consistent with the observed  $^{13}\text{C}$

Table 11 Copolymer Composition, Molecular Weight,  
and Double Bond Composition of Ethylene-1-Butene Copolymers

		Sample 1	Sample 2
Mol-% E	<sup>1</sup> H NMR	32.4	56.2
	<sup>13</sup> C NMR	34.8	58.3
M <sub>n</sub>	<sup>1</sup> H NMR	2030	2350
	<sup>13</sup> C NMR	1810	1920
	SEC	1700	2110
	VPO	2060	2420
MWD(SEC)		2.05	2.17
Double bond end groups by <sup>1</sup> H NMR	CH <sub>2</sub> =C<	75.0	73.1
	-CH=C<	23.0	25.1
	-CH=CH-	1.0	1.4
	CH <sub>2</sub> =CH-	0	0.4
Double bond end groups by <sup>13</sup> C NMR	1-type	61.8	43.7
	2-type	11.2	24.4
	3-type	11.7	19.1
	4-type	14.0	11.8
	-CH=CH-	1.3	1.0

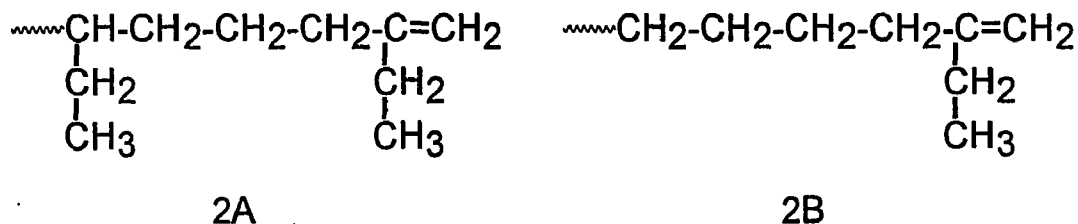
DEPT NMR spectra shown in Figures 16 and 19, which indicated that the signals at 151.5 and 150.2 ppm are quaternary carbons and the signals at 109.1 and 107.4 ppm are secondary carbons. For copolymer samples 1 and 2, the ratio of 1:2 by  $^{13}\text{C}$  NMR is 5.9:1 and 2.0:1 for samples 1 and 2, respectively, consistent with the  $^1\text{H}$  NMR results.

Close inspection of the two  $^{13}\text{C}$  NMR signals for **1** showed each signal to be a pair of signals. This was interpreted in terms of end groups **1A** and **1B**, differing in the identity of the pen-penultimate unit:



**1A** and **1B** have exactly the same calculated double bond carbon and side chain allylic carbon chemical shift values, but different chemical shift values for the backbone allylic carbons. Further support for the presence of **1A** and **1B** came from the  $^{13}\text{C}$  NMR single bond region. There are two signals at 41.6 and 41.1 for the backbone allylic carbons of **1A** and **1B**, respectively, with calculated chemical shift values of 40.5 and 40.0 ppm. There is one signal at 28.6 ppm for the side chain allylic methylene carbon. The calculated chemical shift value is 28.1 ppm for both **1A** and **1B**. Support for the assignments of **1A** and **1B** was also found from the observations that the sum of the signal areas at 41.6 and 41.1 ppm equals the signal area at 28.6 ppm, and the ratio of the signal area at 41.6 ppm to that at 41.1 ppm decreases with increasing ethylene content in the copolymer.

End group **2** may also be present in the corresponding variations **2A** and **2B**, but there was no supporting evidence due to the closeness of chemical shift values of the two structures.



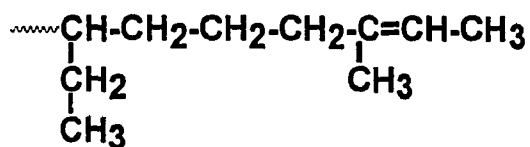
The total vinylidene content found by  $^{13}\text{C}$  NMR, a total of 73.0% and 68.1% for samples 1 and 2, respectively, are in agreement with the results from  $^1\text{H}$  NMR (75.0% and 73.1% respectively).

### 5.2.2 Trisubstituted double bonds

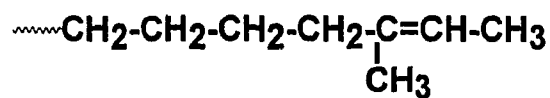
The 5.30-5.10 ppm region of the  $^1\text{H}$  NMR spectrum indicated the presence of more than one type of trisubstituted double bond end groups (Figures 13 and 14). Analysis of the  $^{13}\text{C}$  NMR double bond region (Figures 15 and 17, Table 12) showed that there are at least six different trisubstituted double bond end groups, they are: end groups **3A**, **3C**, **4A**, **4B**, **4C**, and **4D** for sample 1 and end groups **3A**, **3B**, **4A**, **4B**, **4C**, and **4D** for sample 2. Signals for both *E* and *Z* isomers were assigned for end groups **4C** and **4D** with the *E* isomers in greater abundance. (*E* and *Z* refer to *trans* and *cis* placements, respectively, of the larger alkyl groups on each of the carbons of the double bond.) The *E* and *Z* isomers are indicated by subscripts *E* and *Z* in Table 12. Separate signals for *E* and *Z* isomers of **3A**, **3B**, **3C**, **4A**, and **4B** are not observed. Both *E* and *Z* isomers are assumed to be present but not observed due to overlapping of signals.

Table 12  $^{13}\text{C}$  NMR End Group and Repeat Unit Assignments

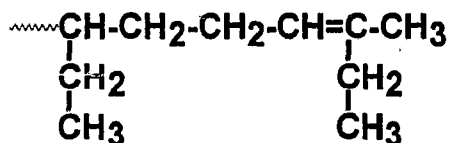
$\delta$ (ppm)	Assignment	$\delta$ (ppm)	Assignment
151.5, 107.4	2	32.0	8
150.2, 109.1	1	30.7	$S_{\gamma\gamma}$ -BEEB
140.5, 118.1	3B	30.2	$S_{\gamma\delta}$ -BEEEB
139.4, 119.2	3A	29.8	$S_{\delta\delta}$ -BEEEEB
138.0, 123.1	3C	29.4	8
136.2, 128.6	4D <sub>E</sub>	29.1	7
135.9, 129.0	4C <sub>E</sub>	28.8	2
135.1, 119.4	4A	28.5	1
134.6, 119.8	4B	28.0	2
130.9, 127.4	5A	27.2	$S_{\text{Br}}$ -BBBB
136.0, 130.1	4C <sub>Z</sub>	26.8	$S_{\beta\delta}$ -EBEE + $S_{\text{Br}}$ -EBBBE
136.0, 129.7	4D <sub>Z</sub>	26.6	$S_{\beta\delta}$ -BBEE + $S_{\text{Br}}$ -BBBE
41.6	1A	26.3	$S_{\text{Br}}$ -EBBE
41.1	1B	26.1	$S_{\text{Br}}$ -EBE
40.5	3A	23.9	$S_{\beta\beta}$ -EBEBE
39.4	$S_{\alpha\alpha}$ -BBBB	23.7	$S_{\beta\beta}$ -BBEBE
39.0	$T_{\delta\delta}$ -EBE	23.2	7
38.7	$S_{\alpha\alpha}$ -BBBE	22.7	8
38.1	$S_{\alpha\alpha}$ -EBBE	19.7	11
36.9	2	14.1	7 + 8
36.4	$T_{\beta\delta}$ -EBB	13.5	3A
34.0	$T_{\beta\beta}$ -EBB	12.4	1 + 2
33.8	$S_{\alpha\gamma}$ -EBEB	10.9	CH <sub>3</sub> -EBE
33.6	$S_{\alpha\delta}$ -EBEB	10.7	CH <sub>3</sub> -BBE
33.4	$S_{\alpha\delta}$ -EBEB	10.6	CH <sub>3</sub> -BBB



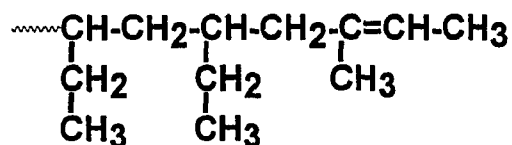
3A



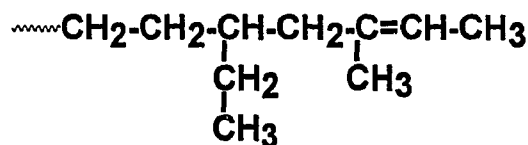
3B



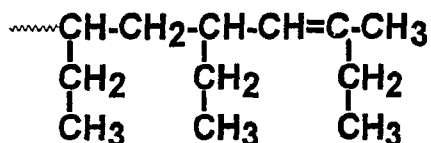
3C



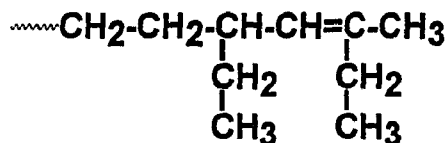
4A



4B



4C



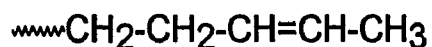
4D

For sample 1, the predominant 3-type of trisubstituted double bond is 3A while the predominant 4-type of trisubstituted double bond is 4A. For sample 2, the predominant 3-type of trisubstituted double bond is 3A with significant amounts of 3B while the predominant 4-type of trisubstituted double bond has comparable amounts of 4A and 4B. The relative amounts of 3 type and 4-type are comparable, somewhat more 4-type for sample 1 but somewhat less 4-type for sample 2.

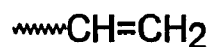
The total trisubstituted double bond content by  $^{13}\text{C}$  NMR, 25.7% and 30.9% for samples 1 and 2, respectively, are in agreement with the results from  $^1\text{H}$  NMR (23.0% and 25.1% respectively).

### 5.2.3 Vinylene and vinyl double bonds

NMR indicated the presence of very small amounts (about 1%) of vinylene and vinyl double bonds. The amounts were near the detection limits for both  $^1\text{H}$  and  $^{13}\text{C}$  NMR. The  $^{13}\text{C}$  NMR spectra identified 5A as the vinylene end group. Vinyl double bonds 6, although detected by  $^1\text{H}$  NMR, were not observed in the  $^{13}\text{C}$  NMR.



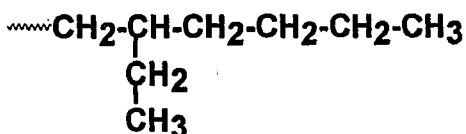
5A



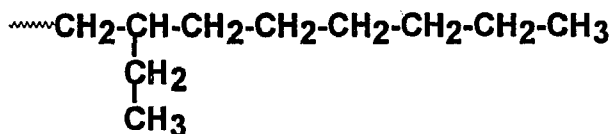
6

### 5.2.4 Saturated end groups

The  $^{13}\text{C}$  NMR single bond region (the signals upfield of 42 ppm in Table 12) indicated two major saturated end groups, 7 and 8:



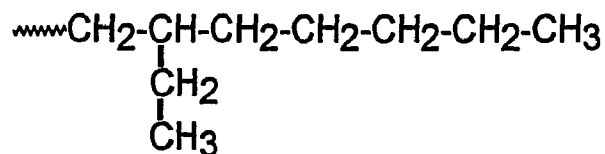
7



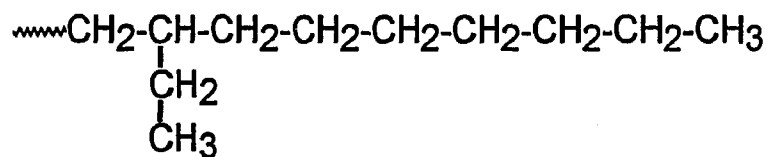
8

Structure 8 differs from 7 in having two additional methylene units at the chain end. The chemical shift values assigned to 7 and 8 are also consistent with 9 and 10, each of which has one additional methylene unit at the chain end compared to 7 and 8. However, mechanistic considerations (see Discussion section) indicate that 7 and 8 exceed 9 and 10 by a factor

of 10000.

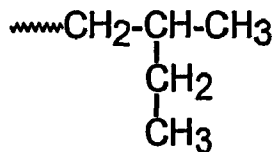


9



10

Structure 11 was assigned as a minor saturated end group based on the small  $^{13}\text{C}$  NMR signal near 20 ppm.



11

The ratio of saturated end groups 7:8:11 is 51:41:8 and 34:53:13 for samples 1 and 2, respectively. Overall, the saturated end groups are in excess of the unsaturated end groups by 10-20% for both copolymer samples. The excess may be no more than 10% or as high as 20%. Experimental limitations prevent a more precise evaluation of the ratio of saturated to unsaturated end groups because the saturated and unsaturated end groups each comprise only about 2% of the polymer.

### 5.3 Results on polymer molecular weight

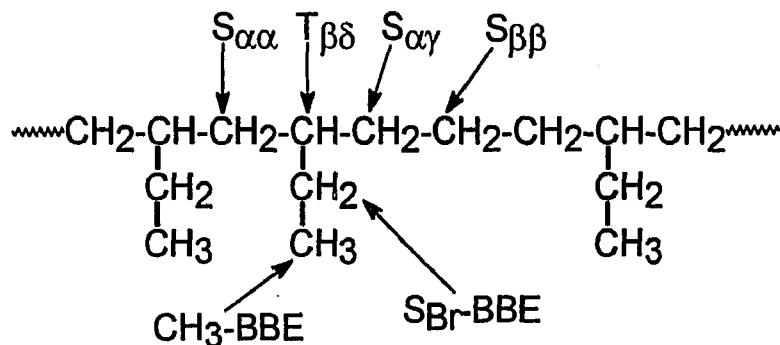
SEC yielded  $M_n=1700$  and  $2110$  for samples 1 and 2, respectively.  $M_n$  values of  $2030$  and  $2350$  were calculated from the  $^1\text{H}$  NMR data for samples 1 and 2, respectively, assuming an average of one double bond per polymer molecule, by comparison of the double bond and single bond signal areas. The corresponding values from  $^{13}\text{C}$  NMR data were  $1810$  and  $1920$ . VPO yielded  $M_n=2060$  and  $2420$ , respectively, for samples 1 and 2. Good agreement was found among the NMR, SEC, and VPO measurements of the number average molecular weight (Table 11).

The polymer molecular weight distribution is narrow. SEC yielded  $M_w/M_n=2.05$  and  $2.17$  for samples 1 and 2, indicative of the single site nature of the zirconocene catalyst.

### 5.4 Results on repeat units

The repeat unit microstructure was determined by matching calculated  $^{13}\text{C}$  chemical shift values<sup>(49)</sup> of possible repeat units with observed chemical shift values. Signal assignments were consistent with the results of  $^{13}\text{C}$  DEPT NMR, signal area differences between samples 1 and 2, and quantitative correlation between different carbon signals. Predominantly isotactic poly(1-butene)<sup>(30)</sup> was used as the model for chemical shift calculations of copolymer repeat units. The assignments (Table 12) are consistent with Cheng's assignments for ethylene/1-butene copolymer.<sup>(39)</sup> The nomenclature used for different repeat units is similar to the nomenclature by Carman and coworkers for ethylene/propylene copolymer.<sup>(57)</sup> The letters S and T represent secondary and tertiary carbons, respectively. Greek subscripts indicate the distance from the designated carbon to the nearest tertiary carbon atoms on

the left and right sides of that carbon. The subscript Br designates the CH<sub>2</sub> of the ethyl branches of 1-butene units. Some examples of this nomenclature are shown in structure 12.



12

The experimental <sup>13</sup>C NMR comonomer triad distributions were determined from the repeat unit assignment (Table 13). This allowed the calculation of the overall comonomer composition, 32 and 59 mol-% ethylene, respectively, for samples 1 and 2. These data were in good agreement with those obtained by comparison of the methyl signal to all other signals: <sup>1</sup>H and <sup>13</sup>C NMR, respectively, gave 32.4 and 34.8 mol-% ethylene for sample 1 and 56.2 and 58.3 mol-% ethylene for sample 2 (Table 11). The triad distribution was fitted to first-order Markovian statistics (terminal model of copolymerization) to obtain the four transition probabilities  $P_{EE}$ ,  $P_{EB}$ ,  $P_{BE}$ ,  $P_{BB}$  for chain terminating in ethylene and 1-butene units reacting with monomers ethylene and 1-butene.<sup>(41)</sup> ( $P_{XY}$  is the probability of monomer Y adding to a propagating chain with X as the terminal unit.) The triad distribution calculated from the transition probabilities compares well with the experimental triad distribution (Table 13). The monomer reactivity ratios for ethylene and 1-butene,  $r_E$  and  $r_B$ , were calculated from the relationships:<sup>(58)</sup>

$$r_E = P_{EE} / [X(1 - P_{EE})] \quad r_B = XP_{BB} / (1 - P_{BB})$$

where  $X$  is the molar feed ratio of ethylene to 1-butene (Appendix 6).

The monomer reactivity ratios are  $r_E=30$ ,  $r_B=0.034$  and  $r_E=80$ ,  $r_B=0.0078$ , respectively, for samples 1 and 2 (Table 13). The ethylene-1-butene system shows *ideal* behavior,  $r_E$  is large while  $r_B$  is small and the product of the two monomer reactivity ratios is near unity. The results are similar to literature observations on ethylene- $\alpha$ -olefin copolymerizations. Heiland and Kaminsky<sup>(59-60)</sup> observed  $r_E=29.2$ ,  $r_B=0.04$ ,  $r_E r_B=1.2$  for ethylene-1-butene polymerization at 70 °C with *rac*-CH<sub>2</sub>CH<sub>2</sub>(Ind)<sub>2</sub>ZrCl<sub>2</sub>. Kaminsky and coworkers<sup>(36)</sup> observed  $r_E=85$ ,  $r_B=0.01$ ,  $r_E r_B=0.85$  at 80 °C with Cp<sub>2</sub>ZrCl<sub>2</sub>. Table 13 also gives the average block lengths of ethylene and 1-butene units,  $n_E$  and  $n_B$ . The ethylene-1-butene copolymers are random with short block lengths of each monomer. 1-Butene has low reactivity but there are considerable amounts of 1-butene in the copolymers because of the very large amount of 1-butene relative to ethylene in the reaction mixture.

### 5.5 Discussion

The proposed mechanism for ethylene-1-butene copolymerization by the zirconocene/MAO initiating system is described in Schemes VII-X. The mechanism builds on that proposed for 1-butene homopolymerization.<sup>(42)</sup> The equations are simplified by showing only one of the ligands for Zr or Al.

MAO alkylates the chloride ligand of the zirconium catalyst to form the initial polymerization sites- zirconium-methyl sites (shown as CH<sub>3</sub>Zr in eq 1 of Scheme VIIA). Polymer chains are subsequently initiated by zirconium-hydride sites (Shown as ZrH in eqs 6 and 8 of Scheme VIIB). formed by various  $\beta$ -hydride transfer reactions (Scheme IX). The various species produced by addition of CH<sub>3</sub>Zr (15, 16, 17) or ZrH (19, 21) to monomer

Table 13 Comonomer Distribution Statistics

	<sup>13</sup> C NMR triad distribution		First order Markovian Statistics	
	Sample		Sample	
	1	2	1	2
[EEE]	0.04	0.19	0.03	0.21
[EEB + BEE]	0.12	0.26	0.12	0.30
[BEB]	0.16	0.14	0.15	0.11
[EBE]	0.11	0.20	0.06	0.18
[BBE + EBB]	0.22	0.13	0.29	0.16
[BBB]	0.36	0.08	0.35	0.04
[E]	0.32	0.59	0.30	0.62
[B]	0.68	0.41	0.70	0.38
n <sub>E</sub>	1.5	3.2		
n <sub>B</sub>	2.2	1.6		
r <sub>E</sub>			30	83
r <sub>B</sub>			0.034	0.0078
r <sub>E</sub> r <sub>B</sub>			1.02	0.65

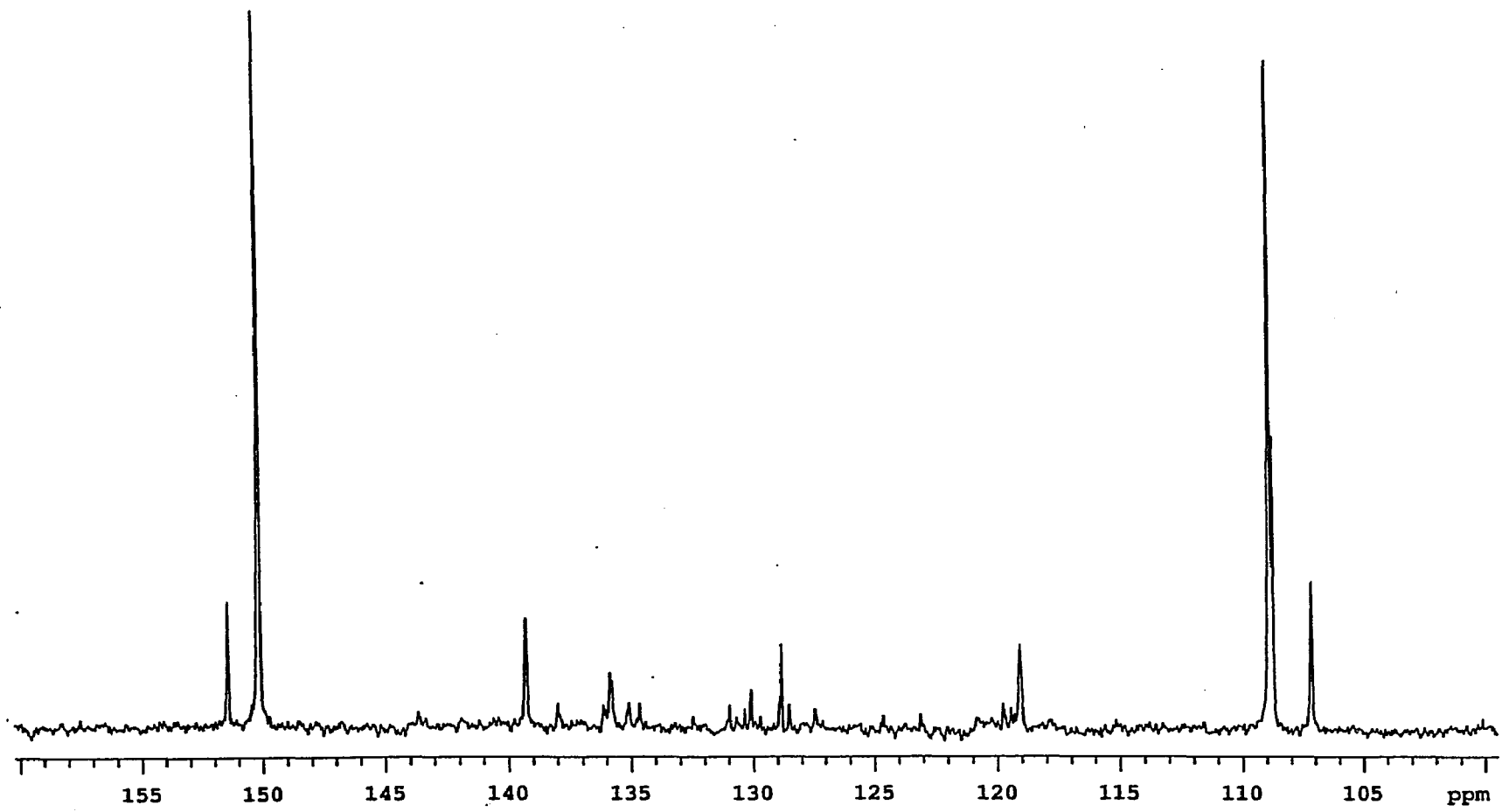


Figure 15  $^{13}\text{C}$  NMR double bond region of poly(ethylene-co-1-butene) sample 1

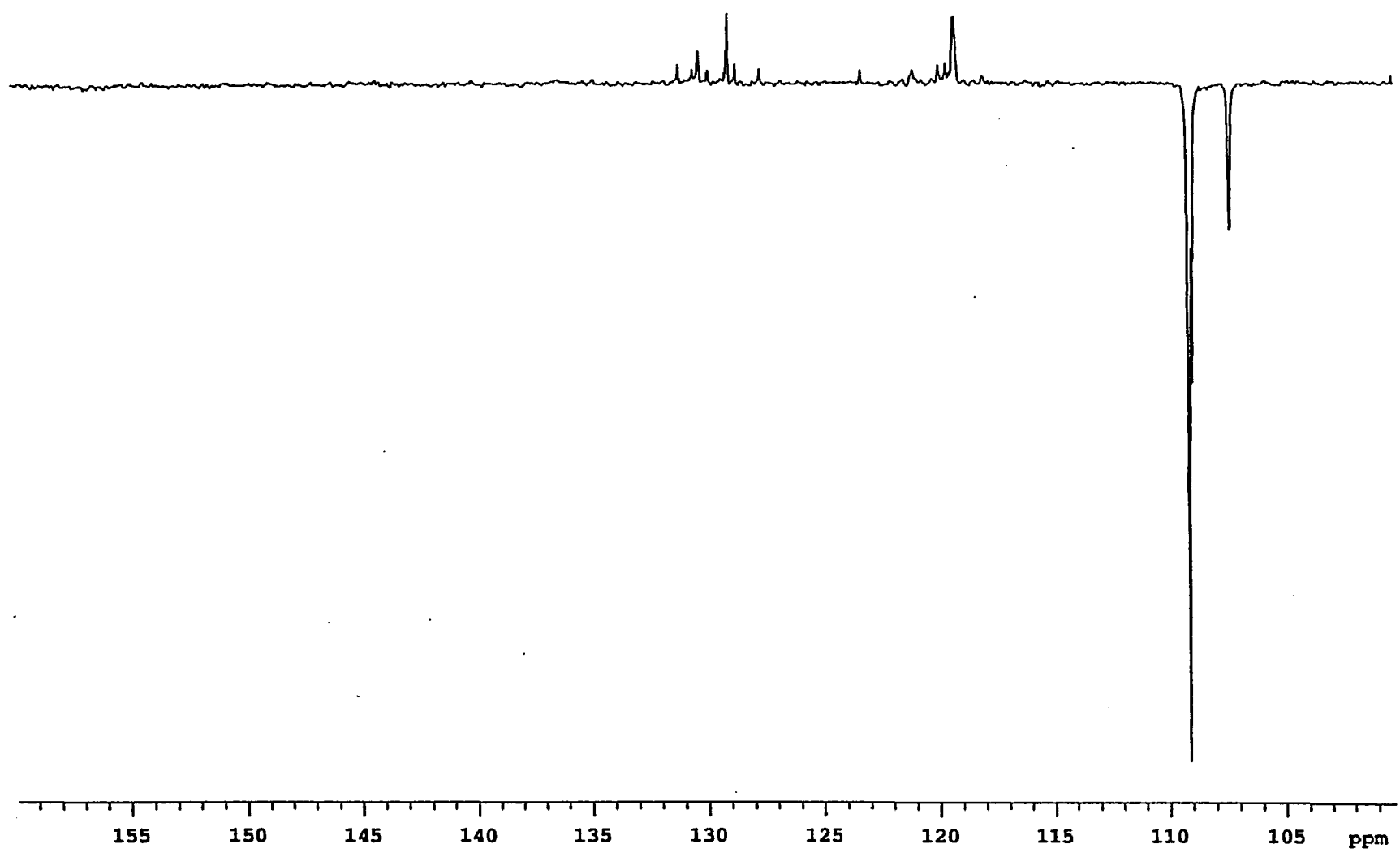


Figure 16  $^{13}\text{C}$  DEPT NMR double bond region of poly(ethylene-co-1-butene) sample 1

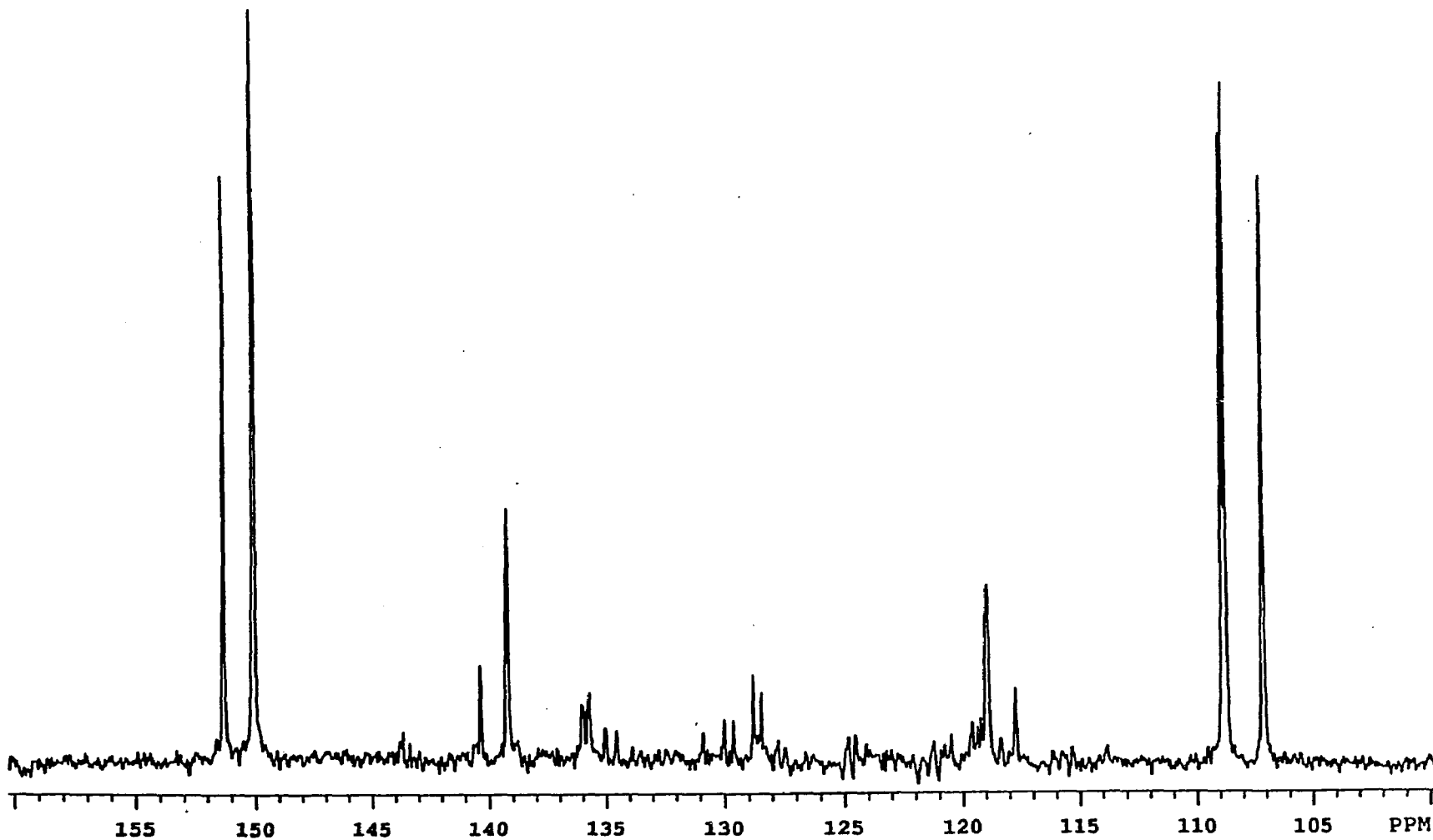


Figure 17  $^{13}\text{C}$  NMR double bond region of poly(ethylene-co-1-butene) sample 2

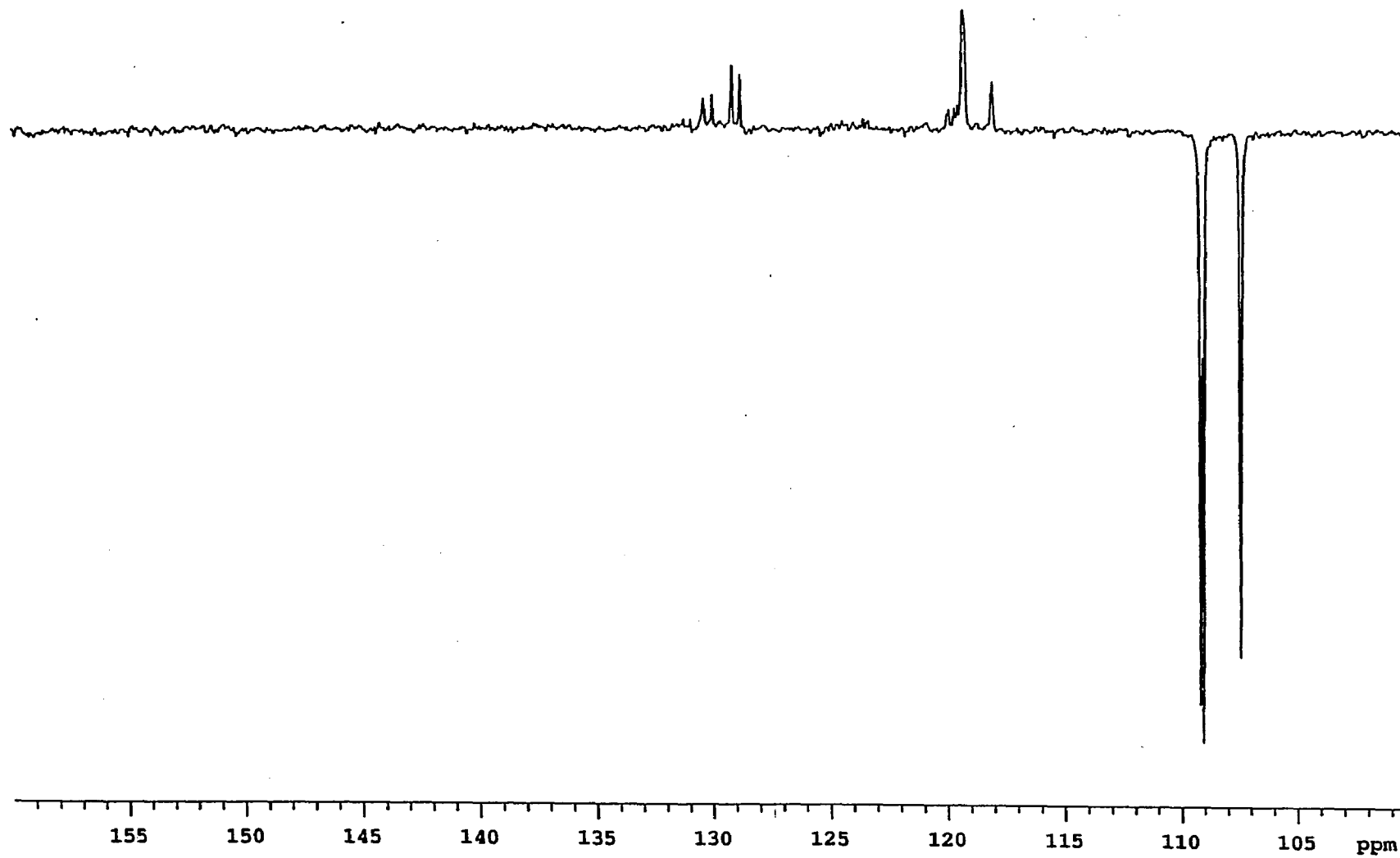


Figure 18  $^{13}\text{C}$  DEPT NMR double bond region of poly(ethylene-co-1-butene) sample 2

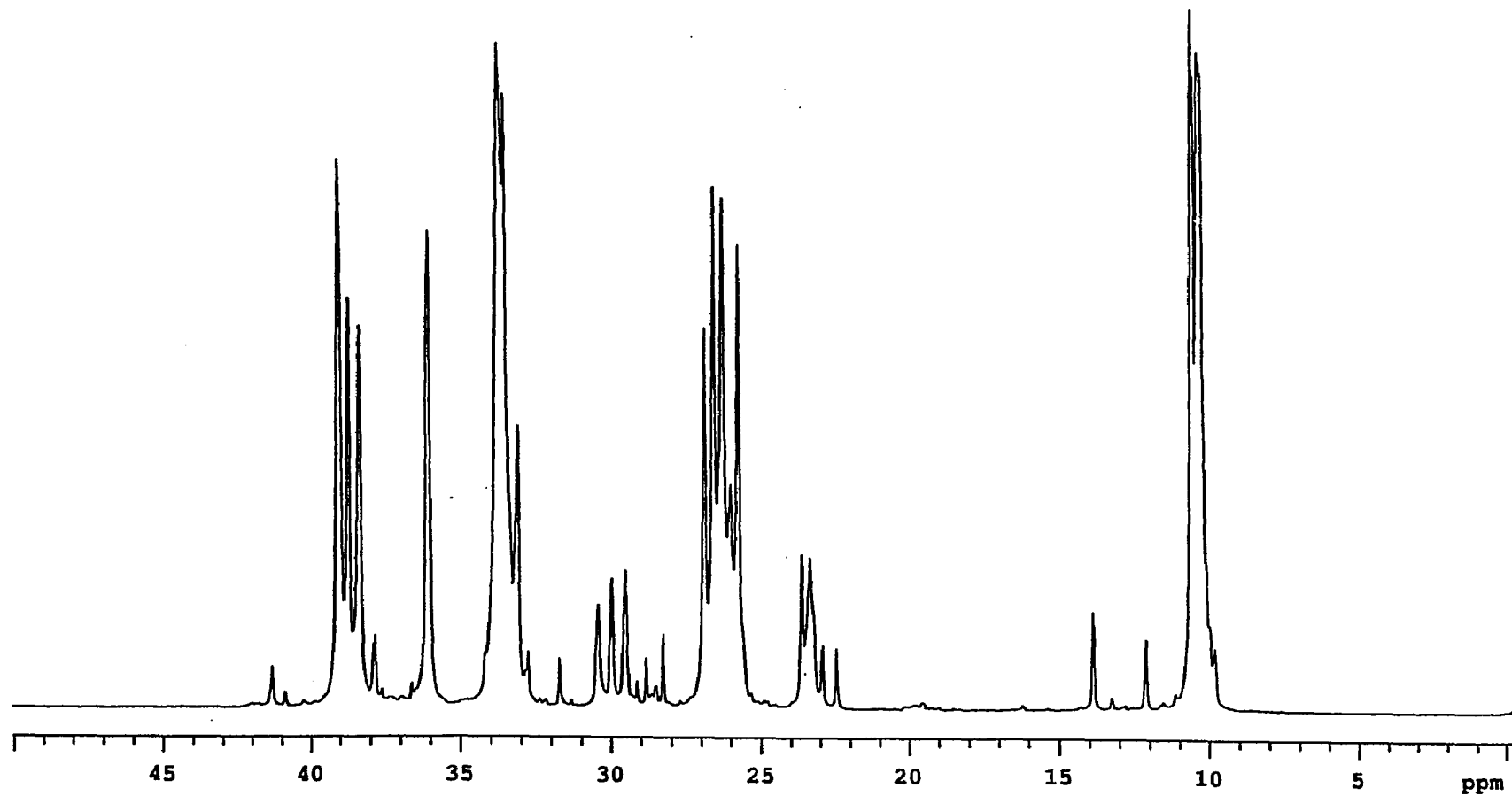


Figure 19  $^{13}\text{C}$  NMR single bond region of poly(ethylene-co-1-butene) sample 1

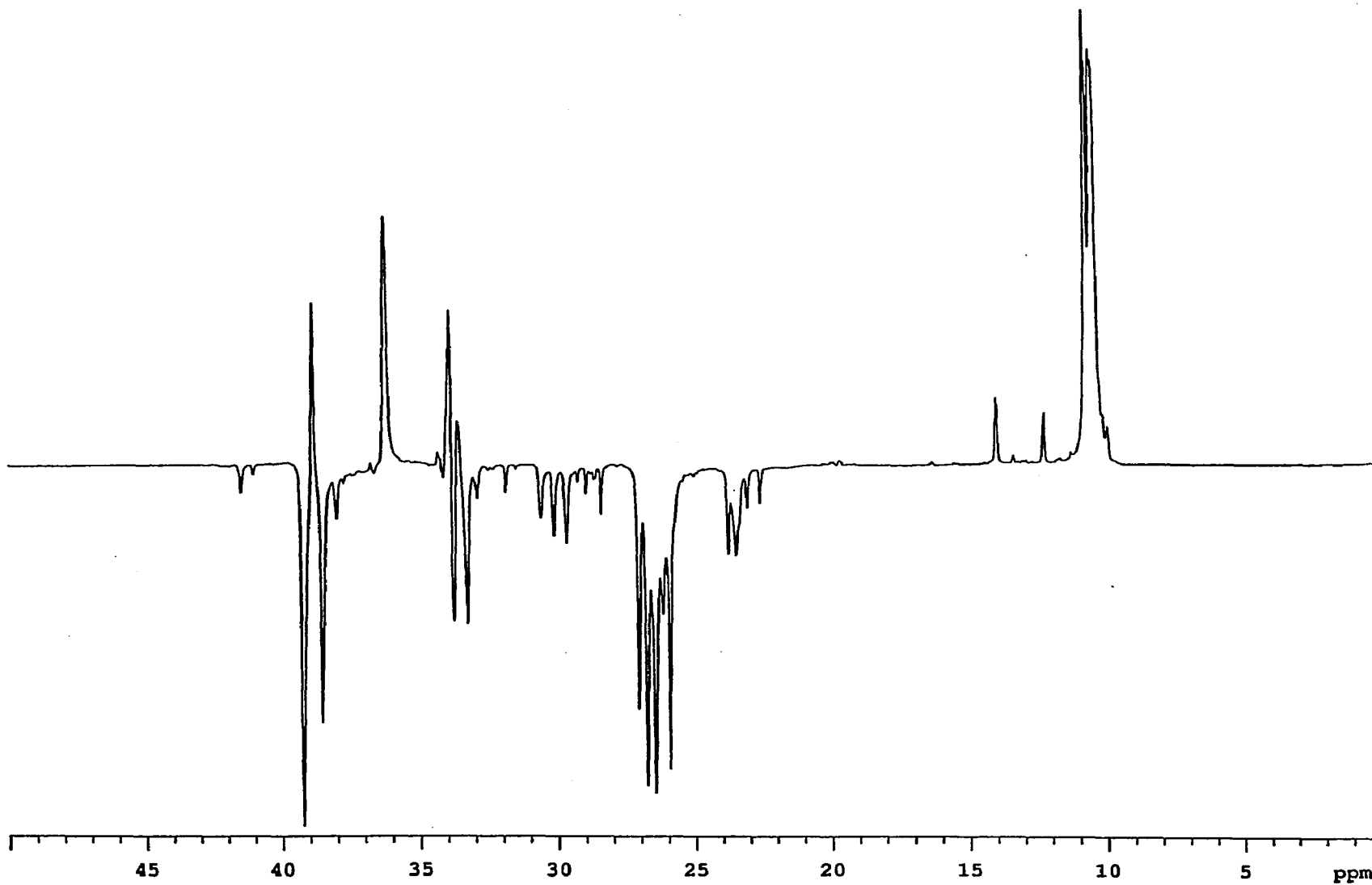


Figure 20  $^{13}\text{C}$  DEPT NMR single bond region of poly(ethylene-co-1-butene) sample 1

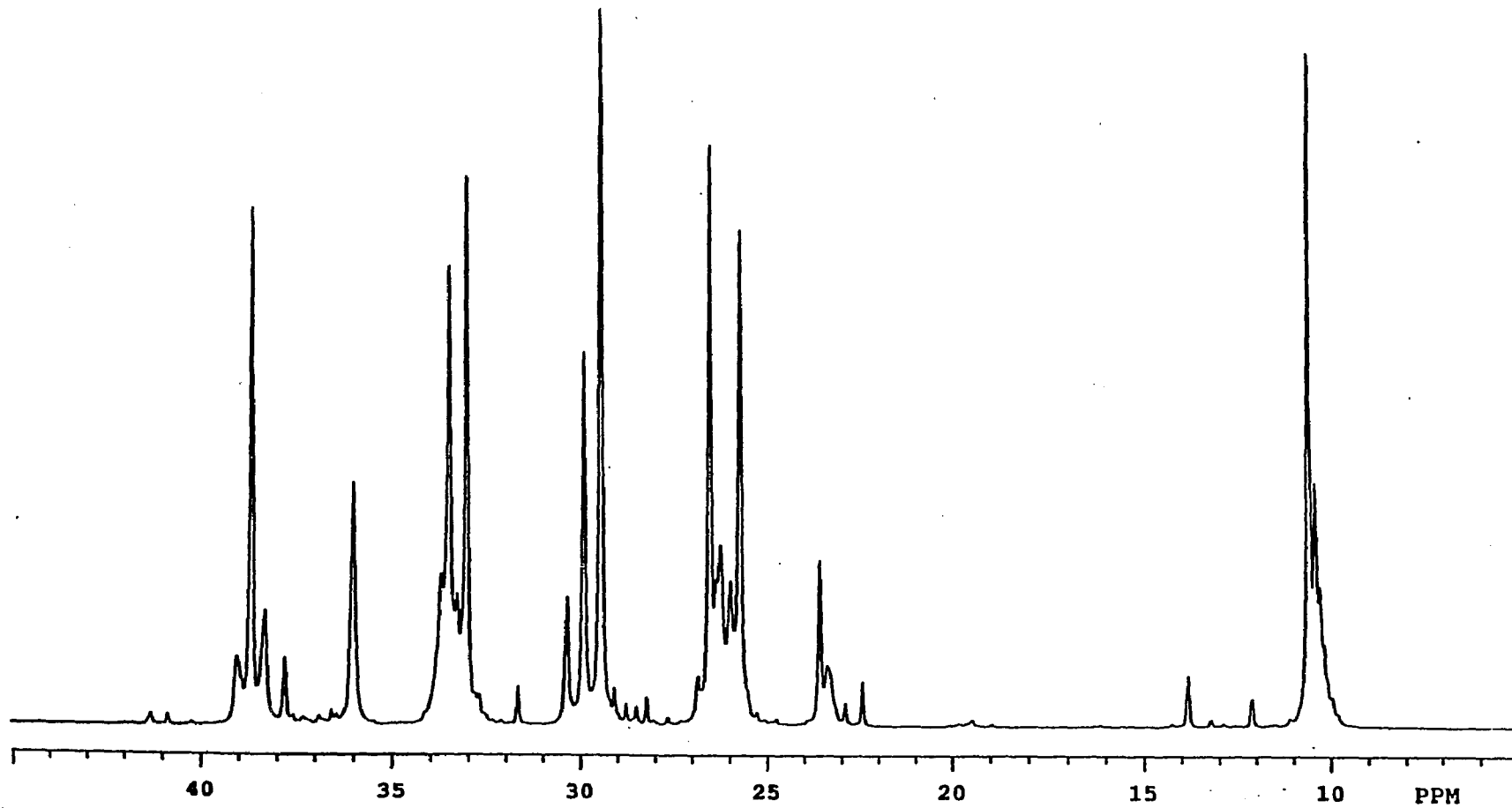


Figure 21  $^{13}\text{C}$  NMR single bond region of poly(ethylene-co-1-butene) sample 2

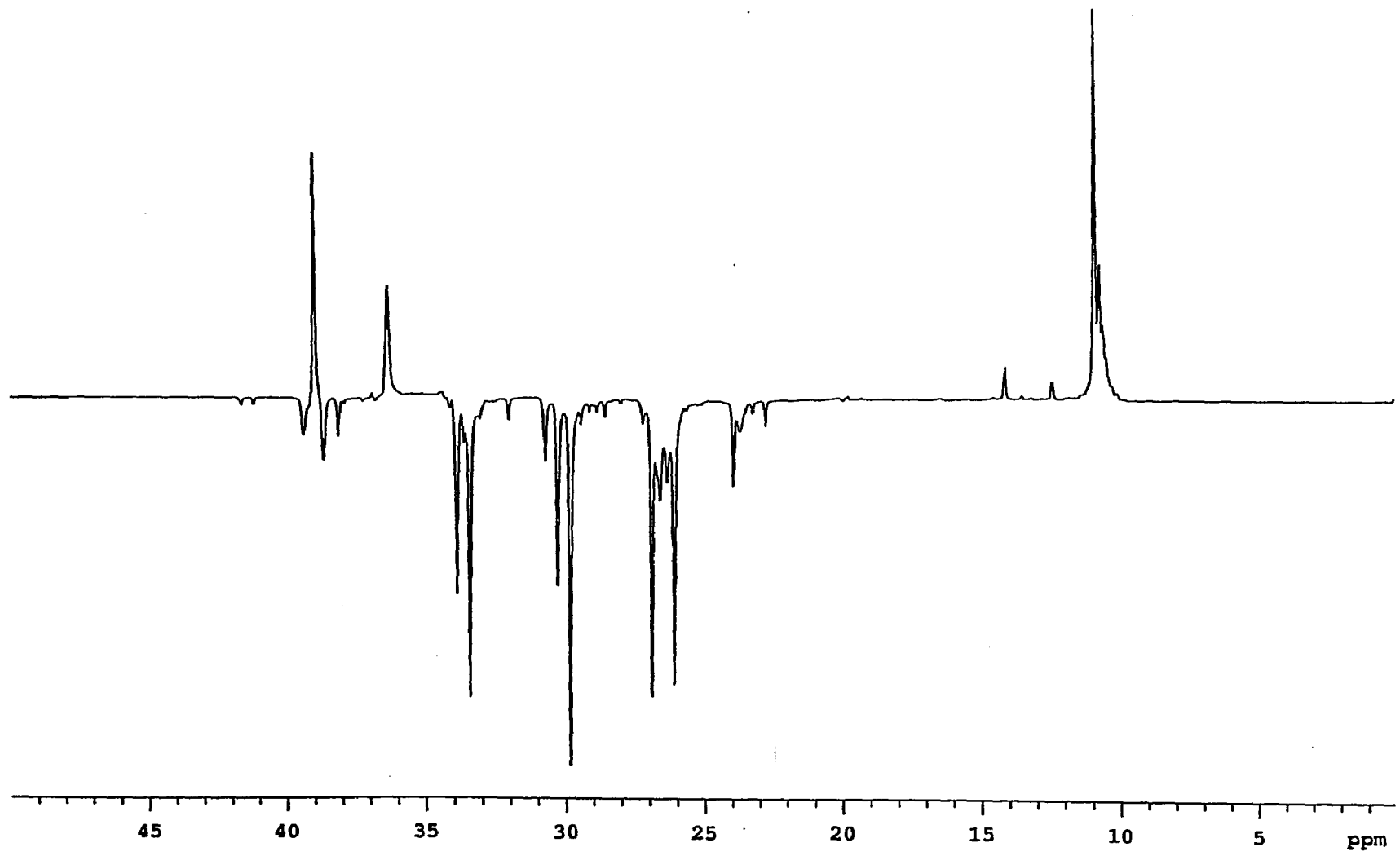


Figure 22  $^{13}\text{C}$  DEPT NMR single bond region of poly(ethylene-co-1-butene) sample 2

differ in the sequence of addition of ethylene and 1-butene monomers. Propagations of **19**, **21**, **16**, and **17** result in saturated end groups **7A**, **8A**, **9A**, **10A**, and **11** respectively (Scheme VIII). Although end groups **9A** and **10A** cannot be distinguished from **7A** and **8A** by NMR, the catalytic efficiency of the polymerization reaction indicates that initiation is carried to better than 99.99% by **19** and **21**, compared to **15** and **16** (and also compared to **17**). On the assumption that each zirconium atom is active, the calculated moles of polymer per mole Zr catalyst is  $1.69 \cdot 10^4$  and  $2.96 \cdot 10^4$  moles of polymer, respectively, for samples 1 and 2. The ratio of **7A**:**8A** is 51:41 and 34:53 for samples 1 and 2, respectively. The increase in this ratio for sample 1 relative to sample 2 is a consequence of the lower ethylene content in the feed for sample 1. The fact that comparable amounts of **7A** and **8A** are formed indicates the much lower reactivity of 1-butene relative to ethylene.

The major unsaturated end groups are vinylidene end group **1** and **2**, which are formed by  $\beta$ -hydride transfer from propagating centers **22**, **24**, **26**, and **28** (eqs 17, 21, 25, 29 of Scheme IX). All propagating centers leading to vinylidene end groups have 1-butene terminal units, indicating that ethylene terminal units are much more reactive toward propagation relative to  $\beta$ -hydride transfer. Propagating centers **22**, **24**, **26**, and **28** differ only in the identity of the penultimate and pen-penultimate units. Vinylidene end group **1** is formed in excess over vinylidene end group **2** (Table 11), indicative of the increased tendency of propagating chains rich in 1-butene units at penultimate and pen-penultimate positions to undergo  $\beta$ -hydride transfer.

The second most abundant unsaturated end groups, trisubstituted double bonds **3** and **4**, are formed by  $\beta$ -hydride transfer from species **23**, **25**,

27, and 29.<sup>(61)</sup> Species 23, 25, 27 and 29 are formed either by rearrangement of propagating species 22, 24, 26, and 28, respectively, or by reverse addition of zirconium hydride to vinylidene end groups 1A, 1B, 2A, and 2B, respectively.  $\beta$ -Hydride transfers from *b* and *c* of species 23 yield 4A and 4C (eqs 19, 20).  $\beta$ -Hydride transfers from *b* and *c* of species 25 yield 4B and 4D (eqs 23, 24).  $\beta$ -Hydride transfers from *b* and *c* of species 27 yield 3A and 3C (eqs 27, 28).  $\beta$ -Hydride transfers from *b* and *c* of species 29 yield 3B and 3D (eqs 31, 32).

<sup>1</sup>H NMR detected very small amounts of vinyl and vinylene end groups (Table 11). The amounts were so low (no more than about 1% each) that no vinyl signals were observed in the <sup>13</sup>C NMR spectra. The most probable route to vinyl end groups is  $\beta$ -hydride transfer from propagating chains possessing ethylene as the terminal unit (30, eq 33). An alternate route to vinyl end groups is  $\beta$ -ethyl transfer from propagating species with 1-butene as the terminal unit (22, 24, 26, and 28, eq 38 in Scheme X). The very low vinyl content (0 and 0.4% for samples 1 and 2, respectively) indicates the almost complete absence of  $\beta$ -ethyl transfer reactions. Propagating chains with ethylene as the terminal unit do not undergo  $\beta$ -hydride transfer.

$\beta$ -Hydride transfer occurs almost exclusively through propagating chains possessing 1-butene terminal units. The very small amount of vinylene end groups (1.0 and 1.4% for samples 1 and 2, respectively) indicates the almost negligible extent of the transfer reactions described by eqs 35-37. Again, there is negligible  $\beta$ -hydride transfer from propagating chains possessing ethylene as the terminal units (eqs 33, 35). Further, the very small amount of vinylene end groups indicates there is very little  $\beta$ -hydride transfer from

propagating centers of type **32** (eqs 36 and 37), formed by reverse (2,1) addition of 1-butene to propagating centers.

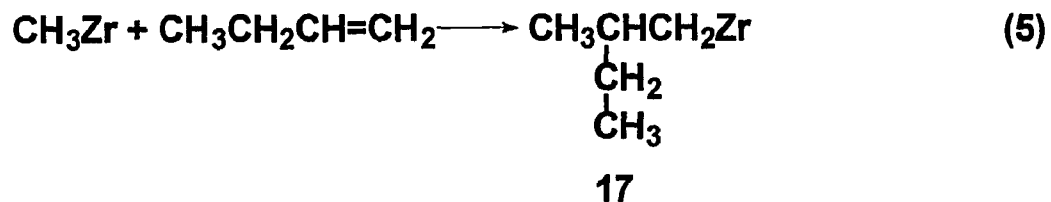
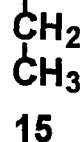
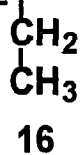
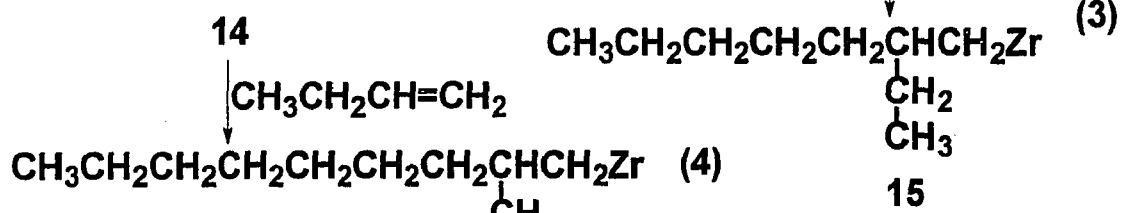
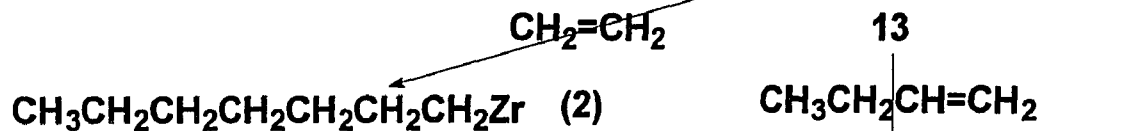
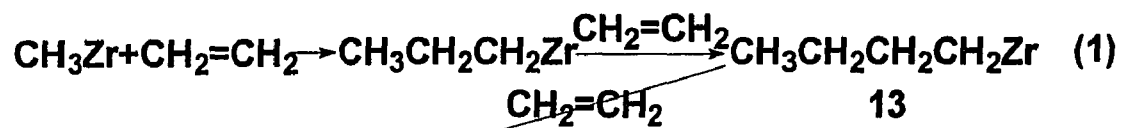
Saturated end groups are formed by the initiation processes as described above. However, chain transfer to aluminum (eqs 39-40, 41-42, 43-44) is a possible second route to saturated end groups. Chain transfer to aluminum involves ligand exchange between zirconium and aluminum from propagating chains terminating in ethylene (eqs 39, 41) or 1-butene (eq 43). The aluminum terminated polymers (**34**, **36**, and **37**) are converted to polymer with saturated end groups (**7B**, **8B**, **9B**, **10B**, and **11B**) when the reaction mixture is hydrolyzed. Saturated end groups **7B**, **8B**, **9B**, **10B**, and **11B**, formed by chain transfer to aluminum, are spectroscopically indistinguishable from **7A**, **8A**, **9A**, **10A**, and **11A**, respectively, formed by the initiation reactions, and this does not allow any conclusion regarding the occurrence of chain transfer to aluminum for propagating chains terminating in ethylene. By analogy to their lack of any tendency toward  $\beta$ -hydride transfer, it is reasonable to conclude that propagating chains terminating in ethylene also do not undergo chain transfer to aluminum because of their high reactivity toward propagation. On the other hand, the amount of saturated end groups **11** is very much larger than can be accounted for by initiation with  $\text{CH}_3\text{Zr}$ . The high catalytic efficiency ( $1.69 \cdot 10^4$  and  $2.96 \cdot 10^4$  moles of polymer per mole of Zr catalyst for samples 1 and 2, respectively) coupled with the significant amounts of saturated end groups **11** (8 and 13% of saturated end groups, respectively, for samples 1 and 2) shows that less than 0.1% of saturated end group **11** (sum of **11A** and **11B**) is formed via initiation by  $\text{CH}_3\text{Zr}$ . More than 99.9% of saturated end group **11** is formed by chain

transfer to aluminum for propagating chains terminating in 1-butene, i.e., there is negligible amount of 11A.

The extent of chain transfer to aluminum for propagating chains terminating in 1-butene is compatible with both the amount of saturated end groups **11B** (8 and 13% of total saturated end groups for samples 1 and 2, respectively) and the ratio of saturated to unsaturated end groups (1.1-1.2:1). Each act of chain transfer to aluminum produces two saturated end groups, one at the terminated propagating chain end and the other occurs when  $\text{CH}_3\text{Zr}$  initiates a new propagating chain. The presence of 8 and 13% of saturated end groups **11B**, respectively, corresponds to 8 and 13% excess of saturated end groups over unsaturated end groups, close to the 10-20% excess experimentally observed.

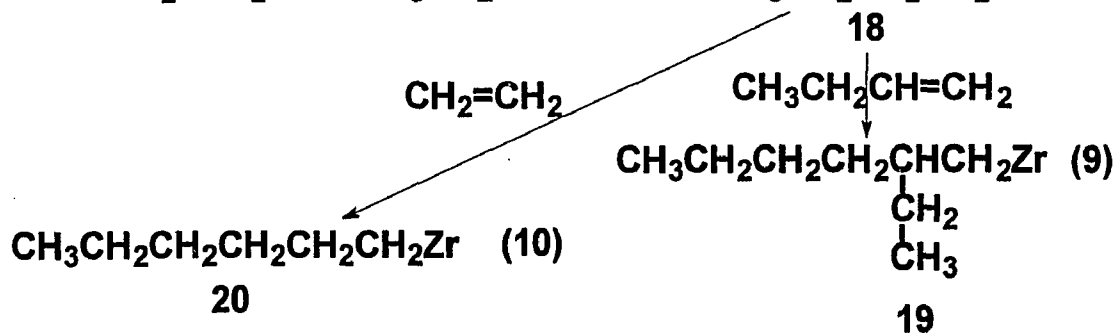
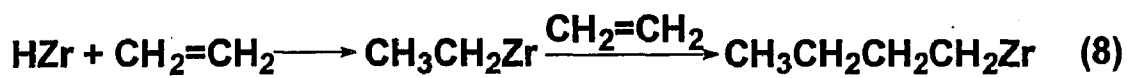
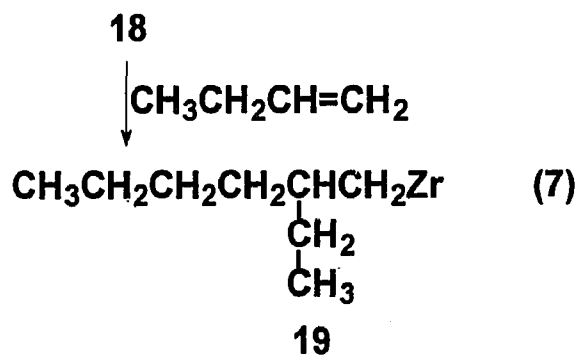
The data on the excess of saturated over unsaturated end groups also yields information on the possibility of long chain branching in the ethylene-1-butene copolymer samples. If vinyl end groups **6** were formed (via  $\beta$ -hydride transfer occurred from propagating chains terminating in ethylene, eq 33 in Scheme IX), subsequent copolymerization of the resulting vinyl-terminated macromer with ethylene and 1-butene would introduce a long chain branch (along with a saturated end group) into the propagating chain. Each incorporated vinyl-terminated macromer would increase the ratio of saturated to unsaturated end groups. There were only negligible amounts (<1%) of vinyl end groups found in the copolymer samples. If significant amounts of vinyl end groups, comparable to the vinylidene or trisubstituted end groups, formed and copolymerized during the reaction, the excess of saturated over unsaturated end groups would be considerably higher than

experimentally observed. The observed excess of saturated over unsaturated end groups is accounted for almost entirely, within experimental error, by chain transfer to aluminum. If there is the formation and copolymerization of vinyl terminated macromer, we estimate that the upper limit for long chain branching is no more than 2-3 long chain branches per 500 monomer units. This amount of long chain branching cannot be excluded, it is within the limits of the NMR analysis for end groups in these samples.

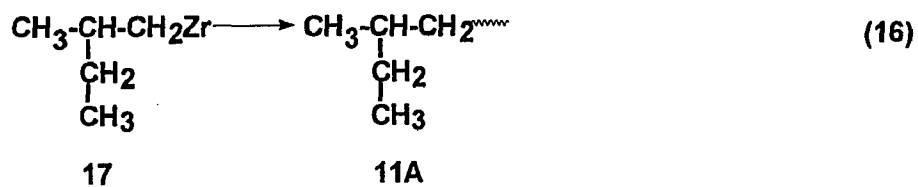
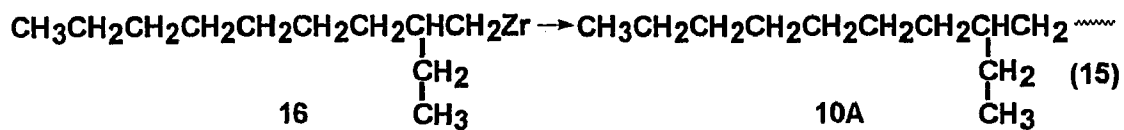
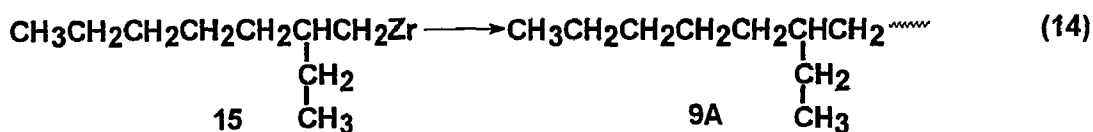
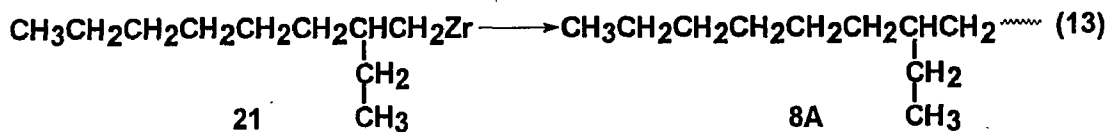
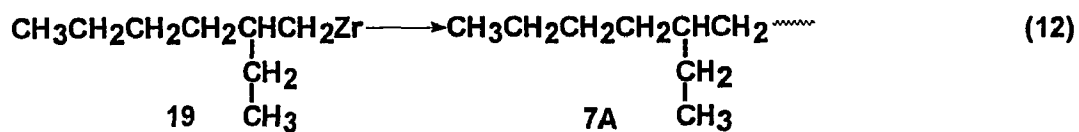
Scheme VIIA Initiation by CH<sub>3</sub>Zr

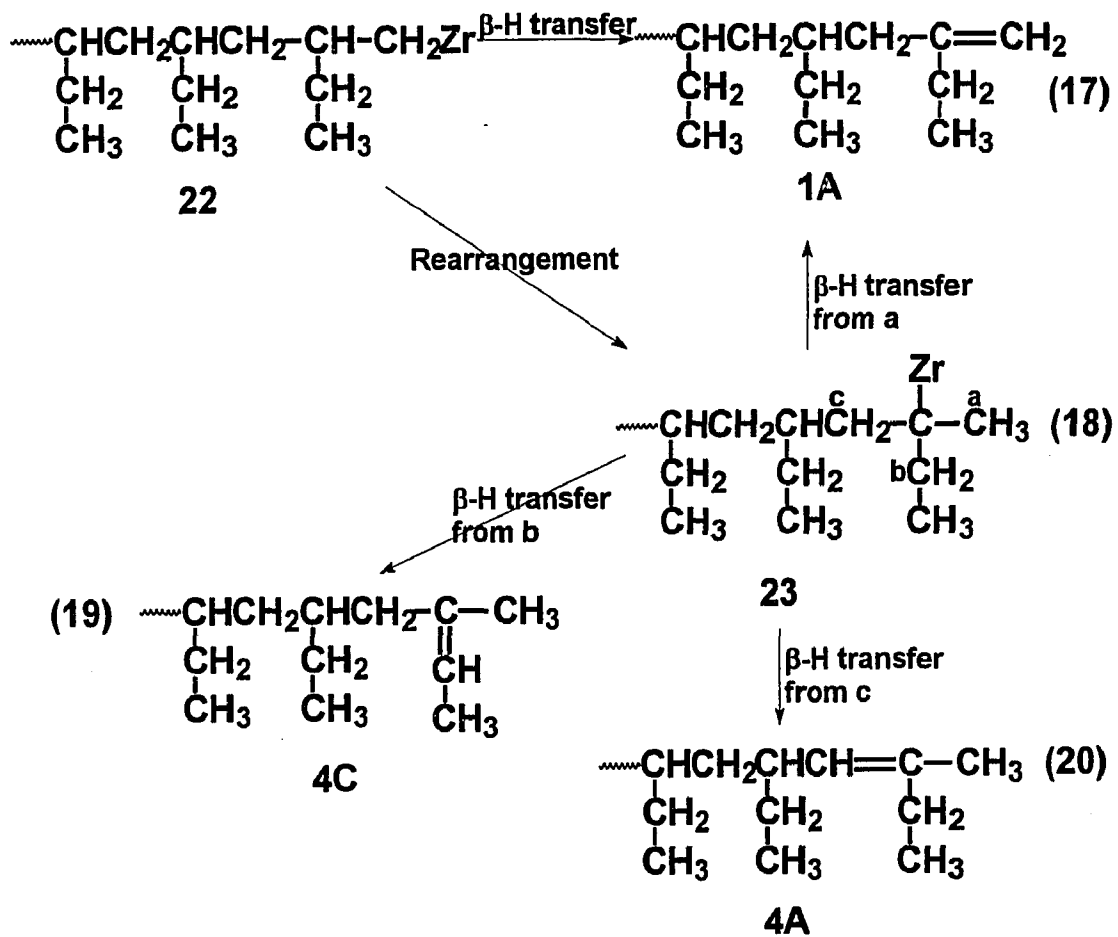
17

## Scheme VIIB Initiation by HZr

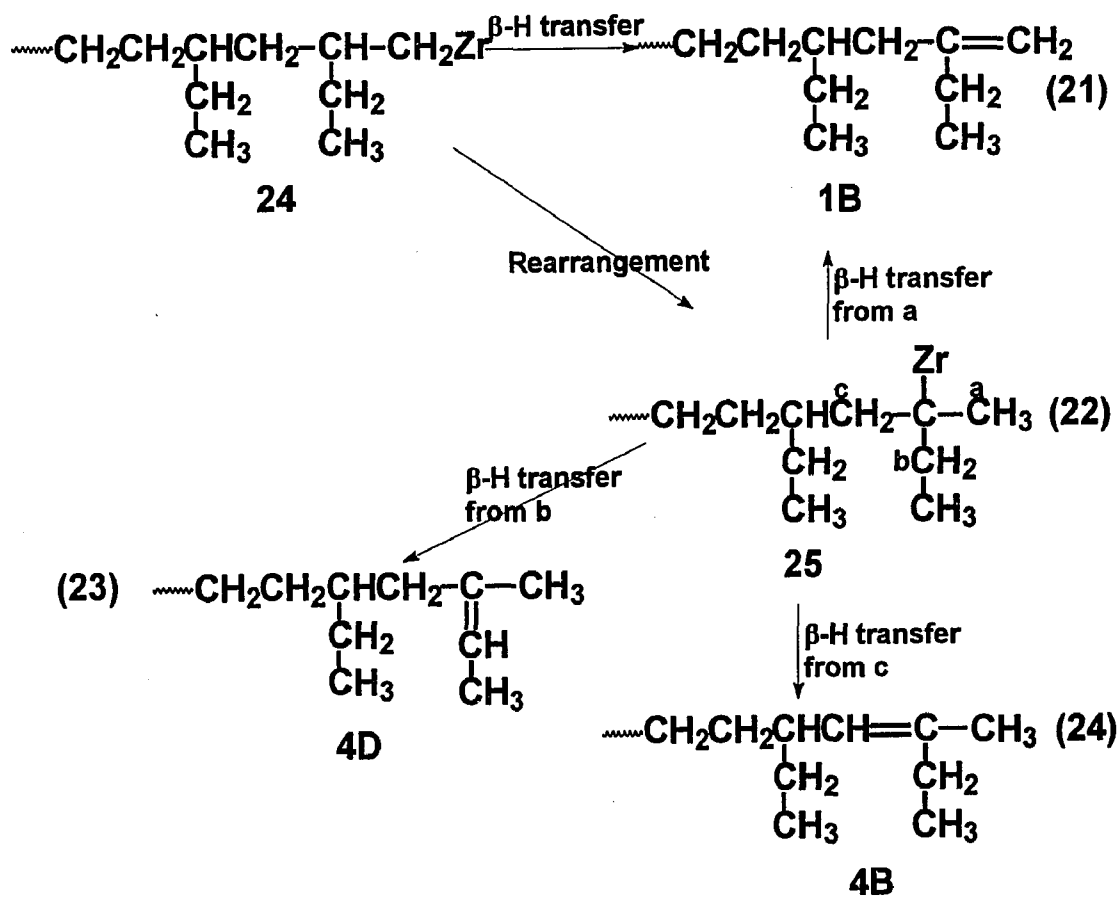


## Scheme VIII Propagation Reactions

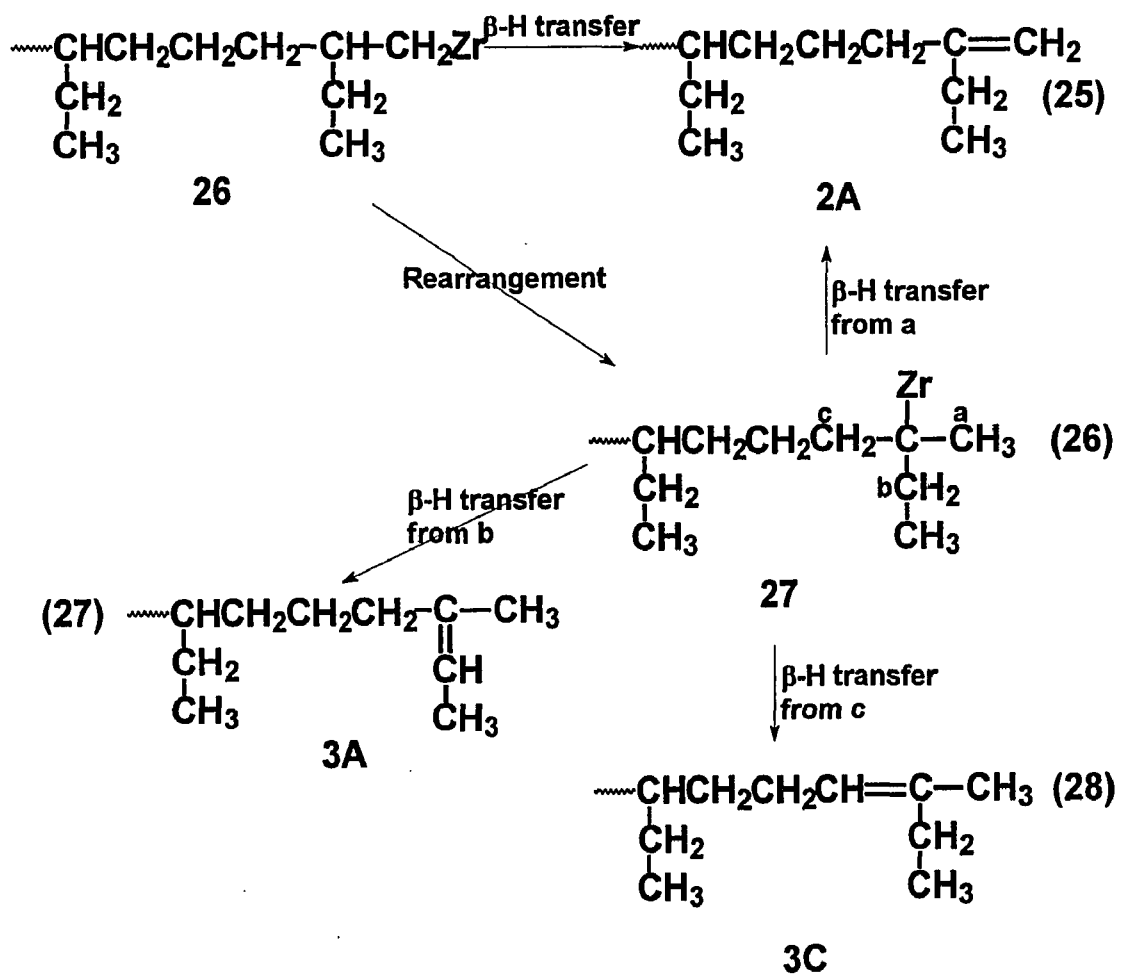


Scheme IX  $\beta$ -Hydride Transfer Reactions

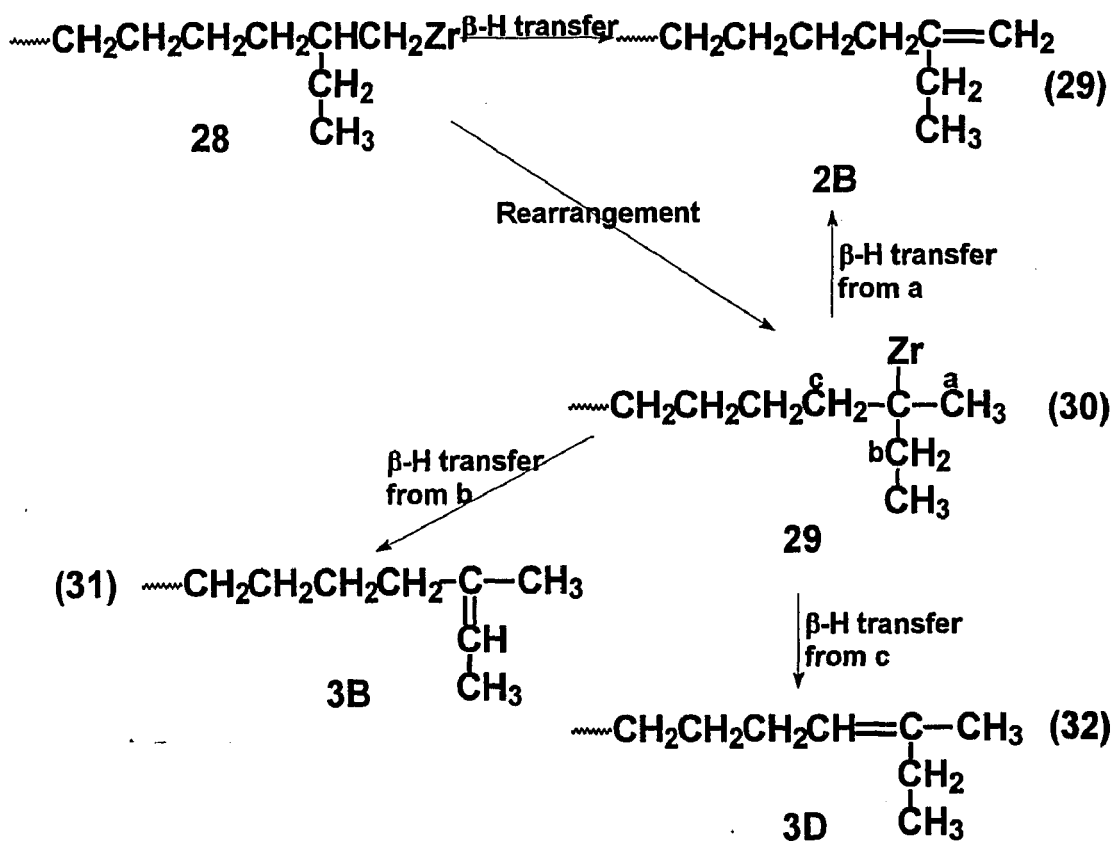
## Scheme IX (continued)



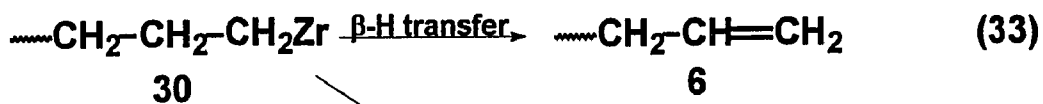
## Scheme IX (continued)



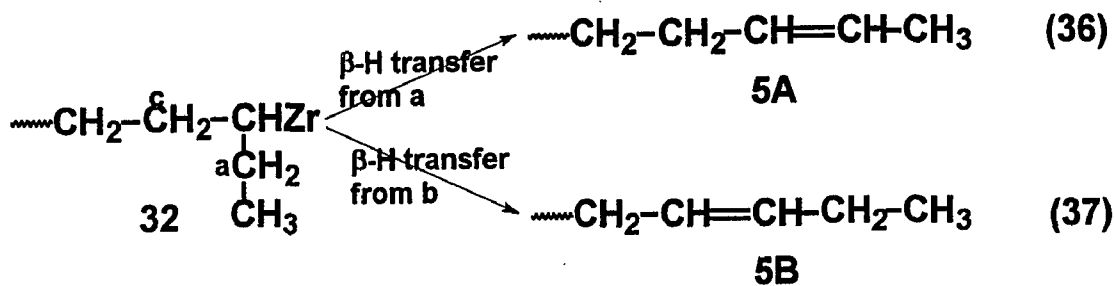
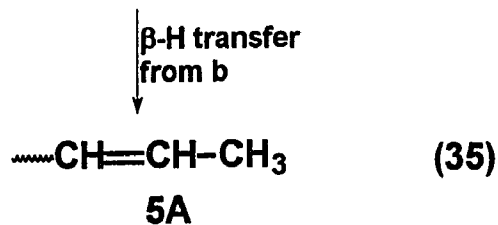
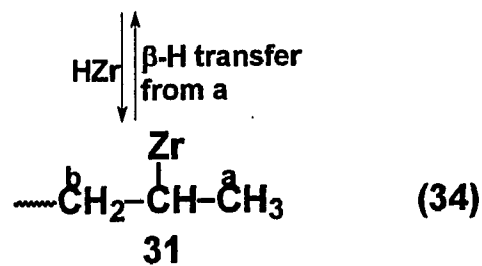
## Scheme IX (continued)



## Scheme IX (continued)

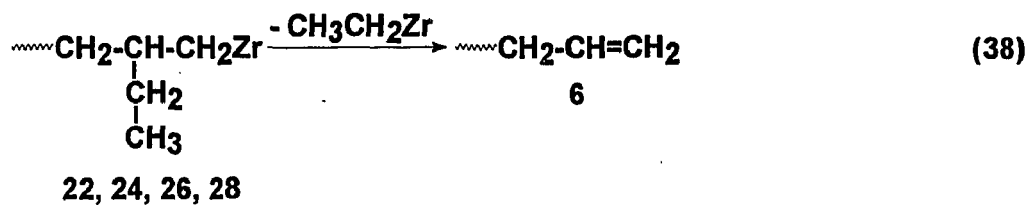


Rearrangement

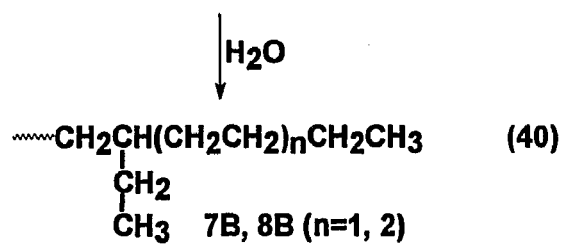
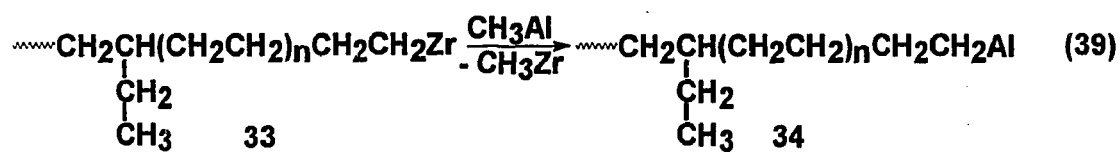


5B

## Scheme X Other Chain Transfer Reactions

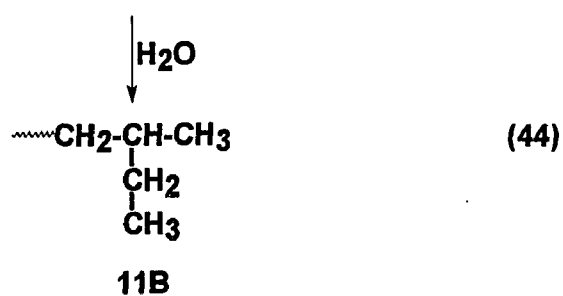
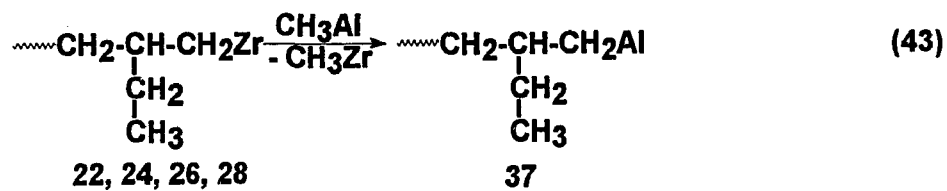
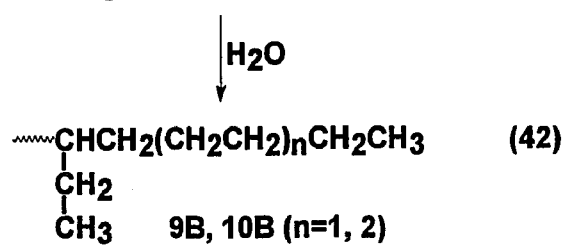
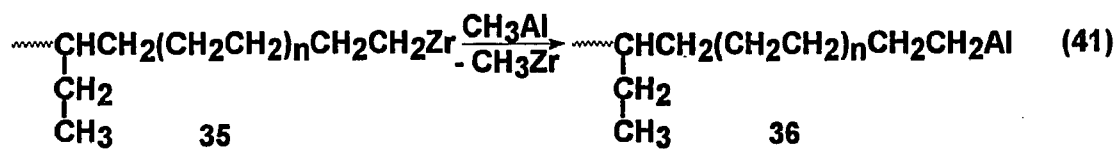
 $\beta$ -Ethyl Transfer

## Transfer to aluminum



## Scheme X (continued)

Transfer to aluminum



## 6.0 Results and Discussion on Microstructure of Poly(1-butene)

### Synthesized under Different Polymerization Conditions

#### 6.1 Double bond end groups

##### 6.1.1 <sup>1</sup>H NMR results

Our previous analysis on microstructures of poly(1-butene) synthesized at 100 °C reveals that there are four types of double bond end groups: vinylidene, trisubstituted, vinylene and vinyl. Vinylidene is the major double bond end group(69.7% by <sup>1</sup>H NMR), and trisubstituted is the next abundant double bond end group(26.9%) with vinylene(2.8%) and vinyl(0.6%) being minor double bond end groups.

Different poly(1-butene) samples were synthesized at different polymerization temperatures, different polymerization time and different catalyst concentrations. Figure 23(600 MHz <sup>1</sup>H NMR) shows the double bond region of poly(1-butene) samples synthesized from 5-100 °C with polymerization time of 60 minutes. Table 14 summarized the double bond end group compositions of poly(1-butene) samples by <sup>1</sup>H NMR analysis corresponding to poly(1-butene) samples in Figure 23.

At 65-100 °C polymerization temperature range, the major unsaturated end groups are vinylidene double bond(~83%), with trisubstituted(~14%) double bond being next abundant unsaturated end groups. Vinylene and vinyl at 65-100 °C polymerization temperature range are only minor unsaturated end groups(~1-2% each). With the polymerization temperature decreasing to 50 °C, there is a significant increase in both vinylene and trisubstituted double bonds(vinylene increases from ~2% to ~7%, trisubstituted increases from ~14% to ~23%) with the sacrifice of vinylidene double bond content from

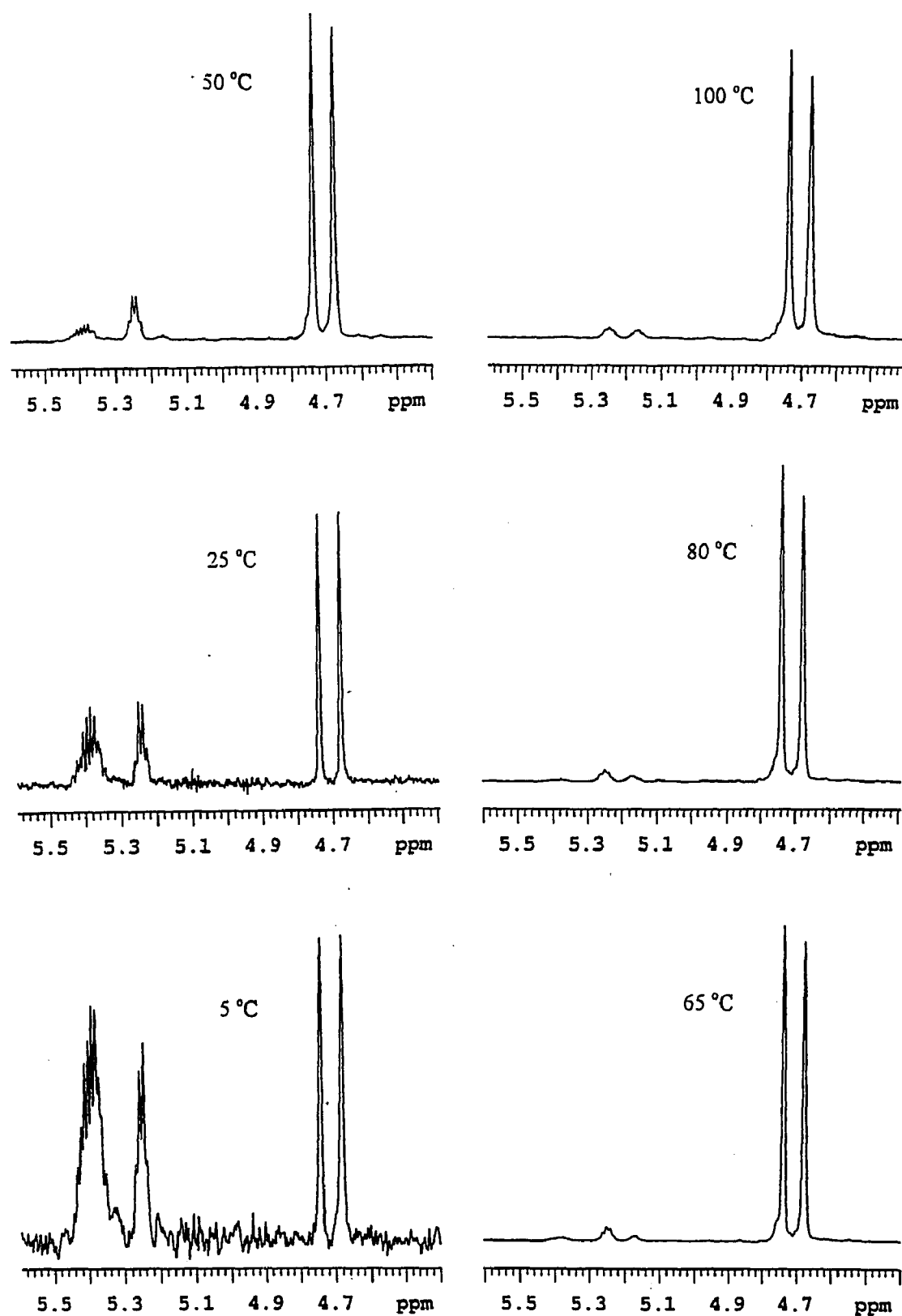


Figure 23.  $^1\text{H}$  NMR double bond regions of poly(1-butene) synthesized at different temperature with 60 minutes polymerization time

Table 14 Double Bond Composition by  $^1\text{H}$  NMR  
for Poly(1-butene) Synthesized at Different Polymerization Temperature\*

	Vinylene	Trisubstituted	Vinyl	Vinylidene
	$\text{R}_1\text{CH}=\text{CHR}_2$	$\text{R}_1\text{CH}=\text{CR}_2\text{R}_3$	$\text{CH}_2=\text{CHR}$	$\text{CH}_2\text{CR}_1\text{R}_2$
100 °C	0.8	14.4	1.7	83.1
80 °C	1.1	13.0	0.8	85.1
65 °C	2.4	13.7	1.5	82.4
50 °C	7.1	23.3	2.7	66.7
25 °C	25.7	30.5	0	43.7
5 °C	41.3	33.5	0	25.2

\* Polymerization time is 60 minutes for all six poly(1-butene) samples.  
Zirconium catalyst concentration is  $7.1 \cdot 10^{-6}$  M, the ratio of cocatalyst  
MAO to zirconium catalyst is 1100/1.

~83% to 67%. When the polymerization temperature becomes 25 °C, the contents of vinylene and trisubstituted double bond increase to ~26% and ~30%, with the further sacrifice of vinylidene double bond content from ~67% to ~44%. With the polymerization temperature further decreasing to 5 °C, the vinylene double bond becomes the most abundant unsaturated end group (~41%) with comparable amounts of trisubstituted double bond (~34%) and vinylidene double bond (~25%). During the entire change of polymerization temperatures, there is no significant change in vinyl double bond content. (0% vinyl content for two samples synthesized at 0 and 25 °C only means that there is no visible signal detected for vinyl double bond in <sup>1</sup>H NMR spectra)

Table 15 reveals the double bond end group compositions by <sup>1</sup>H NMR analysis for poly(1-butene) samples synthesized at different temperatures with polymerization time of 10 minutes and 1 minute. Regardless of different polymerization time, the unsaturated end group compositions change in a similar pattern as discussed above with polymerization time of 60 minutes. Figure 24 shows the double bond region of poly(1-butene) samples listed in Table 15.

### 6.1.2 <sup>13</sup>C NMR results

The <sup>13</sup>C NMR analysis on unsaturated end groups of poly(1-butene) samples synthesized at different polymerization conditions provide useful information on not only the changes in double bond compositions as revealed in <sup>1</sup>H NMR analysis, but details on exact identity of each double bond end group. Figure 25 shows the <sup>13</sup>C NMR double bond region of poly(1-butene) samples synthesized from 5-100 °C with polymerization time of 60

Table 15 Double Bond Composition by  $^1\text{H}$  NMR  
for Poly(1-butene) Synthesized at Different Polymerization Temperature\*

	Vinylene	Trisubstituted	Vinyl	Vinylidene
	$\text{R}_1\text{CH}=\text{CHR}_2$	$\text{R}_1\text{CH}=\text{CR}_2\text{R}_3$	$\text{CH}_2=\text{CHR}$	$\text{CH}_2\text{CR}_1\text{R}_2$
80 °C	1.0	13.1	1.8	84.1
50 °C	8.7	18.7	2.5	70.1
25 °C	28.8	36.9	0	34.3
80 °C	3.2	14.5	0.9	81.4
50 °C	12.0	22.3	3.5	62.2
25 °C	29.3	38.5	0	32.2

\* Polymerization time is 10 minutes for first three poly(1-butene) samples, 1 minute for the rest of samples. Zirconium catalyst concentration is  $7.1 \cdot 10^{-6}$  M, the ratio of cocatalyst MAO to zirconium catalyst is 1100/1.

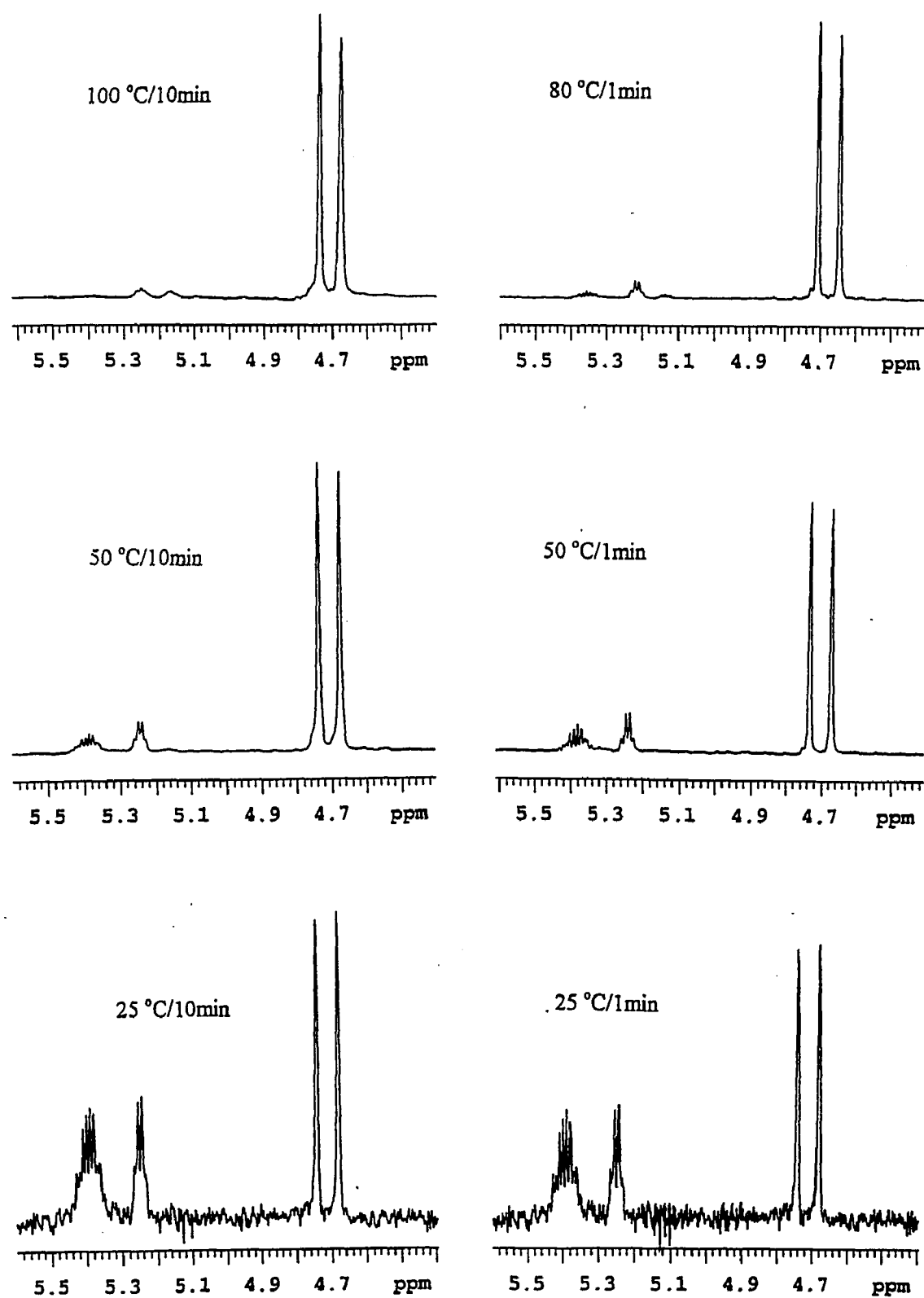


Figure 24.  $^1\text{H}$  NMR double bond region of poly(1-butene) synthesized at different temperature with 10 & 1 minutes polymerization time

minutes. Table 16 summarizes the exact double bond end group types and their compositions by  $^{13}\text{C}$  NMR analysis corresponding to poly(1-butene) samples in Figure 25.

At 65-100 °C polymerization temperature range, the major unsaturated end groups are vinylidene double bond (~80%). At 100 °C, vinylidene 1 is the most abundant vinylidene double bond with vinylidene 2 being minor vinylidene double bond. At 80 °C, vinylidene 1 remains to be the major vinylidene with vinylidene 2 decreasing significantly. At 65 °C, vinylidene 1 becomes completely dominant vinylidene with almost no vinylidene 2 existing. At 65-100 °C polymerization temperature range, the second abundant unsaturated end group is trisubstituted double bond. There are trisubstituted double bond end groups 4, 5, and 6 existing in this temperature range. The minor unsaturated end group detected by  $^{13}\text{C}$  NMR is vinylene 9.

With the polymerization temperature decreasing to 50 °C, vinylidene 1 becomes the only vinylidene double bond end group, and there exist only two trisubstituted double bond end groups 5 and 6 with 4 disappearing almost completely. At 50 °C, vinylene 9 increases significantly to almost comparable amount as trisubstituted double bond end group 5. When polymerization temperature decreases to 25 °C, 5 becomes the only remaining trisubstituted double bond end group, and vinylene 9 further increases to exceed 5 in concentration. With polymerization temperature further decreasing to 5 °C, vinylene 9 becomes the most abundant unsaturated end group with remaining to be only trisubstituted double bond end group 5 and vinylidene double bond end group 1.

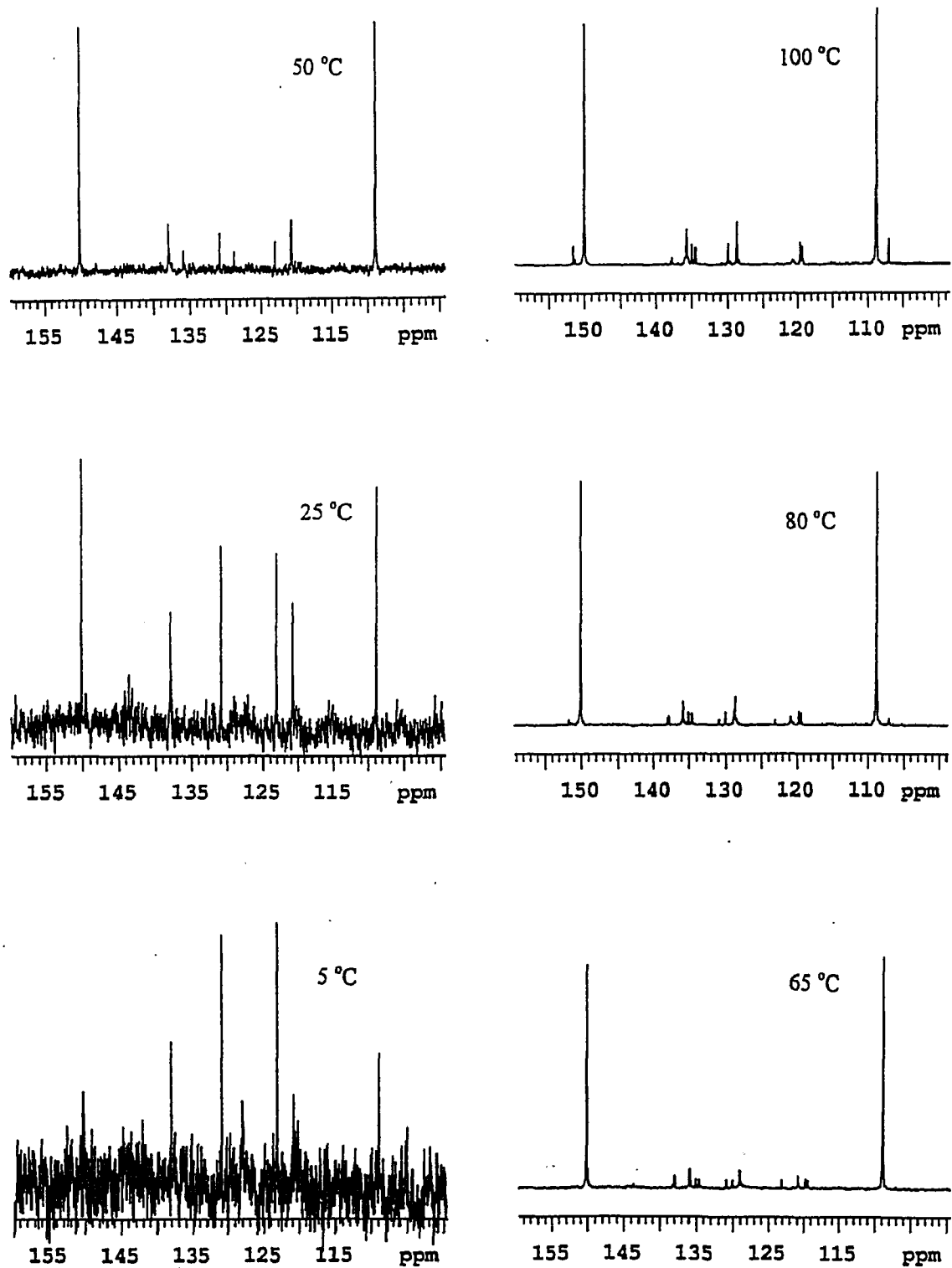


Figure 25.  $^{13}\text{C}$  NMR double bond region of poly(1-butene) synthesized at different temperature with 60 minutes polymerization time

Table 16 Assignments and Compositions of Double Bond  
End Groups by  $^{13}\text{C}$  NMR Analysis

$\delta(\text{ppm})$	Assignments	Percentages(%) at different temperatures					
		100°C	80°C	65°C	50°C	25°C	5°C
152.3	2	4.0	2.0	0	0	0	0
150.5	1	74	77	78	63	40	23
138.3	5	0.8	3.0	5.6	21	33	34
136.3	6 <sub>t,c</sub>	13	10	8.4	6	0	0
135.5	4 <sub>t</sub>	4.4	4.0	3.7	1.0	0	0
135.0	4 <sub>c</sub>	3.6	3.0	2.3	1.0	0	0
131.3	9 or 10	0.2	1.0	2.0	8	27	43
130.5	6 <sub>c</sub>	5.5	4.9	3.5	1.0	0	0
129.3	6 <sub>t</sub>	6.5	5.1	4.9	5.0	0	0
123.5	9 or 10	0.2	1.0	2.0	8.0	27	43
121.3	5	0.8	3.0	5.6	21	33	34
120.2	4 <sub>t</sub>	4.4	4.0	3.7	1.0	0	0
119.9	4 <sub>c</sub>	3.6	3.0	2.3	1.0	0	0
109.4	1	74	77	78	63	40	23
107.5	2	4	2.0	0	0	0	0

### 6.1.3 Discussion in terms of chain transfer reactions

Different chain transfer reactions are described in Scheme V.

At 65-100 °C polymerization temperature range, chain transfer reaction (5) yields unsaturated end groups **1**, (6) and (7) yield **4**, (6) and (8) yield **6**, (9) yields **2**, (10) and (11) yield **5**, and (13) yields **9**. All these chain transfer reactions are just different variations of  $\beta$ -Hydride transfer reactions.

At 50 °C polymerization temperature, chain transfer reactions (7) and (9) become unimportant. When polymerization temperature decreases to 25 and 0 °C, (7), (8) and (9) three chain transfer reactions become unimportant. But no matter at what polymerization temperature between 0-100 °C,  $\beta$ -Hydride transfer reaction is the only important type of chain transfer reaction in 1-butene polymerization initiated by our zirconium metallocene catalyst. This conclusion is consistent with those documented in the literature for this type of metallocene catalyst system.

### 6.2 Saturated end groups

<sup>13</sup>C NMR spectrum single bond regions of poly(1-butene) samples shows unambiguously that regardless of polymerization conditions, the major saturated end group is **12**, referred to as n-butyl saturated end group. **13** and **14** are minor saturated end groups(See section 4.1.5). The ratios of **12:13** and **12:14** remain almost unchanged with decreasing polymerization temperature. Table 17 summarizes the relative ratios of **12:14** for samples synthesized at different polymerization temperatures with 60 minutes polymerization time.

The total content of saturated end groups is still slightly higher than the total content of unsaturated end groups, indicating that chain transfer to

Table 17 Compositions of Saturated End Groups  
for Poly(1-butene) Synthesized at Different Polymerization Temperature\*

Polymerization temperature	Ratio of Saturated End group <b>12:14</b>
100 °C	10:1
80 °C	10:1
65 °C	10:1
50 °C	10:1
25 °C	10:1
5 °C	10:1

\* Polymerization time is 60 minutes for all six poly(1-butene) samples.  
Zirconium catalyst concentration is  $7.1 \cdot 10^{-6}$  M, the ratio of cocatalyst MAO to zirconium catalyst is 1100/1.

aluminum and/or chain transfer to vinylidene end groups have to be counted at 0-100 °C polymerization temperature range, even though they are just minor chain transfer reactions.

### 6.3 Structure of repeat units

#### 6.3.1 Stereoselectivity

Figure 26 illustrates  $^{13}\text{C}$  NMR region of the side chain methylene carbon for poly(1-butene) samples synthesized at different polymerization temperatures (with 60 minutes polymerization time). The stereoisomeric pentad fractions and overall racemic fractions corresponding to poly(1-butene) samples shown in Figure 26 are listed in Tables 18-23.

At 100 °C polymerization temperature, the isotacticity of the poly(1-butene) sample is extremely low (~22%), which can be explained by the effect of reverse repeat units. When the polymerization temperature decreases to 80 °C, the isotacticity increases dramatically to about 76%. With 5 °C polymerization temperature, the isotacticity reaches the level close to 100%. The general trend is that the isotacticity of poly(1-butene) samples increases accordingly with the decreasing polymerization temperature (100-5 °C).

#### 6.3.2 Regioselectivity

Figure 27 illustrates the main chain methylene and methine region of  $^{13}\text{C}$  NMR spectra for poly(1-butene) samples synthesized at different polymerization temperatures (with 60 minutes polymerization time). The ratio of signal area at 36.8 ppm (BBBBB) to signal area of repeat unit methine carbons represent the percentage of reverse repeat units. Table 24 summarizes the percentage of repeat unit according to different polymerization temperature. With 100 °C polymerization temperature, the

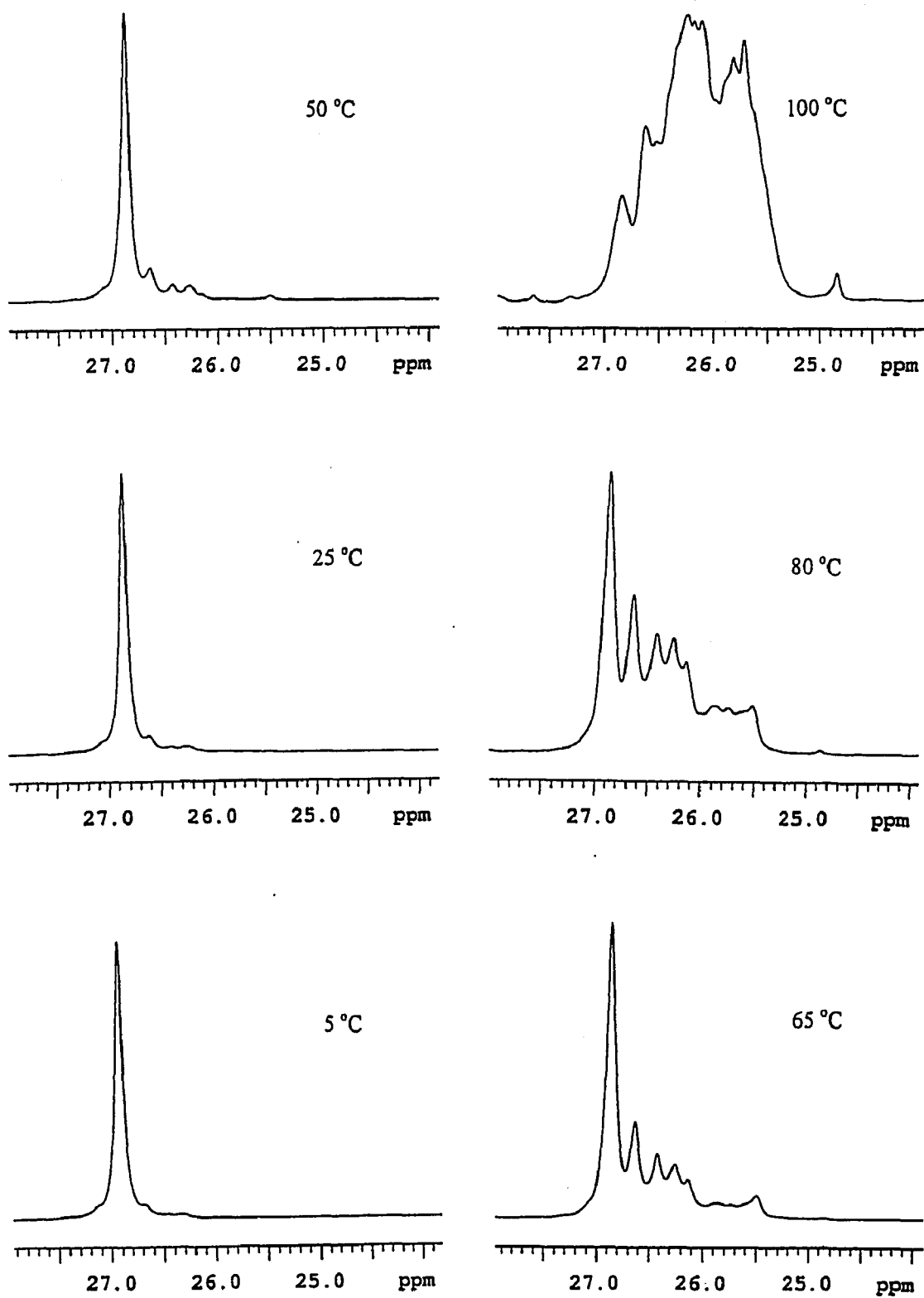


Figure 26.  $^{13}\text{C}$  NMR side chain methylene region (pentad fractions) of poly(1-butene) synthesized at different temperature with 60 minutes polymerization time

Table 18 Pentad and Racemic Fractions of Poly(1-butene)  
Synthesized at 100 °C with 60 minutes of Polymerization Time

Pentad	$\delta$ (ppm)	Fraction
mmmm	27.1	0
mmmr	26.9	0
rmmr		
mmrr	26.7	0
mmrm		
rmrr	26.6	0.116
mrmr	26.4	0.333
rrrr		
mrrr	26.1	0.551
mrrm		
Dyad		Fraction
m		0.22*
r		0.78

\* The m dyad fraction should not be less than 0.50 for our poly(1-butene) samples. The number 0.22 may be caused by the shift of NMR signals due to the large amount of reverse repeat units (Table 24).

Table 19 Pentad and Racemic Fractions of Poly(1-butene)  
 Synthesized at 80 °C with 60 minutes of Polymerization Time

Pentad	$\delta$ (ppm)	Fraction
mmmm	27.1	0.392
mmmr	26.9	0.169
rmmr		
mmrr	26.7	0.184
mmrm		
rmrr	26.6	0.120
mrrr	26.4	0.090
rrrr		
mrrr	26.1	0.045
mrrm		
Dyad		Fraction
m		0.76
r		0.24

Table 20 Pentad and Racemic Fractions of Poly(1-butene)  
 Synthesized at 65 °C with 60 minutes of Polymerization Time

Pentad	$\delta$ (ppm)	Fraction
mmmm	27.1	0.565
mmmr	26.9	0.143
rmmr		
mmrr	26.7	0.116
mmrm		
rmrr	26.6	0.101
mrrr	26.4	0.045
rrrr		
mrrr	26.1	0.030
mrrm		
Dyad		Fraction
m		0.84
r		0.16

Table 21 Pentad and Racemic Fractions of Poly(1-butene)  
Synthesized at 50 °C with 60 minutes of Polymerization Time

Pentad	$\delta(\text{ppm})$	Fraction
mmmm	27.1	0.827
mmmr	26.9	0.066
rmmr		
mmrr	26.7	0.033
mmrm		
rmrr	26.6	0.056
mrmr	26.4	0.005
rrrr		
mrrr	26.1	0.013
mrrm		
Dyad		Fraction
m		0.94
r		0.06

Table 22 Pentad and Racemic Fractions of Poly(1-butene)  
 Synthesized at 25 °C with 60 minutes of Polymerization Time

Pentad	$\delta(\text{ppm})$	Fraction
mmmm	27.1	0.899
mmmr	26.9	0.041
rmmr		
mmrr	26.7	0.014
mmrm		
rmrr	26.6	0.041
mrmr	26.4	0
rrrr		
mrrr	26.1	0.005
mrrm		
Dyad	Fraction	
m	0.97	
r	0.03	

Table 23 Pentad and Racemic Fractions of Poly(1-butene)  
 Synthesized at 5 °C with 60 minutes of Polymerization Time

Pentad	$\delta(\text{ppm})$	Fraction
mmmm	27.1	0.990
mmmr	26.9	0.010
rmmr		
mmrr	26.7	0
mrrm		
rmrr	26.6	0
rrmr	26.4	0
rrrr		
mrrr	26.1	0
mrrm		
Dyad	Fraction	
m	0.99	
r	0.01	

reverse repeat unit comprises of about 34% of entire repeat units. When polymerization temperature drops to 80 °C, the percentage of reverse repeat units decreases sharply to 11%. With the further decreasing of polymerization temperature, the percentage of reverse repeat units further decreases. When polymerization temperature drops to 5 °C, the percentage of reverse repeat unit becomes only 0.3%.

The general trends for the effects of polymerization temperature on stereoselectivity and regioselectivity are: the lower the polymerization temperature, the higher the stereoselectivity and regioselectivity in terms of isotactic content and normal monomer addition(1,2-addition) respectively.

Most of literature studies of temperature effects on stereoselectivity of  $\alpha$ -olefin polymerization were performed on propylene polymerization.<sup>(23, 62-64)</sup> Generally, the literature studies reveal similar trend of polypropylene tacticity dependence on polymerization temperature as our studies on 1-butene polymerization regardless of the identity of their homogeneous catalyst. The mmmm pentad fraction of polypropylene has been reported to be 98% and 96%, at 0 °C and 80 °C polymerization temperature respectively, using *rac*-dimethyl-silybis(2-methyl-4-*t*-butyl-cyclopentadienyl)zirconium dichloride/MAO catalyst system by Rieger et al.<sup>(62)</sup>

The literature regioselectivity studies of  $\alpha$ -olefin polymerization using homogeneous metallocene catalysts reveal mixed results. For propylene polymerization, Brintzinger et al. has reported the occurrence of reverse repeat unit(2,1-insertion) using catalysts *rac*-Me<sub>2</sub>Si(Benz[e]Indenyl)<sub>2</sub>ZrCl<sub>2</sub>/MAO (**BI**) and *rac*-Me<sub>2</sub>Si(2-Me-Benz[e]Indenyl)<sub>2</sub>ZrCl<sub>2</sub>/MAO (**MBI**)<sup>(65)</sup>. But the trend of dependence of 2,1-insertion on temperature is just the

opposite of what we observed in 1-butene polymerization, e.g., lower the polymerization temperature, higher the 2,1-insertion percentage. Busico et al. reported to observe both reverse(2,1-insertion) repeat units and 1,3 repeat units formed through monomer isomerization for propylene polymerization using *rac*-(Ethylene)bis(1-indenyl)ZrCl<sub>2</sub>/MAO and *rac*-(dimethylsilyl)bis(1-indenyl)ZrCl<sub>2</sub>/MAO catalysts<sup>(66)</sup>. For 1-butene polymerization, Asakura et al. reported the occurrence of reverse repeat units(2,1-insertion) by studying 1-D and 2-D NMR spectra of poly(1-butene) samples prepared by Ti(OC<sub>4</sub>H<sub>9</sub>)<sub>4</sub>/Al<sub>2</sub>(C<sub>2</sub>H<sub>5</sub>)<sub>3</sub>Cl<sub>3</sub>/C<sub>2</sub>H<sub>5</sub>OH catalyst<sup>(67-68)</sup>. Kioka and Busico have reported in separate papers that there occurred both 2,1-insertion and 1,4-insertion in 1-butene polymerization<sup>(69-70)</sup>. Kioka's catalyst is *rac*-C<sub>2</sub>H<sub>4</sub>(ind)<sub>2</sub>ZrCl<sub>2</sub>/MAO and Busico's catalysts are *rac*-C<sub>2</sub>H<sub>4</sub>(ind)<sub>2</sub>ZrCl<sub>2</sub>/MAO and *rac*-Me<sub>2</sub>Si(2-Me-benz[e]ind)<sub>2</sub>ZrCl<sub>2</sub>/MAO. But neither studied the effects of polymerization temperature on regioirregular repeat units. In our studies of 1-butene polymerization, only reverse repeat units(2,1-insertion) were observed to be present and the percentage of 2,1-insertion decreases with decreasing polymerization temperature.

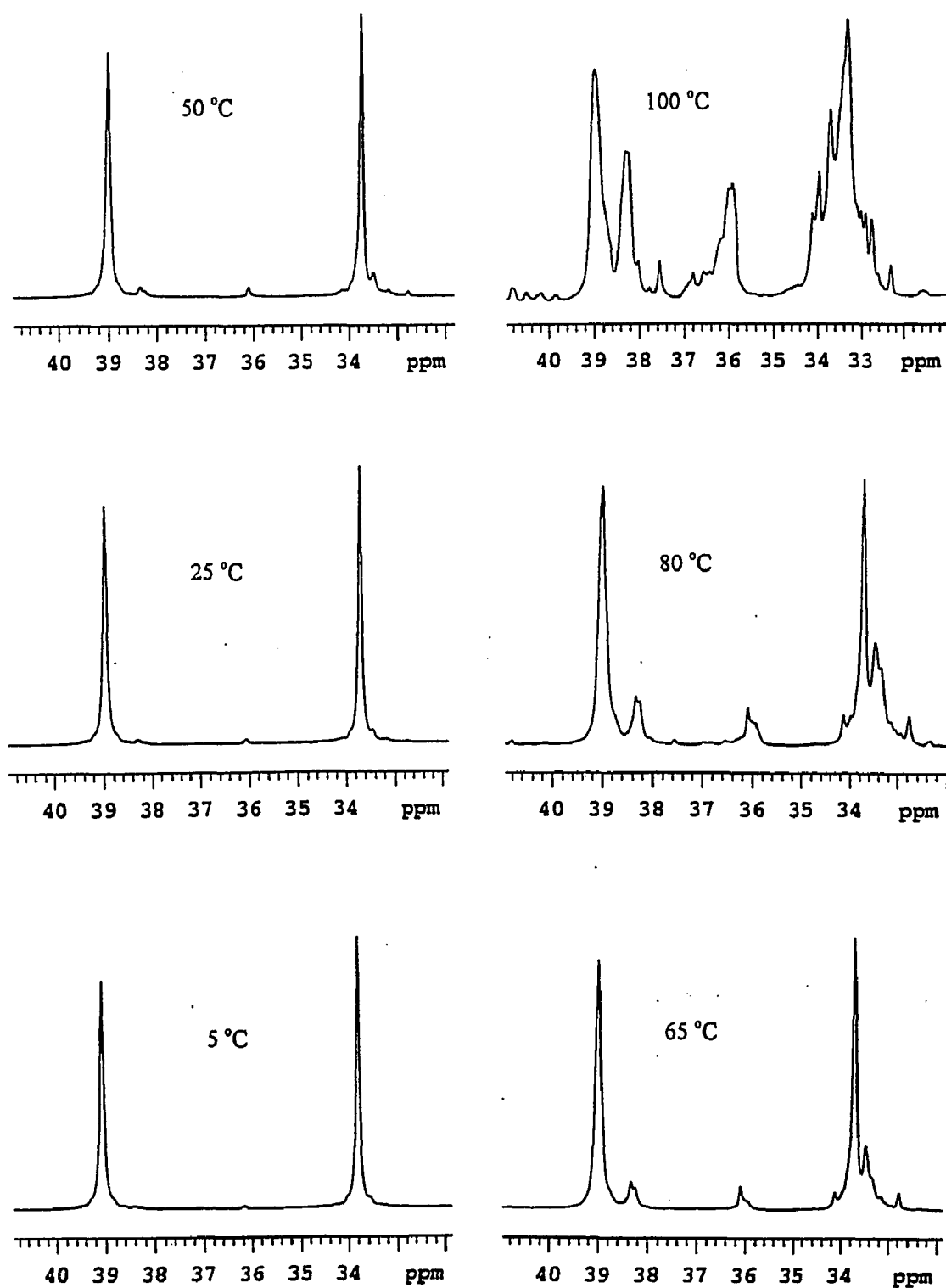


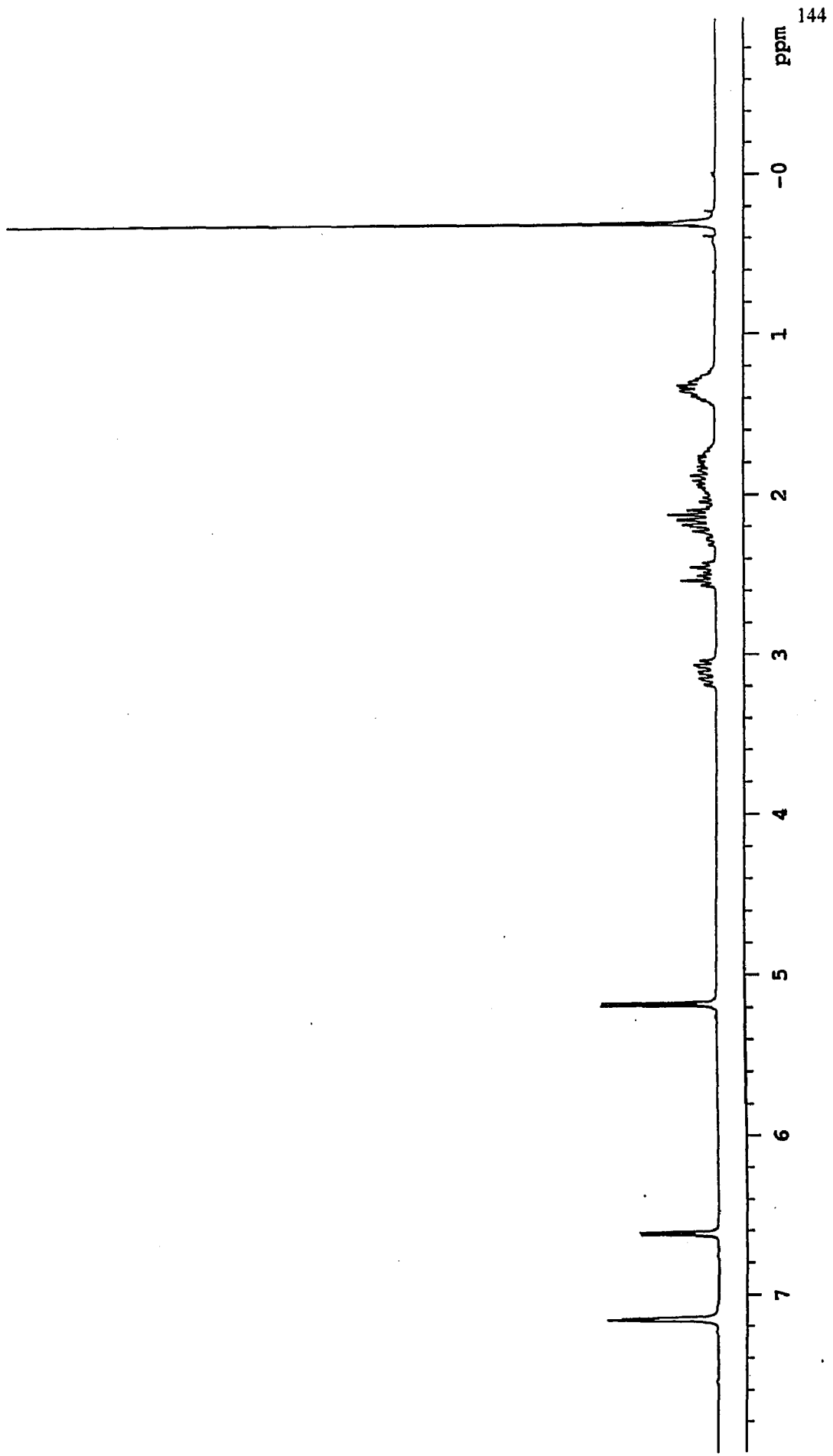
Figure 27.  $^{13}\text{C}$  NMR main chain methylene and methine region (regioselectivity) of poly(1-butene) synthesized at different  $T(^{\circ}\text{C})$  with 60 min polymerization time

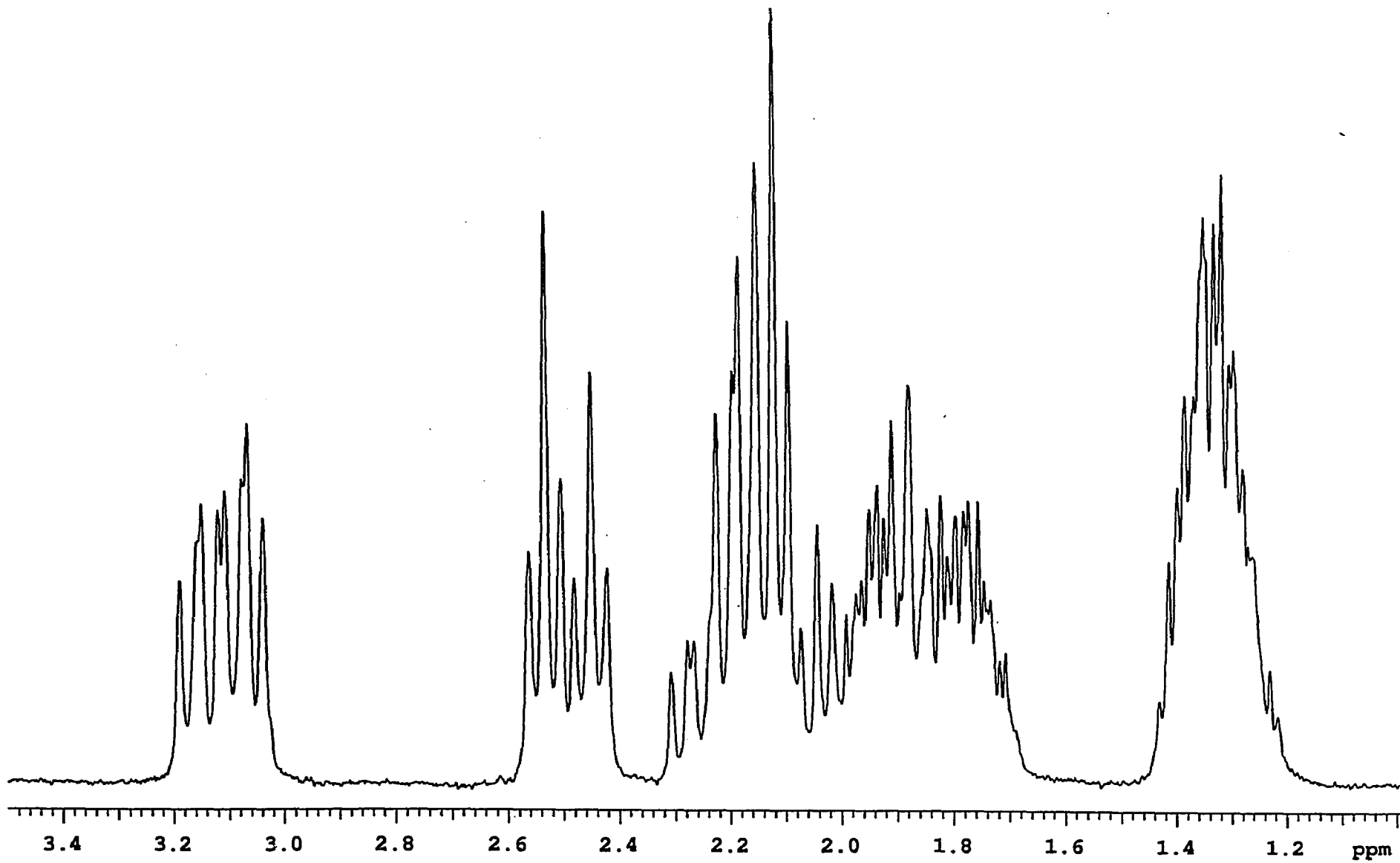
Table 24 Percentage(%) of Reverse Repeat Units for Poly(1-butene)  
Synthesized at Different Polymerization Temperature\*

Polymerization temperature	Percentage(%) of reverse repeat units
100 °C	34
80 °C	11
65 °C	6
50 °C	2
25 °C	1
5 °C	0.3

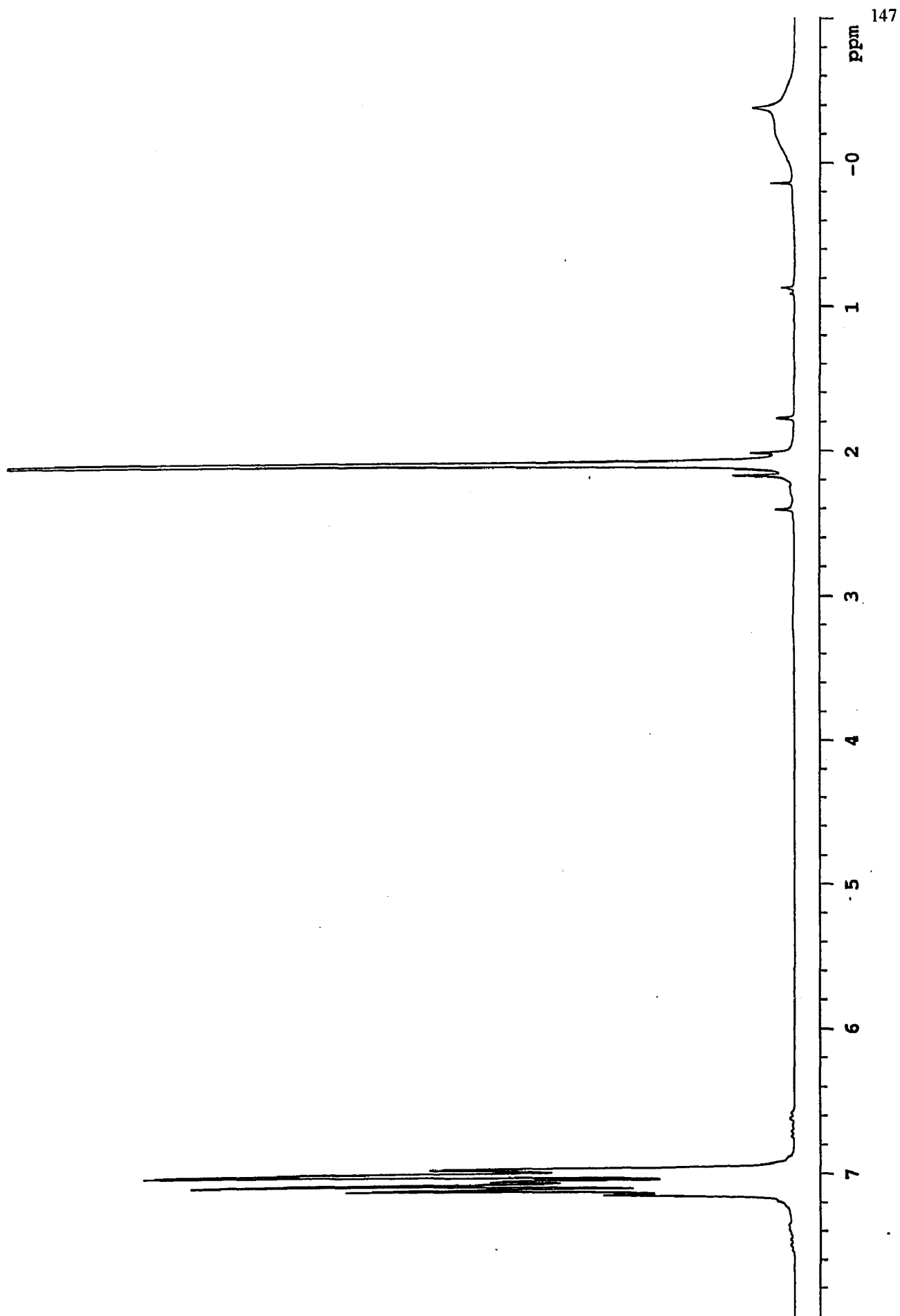
\* Polymerization time is 60 minutes for all six poly(1-butene) samples.  
Zirconium catalyst concentration is  $7.1 \cdot 10^{-6}$  M, the ratio of cocatalyst MAO to zirconium catalyst is 1100/1.

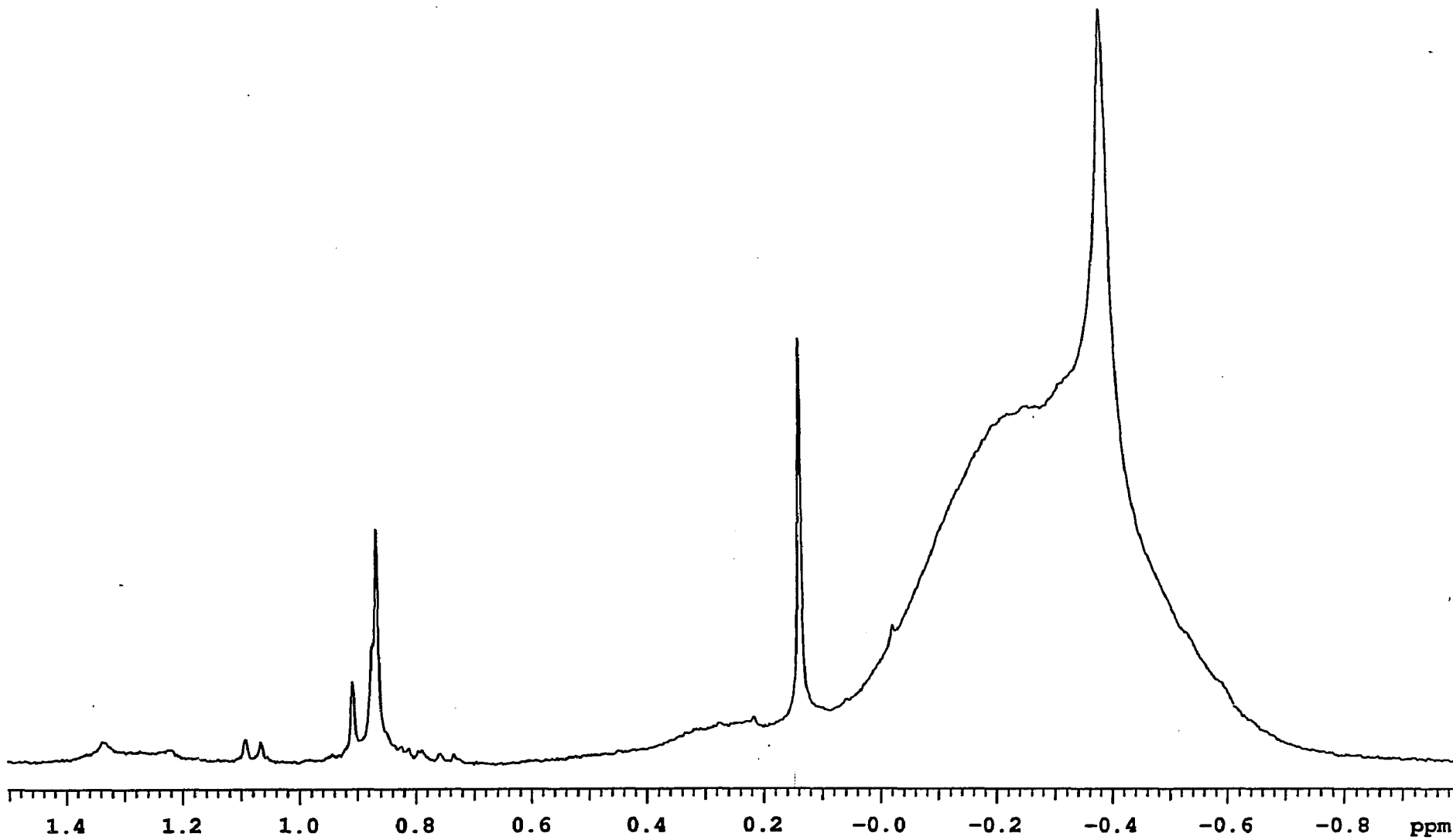
Appendix 1  $^1\text{H}$  NMR of *rac*-zirconium metallocene catalyst



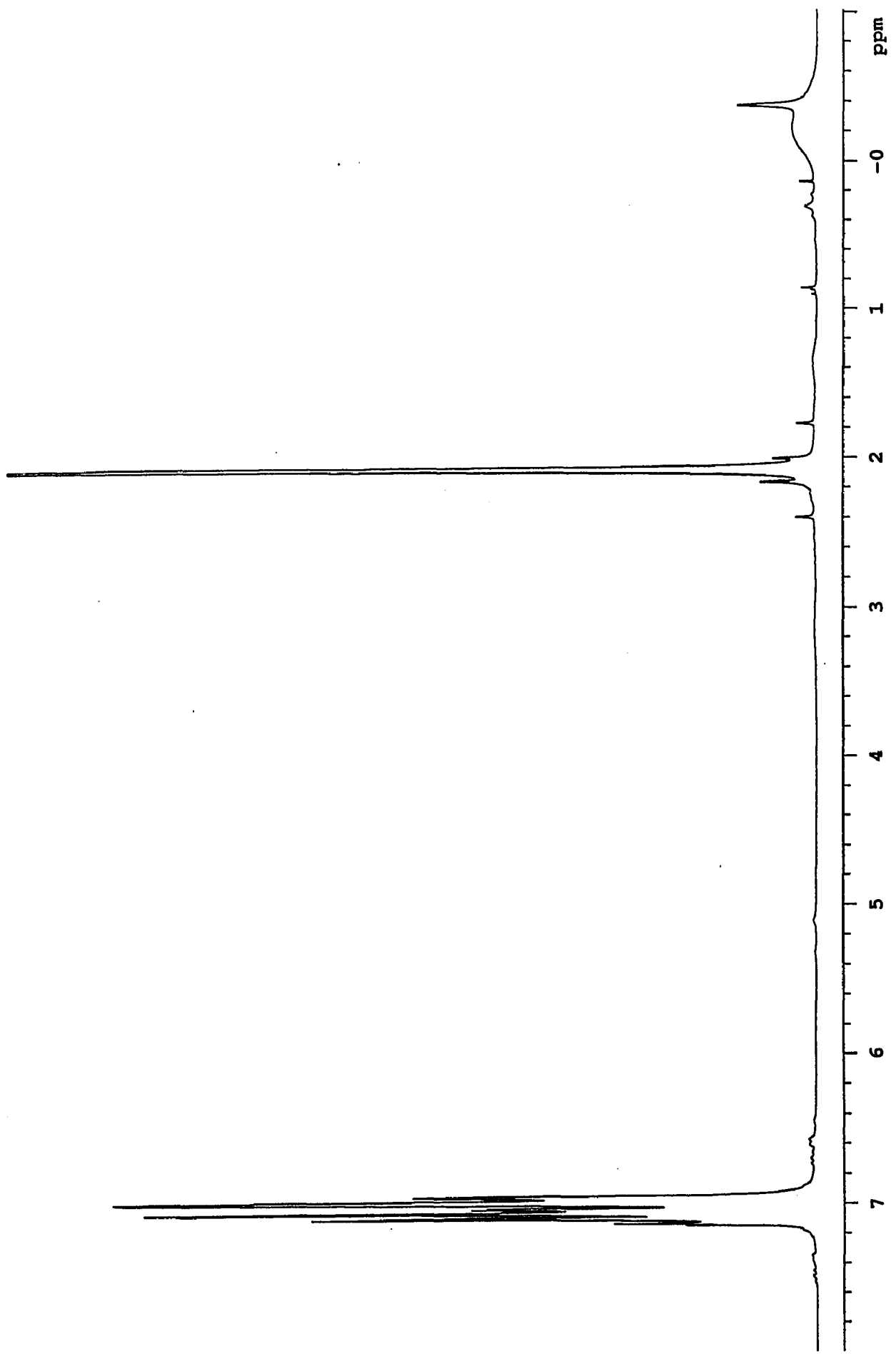


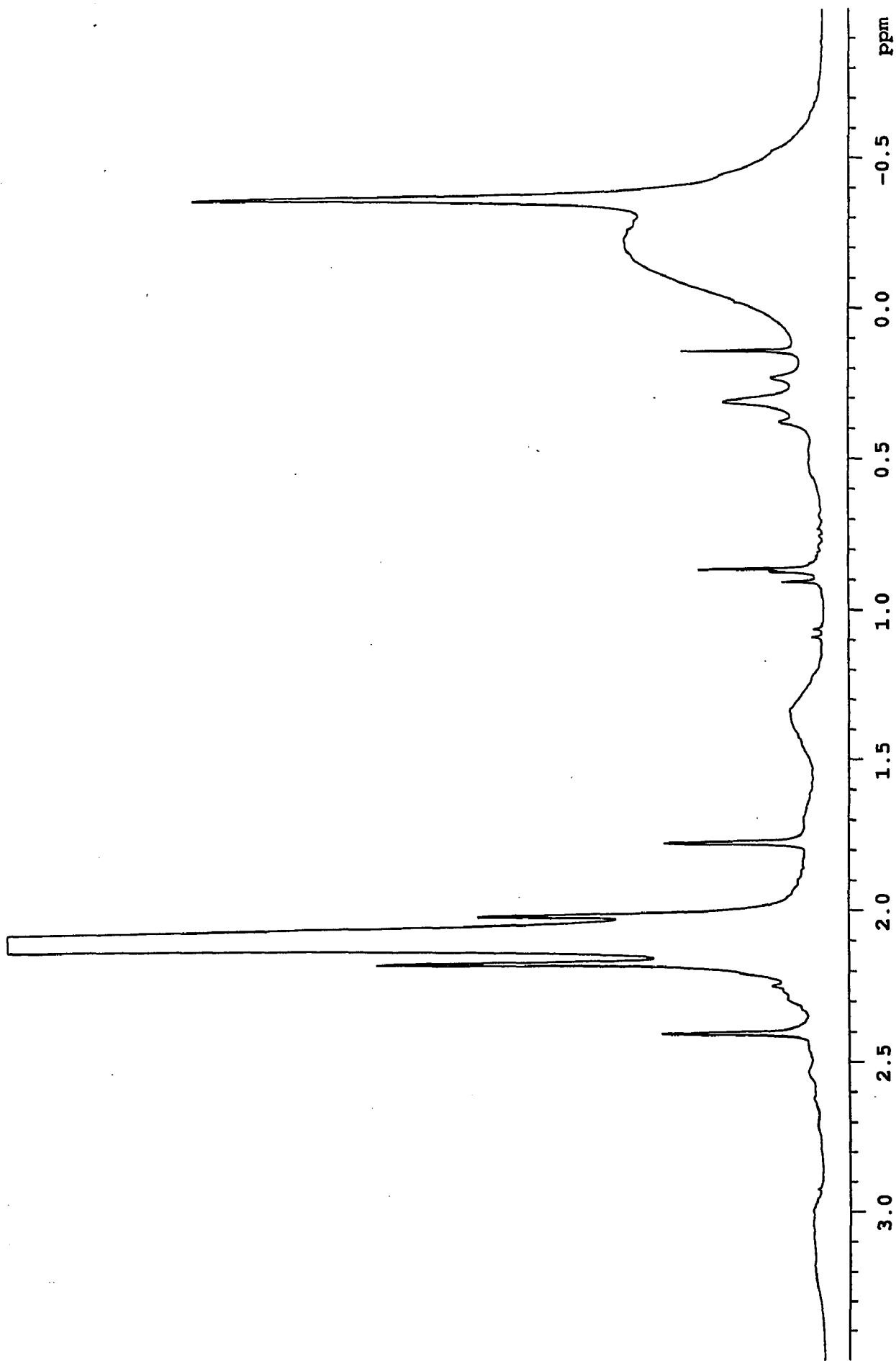
## Appendix 2 $^1\text{H}$ NMR of cocatalyst MAO





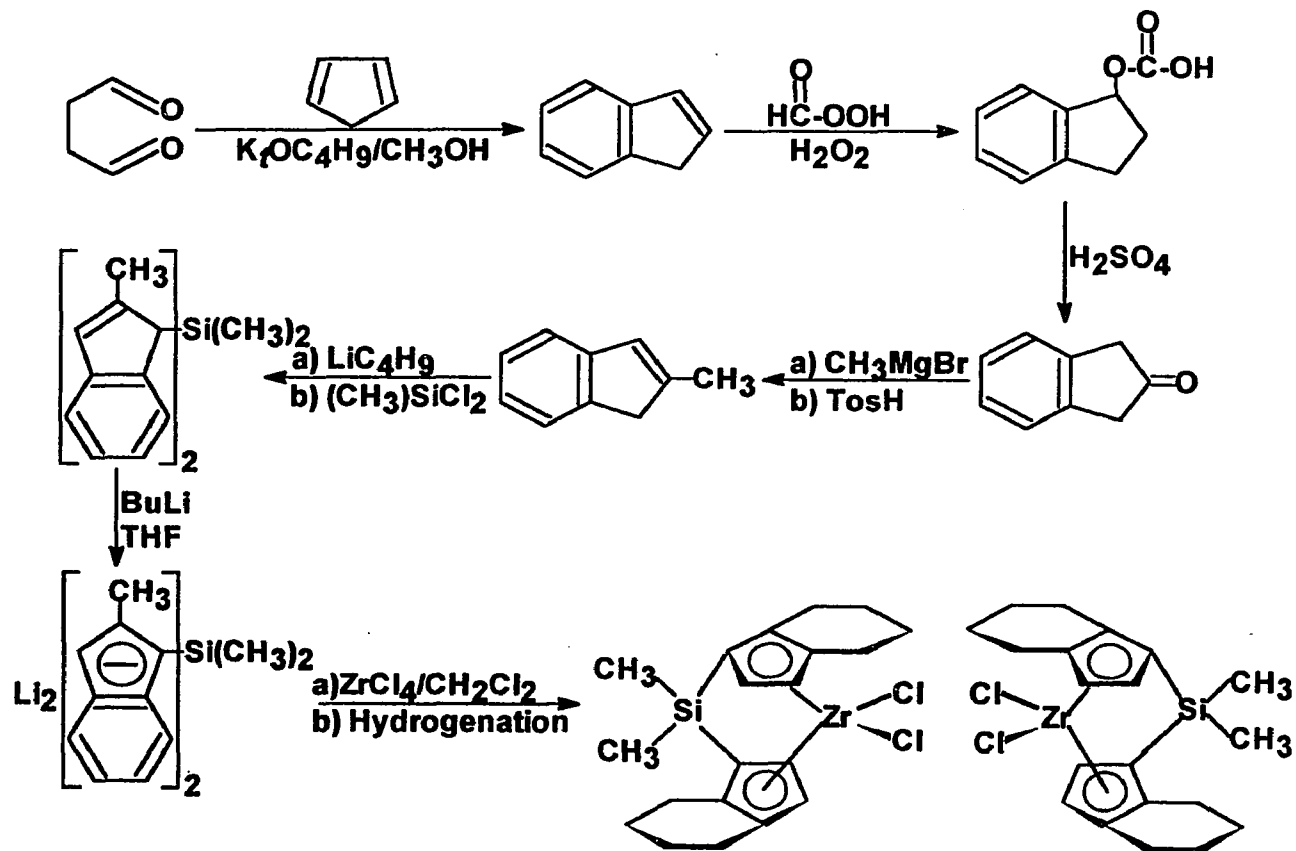
Appendix 3  $^1\text{H}$  NMR of catalyst system *rac*-zirconium metallocene/MAO





#### Appendix 4 Synthesis routine for zirconium metallocene catalyst

# Zirconium Metallocene



Dimethyl silyl(4,5,6,7-tetrahydro-1-indenyl) Zirconium dichloride

## Appendix 5 Relationship between dyad, triad, tetrad and pentad fractions

*Dyad tacticity* is defined as the fractions of pairs of adjacent repeating units that are isotactic or syndiotactic to one another. The fractions of isotactic and syndiotactic dyads are referred to as (m) and (r), respectively. Triad tacticity describes isotactic, syndiotactic, and heterotactic triads whose fractions are designated as (mm), (rr), and (mr), respectively. The dyad and triad fractions each total unity by definition, that is:

$$(m) + (r) = 1$$

$$(mm) + (rr) + (mr) = 1$$

and the two are related by

$$(m) = (mm) + 0.5(mr)$$

$$(r) = (rr) + 0.5(mr)$$

The tetrad tacticity distribution consists of the isotactic sequence mmm, the syndiotactic sequence rrr, and the heterotactic sequences mmr, rmr, mrm and rrm. The sum of the tetrad fractions is unity, and the following relationships exist:

$$(mm) = (mmm) + 0.5(mmr)$$

$$(rr) = (rrr) + 0.5(mrr)$$

$$(mr) = (mmr) + 2(rmr) = (mrr) + 2(mrm)$$

The pentad tacticity distribution consists of the isotactic sequence mmmmm, the syndiotactic sequence rrrrr, and the heterotactic sequences rmmr, mrrm, mmrr, rrrm, mrrm and rrrm. The sum of the pentad sequences is unity, and the following relationships exist:

$$(mmmr) + 2(rmmr) = (mmrm) + (mmrr)$$

$$(mrrr) + 2(mrrm) = (rrmr) + (rrmm)$$

$$(mmm) = (mmmm) + 0.5(mmmr)$$

$$(mmr) = (mmm) + 2(rmm) = (mmr) + (mmr)$$

$$(rnr) = 0.5(mrnr) + 0.5(rnrr)$$

$$(mrm) = 0.5(mrnr) + 0.5(mmrm)$$

$$(rrm) = 2(mrrm) + (mrrr) = (mmrr) + (rnr)$$

$$(rrr) = (rrr) + 0.5(mrrr)$$

By applying above necessary relationships, we can obtain following expressions:

$$(m) = (mm) + 0.5(mr)$$

$$= (mmm) + (mnr) + (rnr)$$

$$= (mmmm) + 1.5(mmnr) + 2(rmmr) + 0.5(mrnr) + 0.5(rnr)$$

$$(r) = (rr) + 0.5(mr)$$

$$= (rrr) + 0.5(mrr) + 0.5(mnr) + rnr$$

$$= (rrrr) + (mrrr) + (mrrm) + 0.5[(mmnr) + (rmmr) + (mnr) + (rnr)]$$

## Appendix 6. Derivation of comonomer reactivity ratio

$R_{EE}$  represents the rate of monomer E added to monomer E at propagating chain terminal and  $k_{EE}$  is the corresponding rate constant;  $R_{EB}$  represents the rate of monomer B added to monomer E at chain propagating terminal and  $k_{EB}$  is the corresponding rate constant;  $R_{BB}$  represents the rate of monomer B added to monomer B at propagating chain terminal and  $k_{BB}$  is the corresponding rate constant;  $R_{BE}$  represents the rate of monomer E added to monomer B at chain propagating terminal and  $k_{BE}$  is the corresponding rate constant.  $X$  represents  $X_E/X_B$ , in which  $X_E$  represents the molar concentration of monomer E in feed, and  $X_B$  represents the molar concentration of monomer B in feed.

In first order Markovian statistics,  $P_{EE}$  represents the probability of monomer E added to monomer E at propagating chain terminal;  $P_{EB}$  represents the probability of monomer B added to monomer E at propagating chain terminal;  $P_{BB}$  represents the probability of monomer B added to monomer B at propagating chain terminal;  $P_{BE}$  represents the probability of monomer E added to monomer B at propagating chain terminal. Therefore following relations exist:

$$P_{EB} + P_{EE} = 1$$

$$P_{BE} + P_{BB} = 1$$

The comonomer reactivity ratios are defined as:

$$r_E = k_{EE}/k_{EB}$$

$$r_B = k_{BB}/k_{BE}$$

If  $[E^*]$  is the concentration of propagating center with E as terminal unit;  $[B^*]$  is the concentration of propagating center with B as terminal,  $[E]$  represents the steady concentration of monomer E during polymerization, and

[B] represents the steady concentration of monomer B during polymerization, there exist following expressions:

$$R_{EE} = k_{EE}[E^*][E]$$

$$R_{EB} = k_{EB}[E^*][B]$$

$$R_{BB} = k_{BB}[B^*][B]$$

$$R_{BE} = k_{BE}[B^*][E]$$

The propagating probability  $P_{EE}$  will be written as:

$$\begin{aligned} P_{EE} &= R_{EE}/(R_{EE} + R_{EB}) \\ &= \{k_{EE}[E^*][E]\}/\{k_{EE}[E^*][E] + k_{EB}[E^*][B]\} \\ &= \{k_{EE}[E]\}/\{k_{EE}[E] + k_{EB}[B]\} \\ &= k_{EE}X_E/(k_{EE}X_E + k_{EB}X_B) \\ &= k_{EE}X_E/\{k_{EE}X_E + k_{EB}(X_E/X)\} \\ &= k_{EE}X/(k_{EE}X + k_{EB}) \\ &= X/(X + k_{EB}/k_{EE}) \\ &= X/(X + 1/r_E) \end{aligned}$$

The rearrangement of above equation gives rise to the monomer E reactivity ratio as:

$$r_E = P_{EE}/(X - XP_{EE}) \quad (\text{eq.1})$$

The propagating probability  $P_{BB}$  will be written as:

$$\begin{aligned} P_{BB} &= R_{BB}/(R_{BB} + R_{BE}) \\ &= \{k_{BB}[B^*][B]\}/\{k_{BB}[B^*][B] + k_{BE}[B^*][E]\} \\ &= \{k_{BB}[B]\}/\{k_{BB}[B] + k_{BE}[E]\} \\ &= k_{BB}X_B/(k_{BB}X_B + k_{BE}X_E) \\ &= k_{BB}/(k_{BB} + k_{BE}X) \\ &= 1/\{1 + (k_{BE}/k_{BB})X\} \end{aligned}$$

$$= 1/(1 + X/r_B)$$

The similar rearrangement of above equation gives rise to monomer B reactivity ratio as:

$$r_B = XP_{BB}/(1 - P_{BB}) \quad (\text{eq. 2})$$

In first order Markovian statistics, the following relationships between comonomer sequence distributions and propagating probabilities:

$$[EEE] = X_E(1 - P_{EB})^2$$

$$[EEB + BEE] = 2X_E(1 - P_{EB})P_{EB}$$

$$[BEB] = X_E P_{EB}^2$$

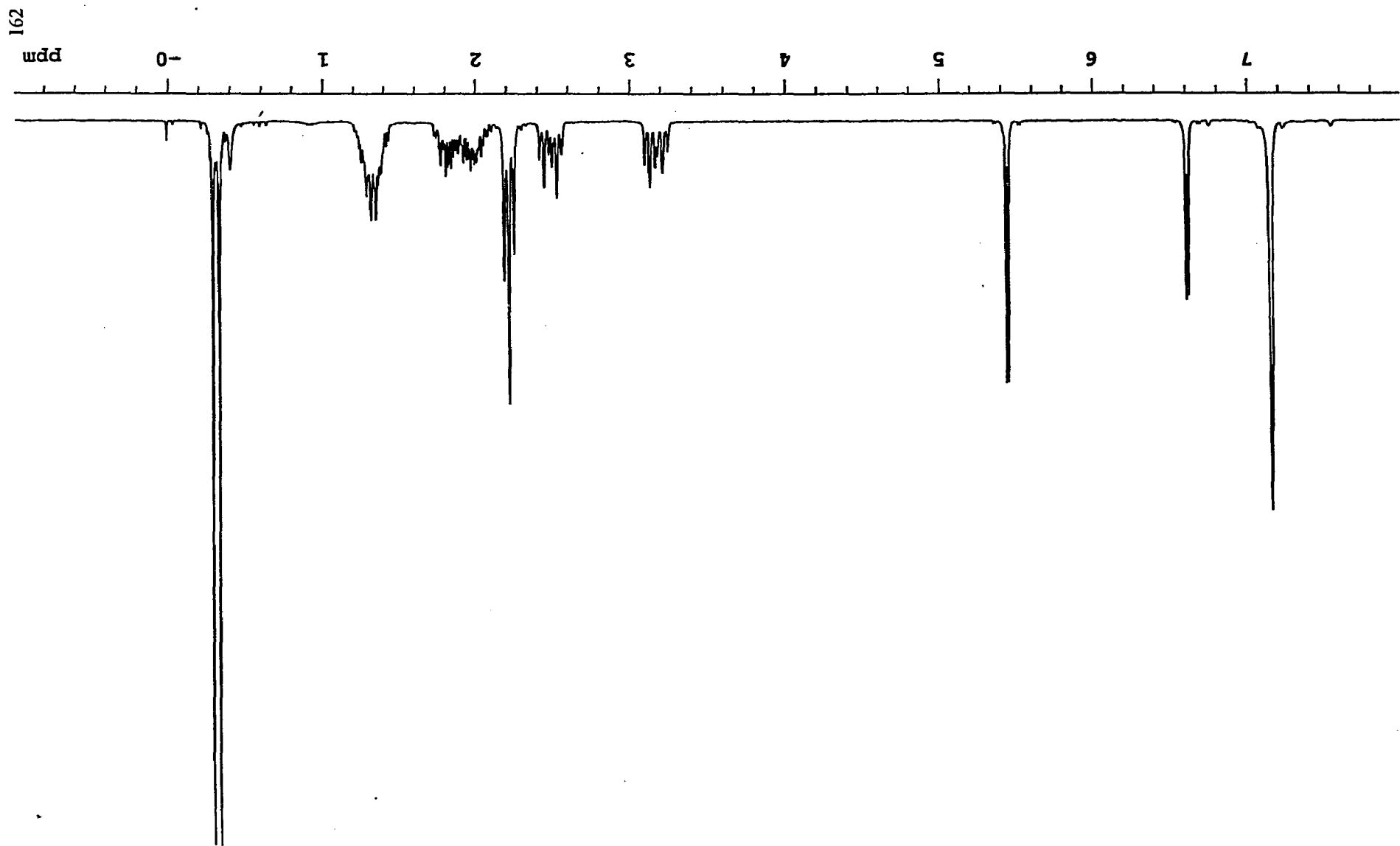
$$[EBE] = X_B P_{BE}^2$$

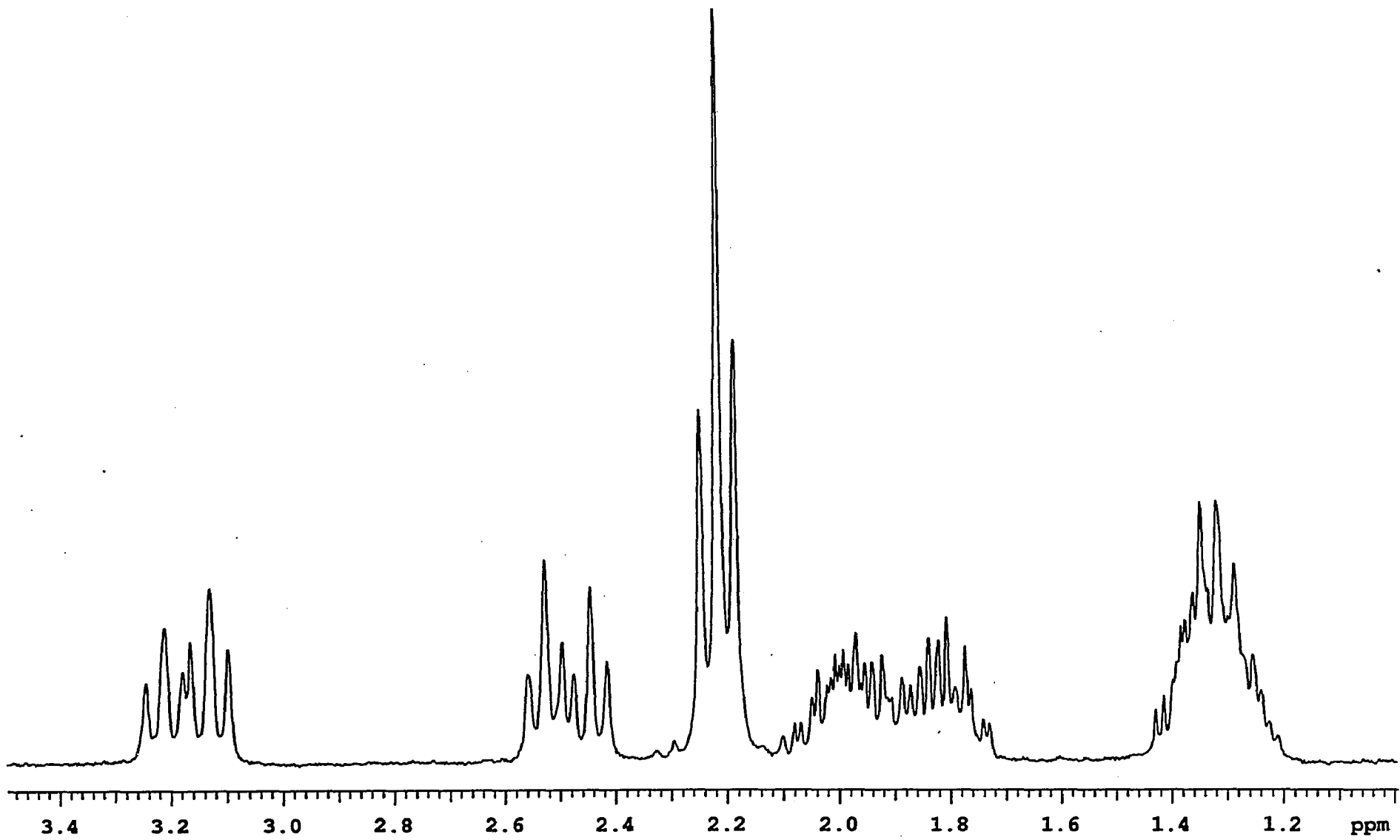
$$[BBE + EBB] = 2X_B(1 - P_{BE})P_{BE}$$

$$[BBB] = X_B(1 - P_{BE})^2$$

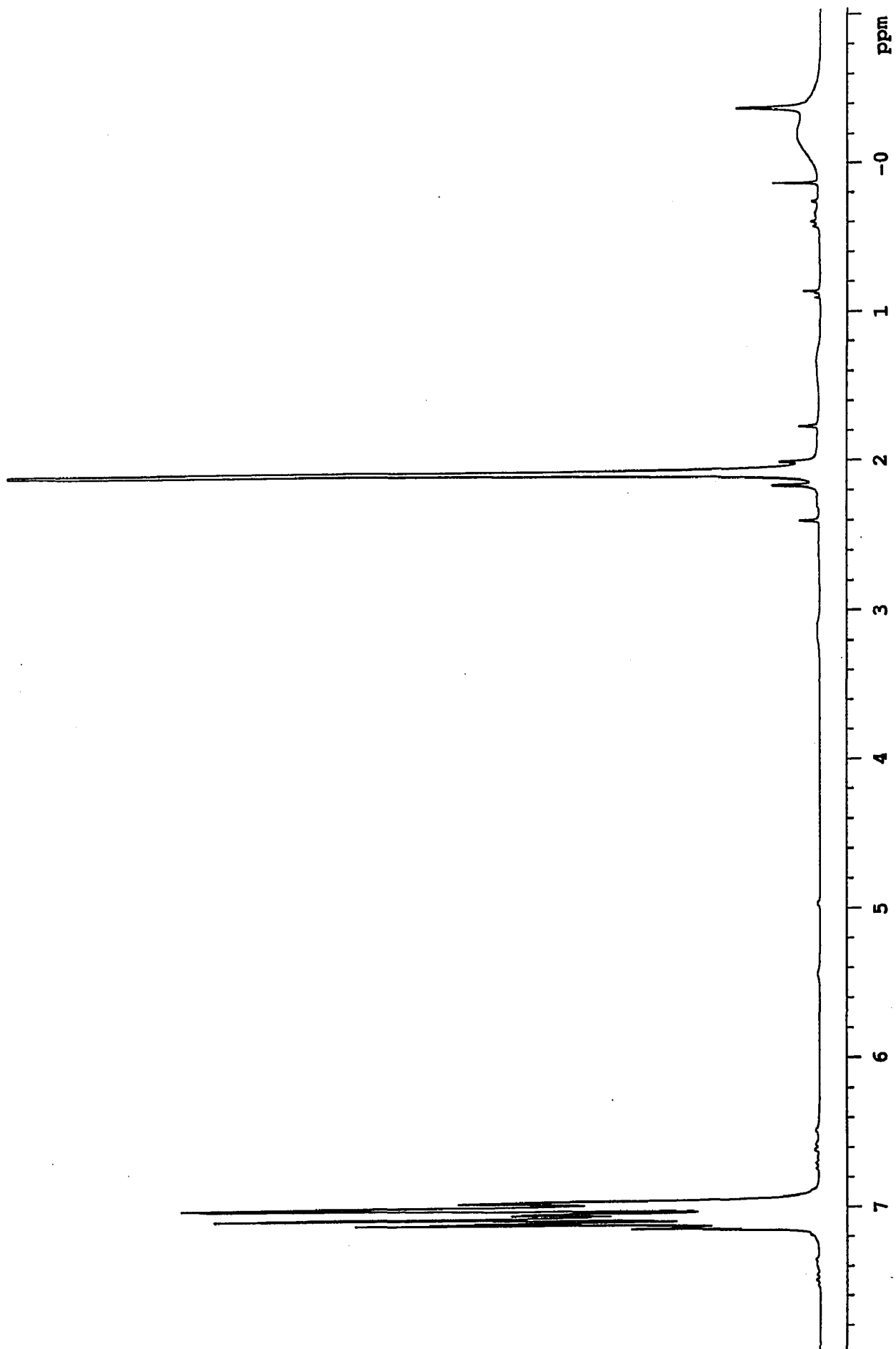
The first three equations are solved to get the independent trial values for  $P_{EB}$ , and the second three are solved for trial values for  $P_{BE}$ . The average  $P_{EB}$  and  $P_{BE}$  can be converted to average  $P_{EE}$  and  $P_{BB}$ , which can in turn be substituted into (eq.1) and (eq.2) to obtain monomer reactivity ratios  $r_E$  and  $r_B$ .

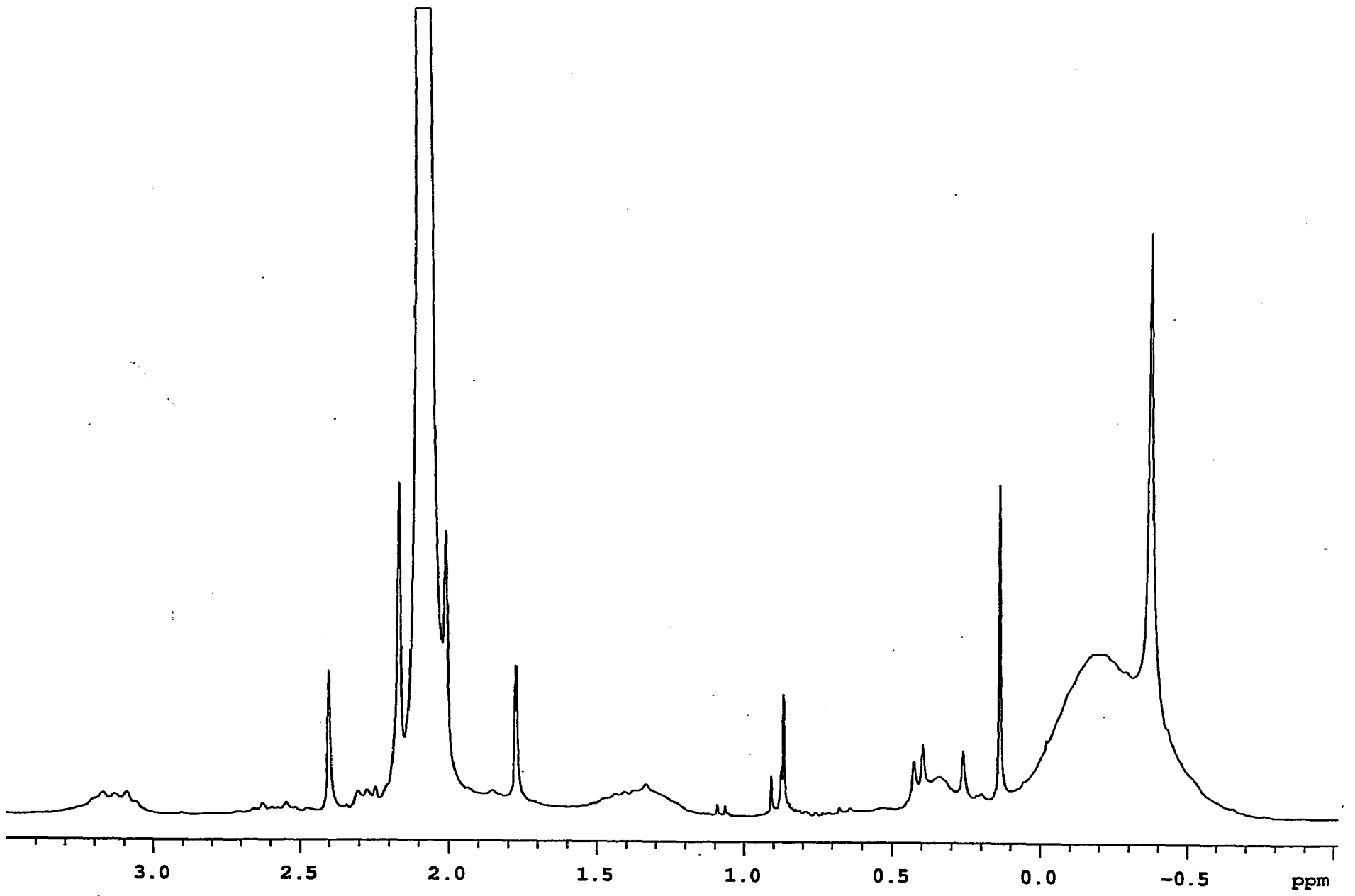
Appendix 7  $^1\text{H}$  NMR of *meso*-zirconium metallocene catalyst



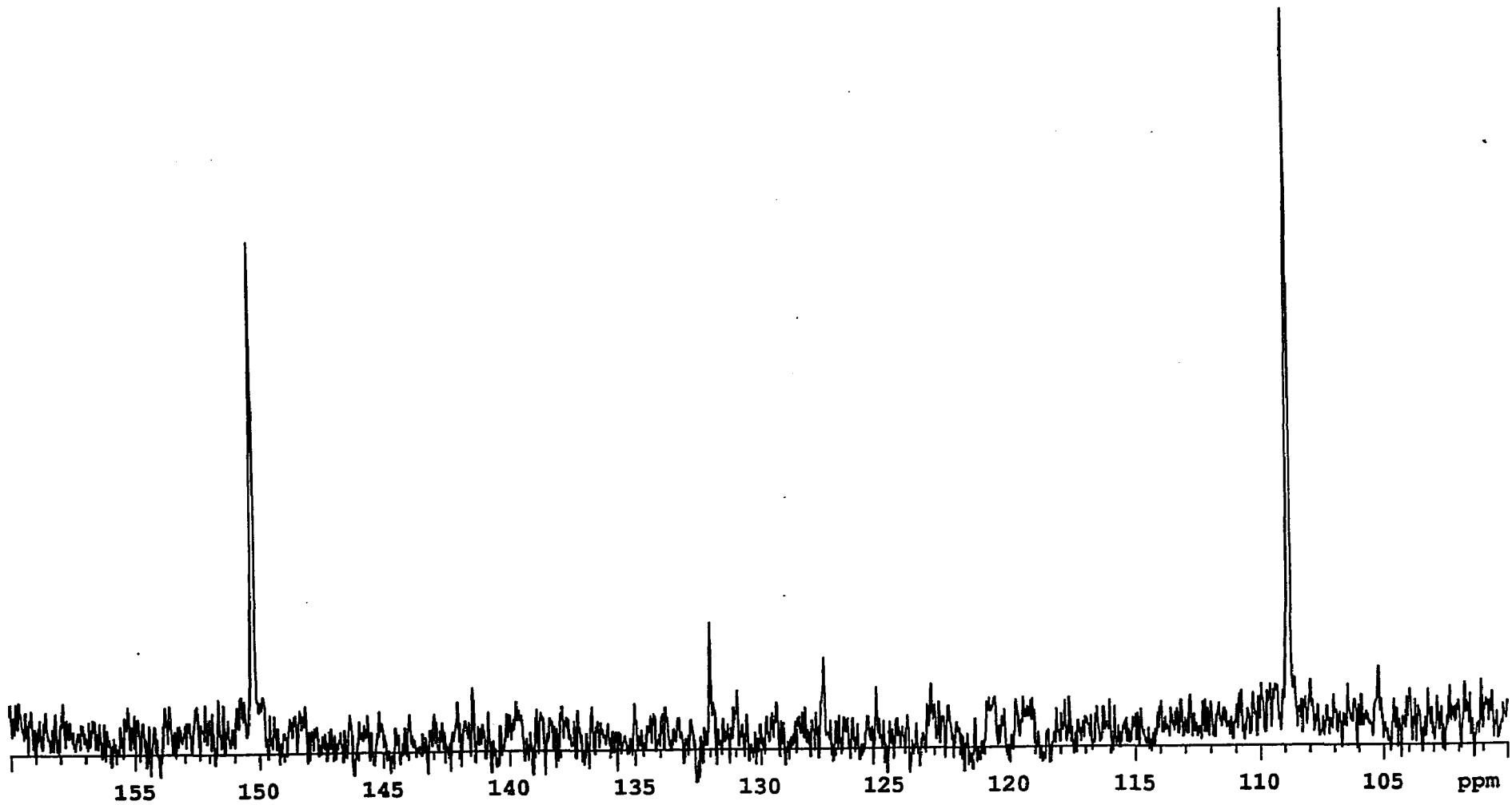


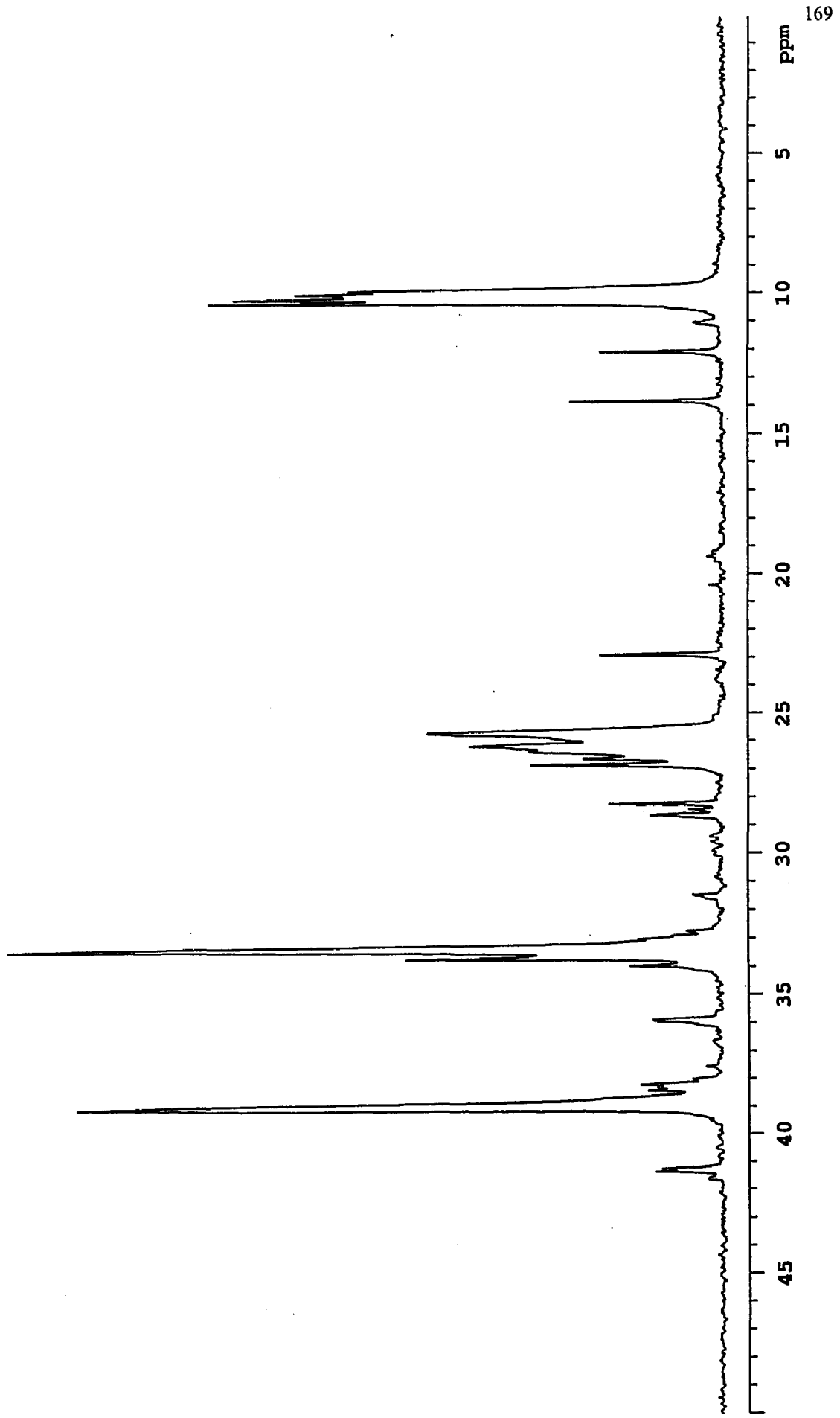
Appendix 8  $^1\text{H}$  NMR of catalyst system *meso*-zirconium metallocene/MAO



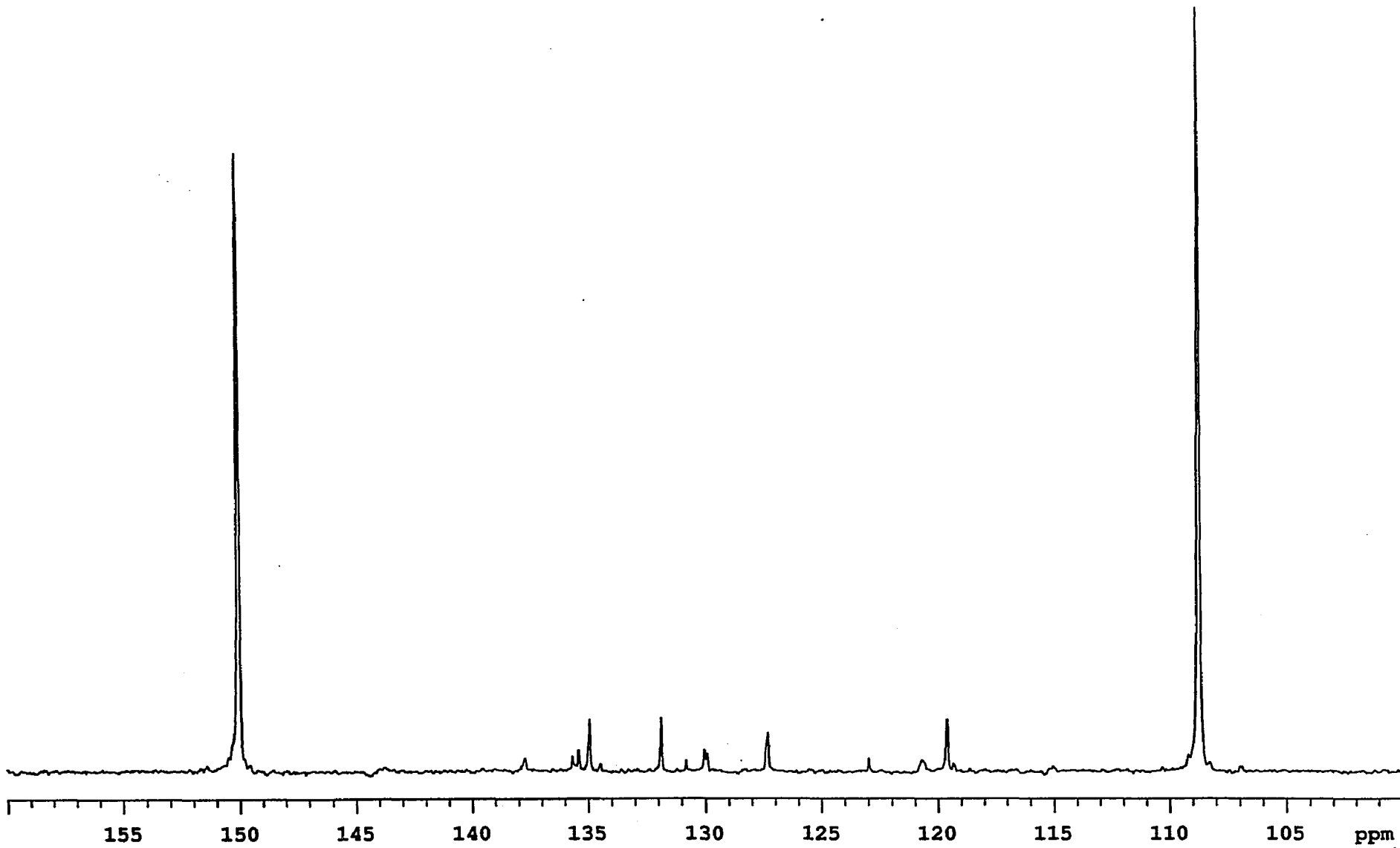


Appendix 9  $^{13}\text{C}$  NMR of poly(1-butene) synthesized  
by *meso*-zirconium metallocene catalyst at 25 °C/60min

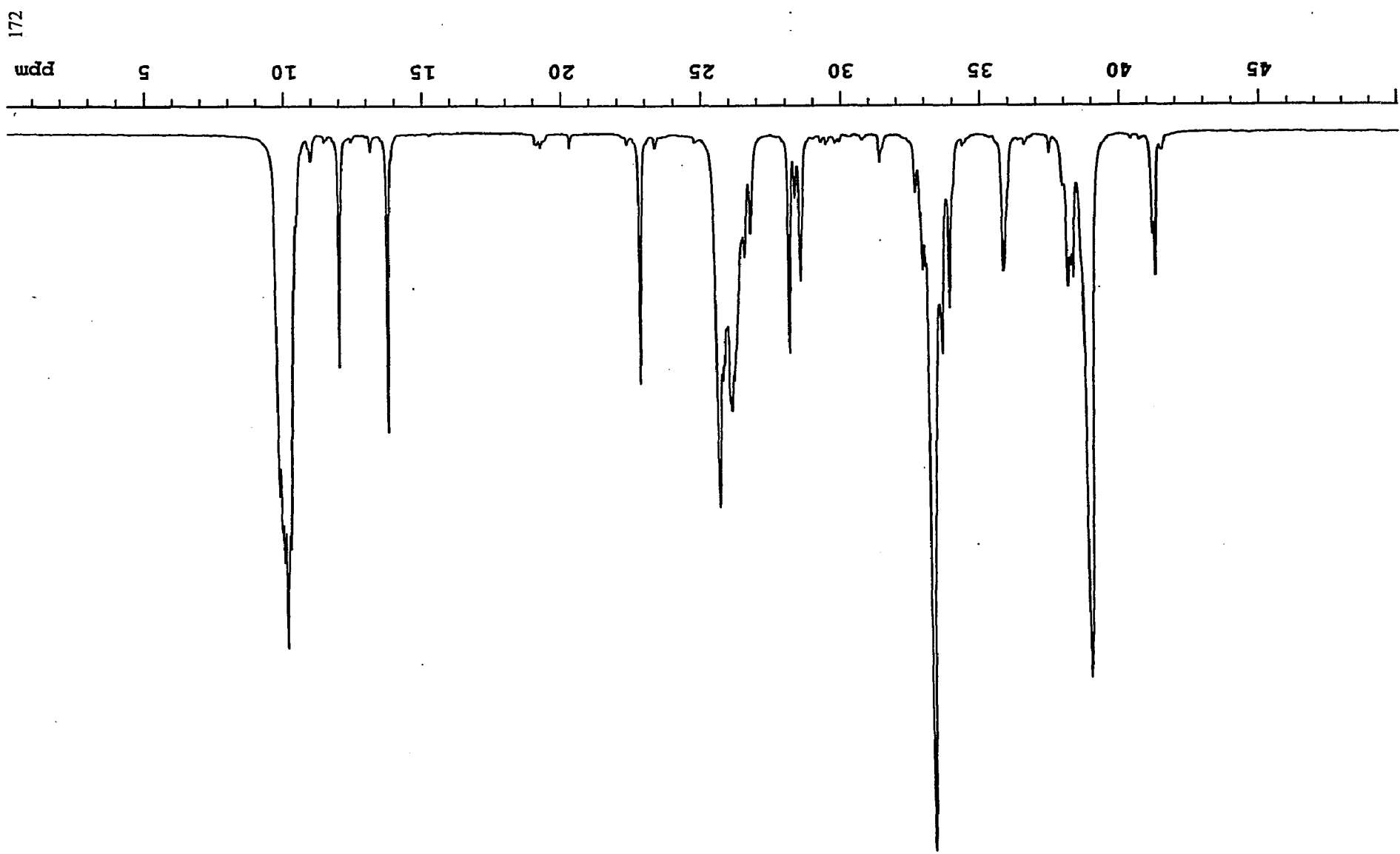




Appendix 10  $^{13}\text{C}$  NMR of poly(1-butene) synthesized  
by *meso*-zirconium metallocene catalyst at 50 °C/60min



ppm  
171



172

ppm

5

10

15

20

25

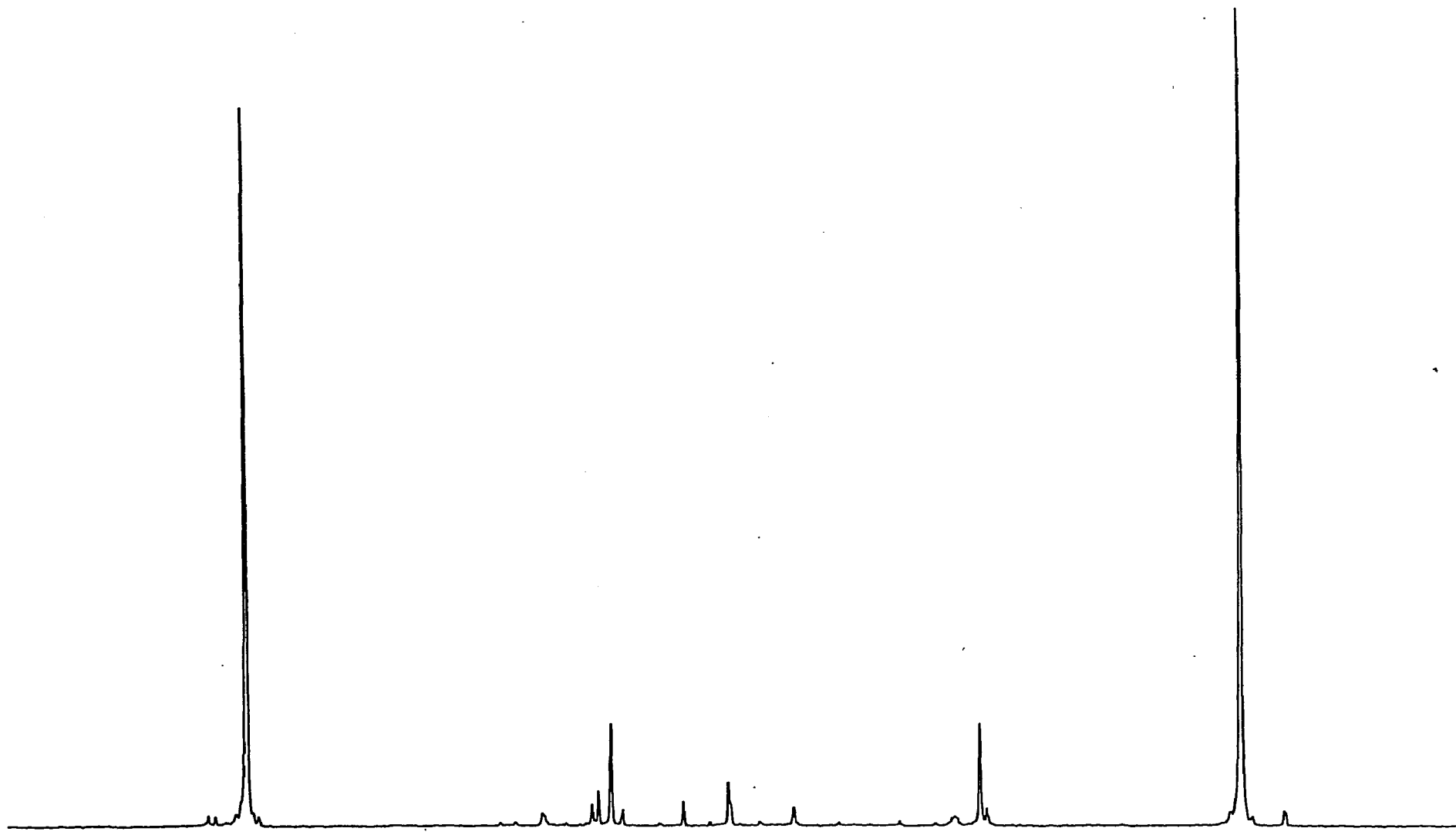
30

35

40

45

Appendix 11  $^{13}\text{C}$  NMR of poly(1-butene) synthesized  
by *meso*-zirconium metallocene catalyst at 80 °C/60min



155

150

145

140

135

130

125

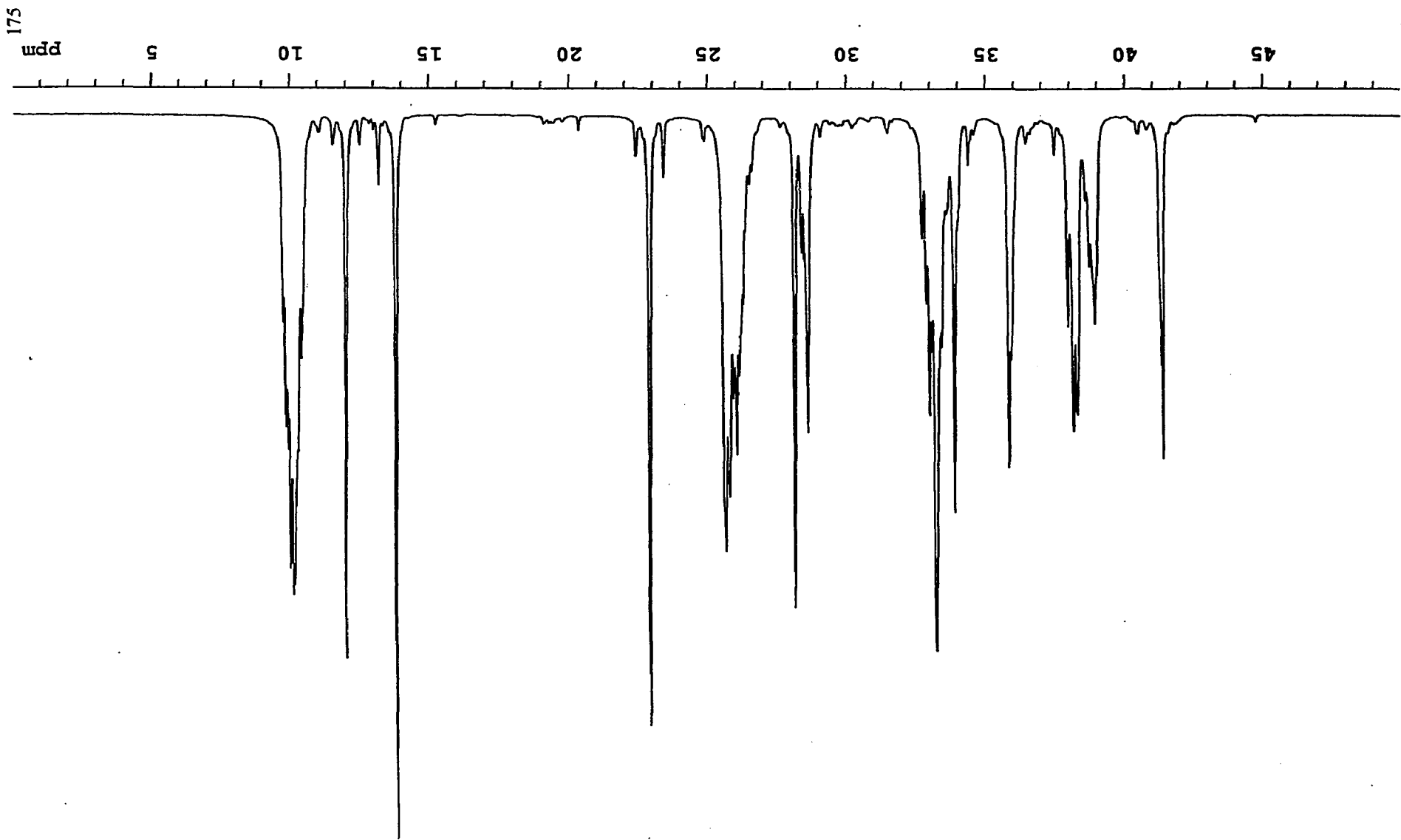
120

115

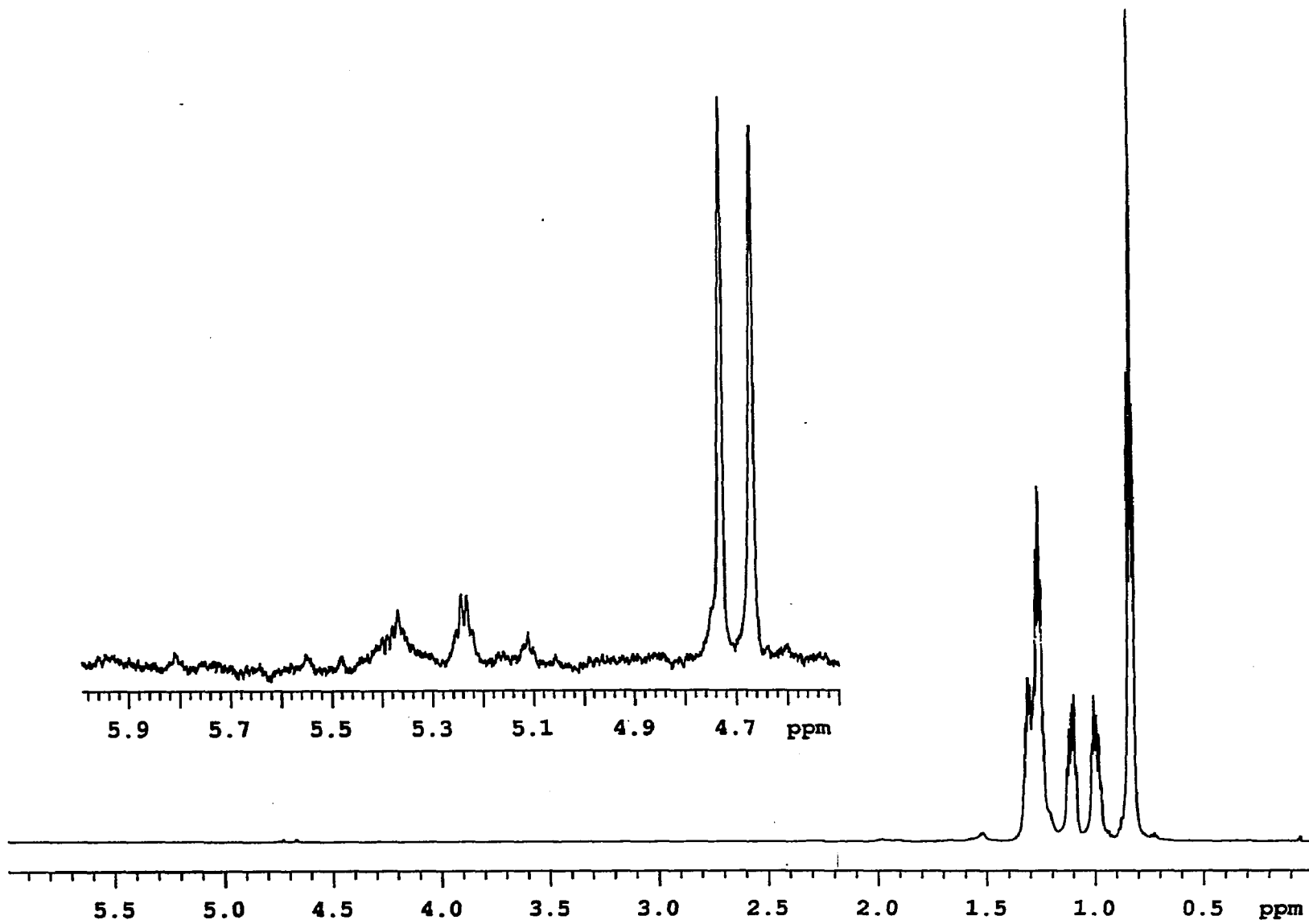
110

105

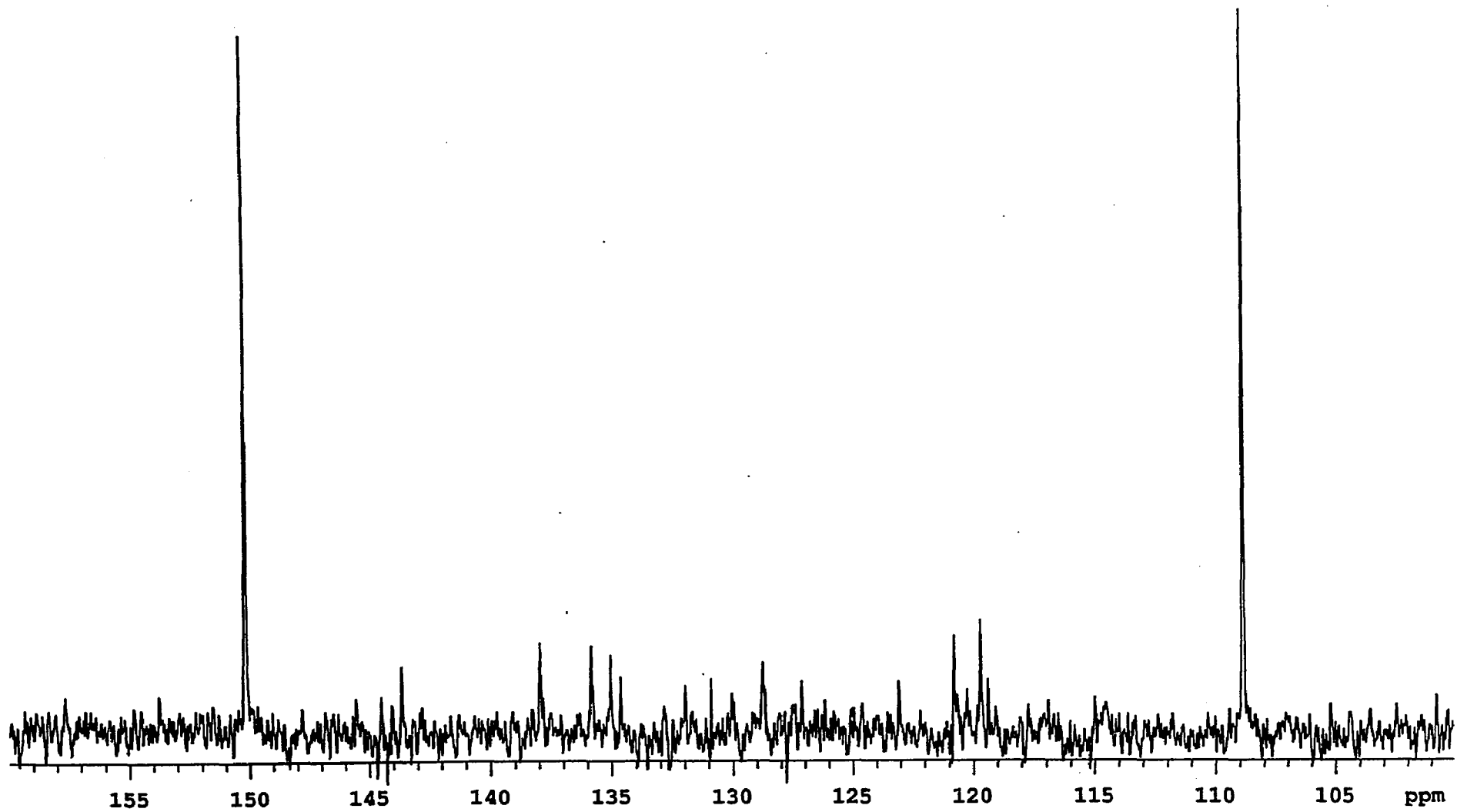
ppm

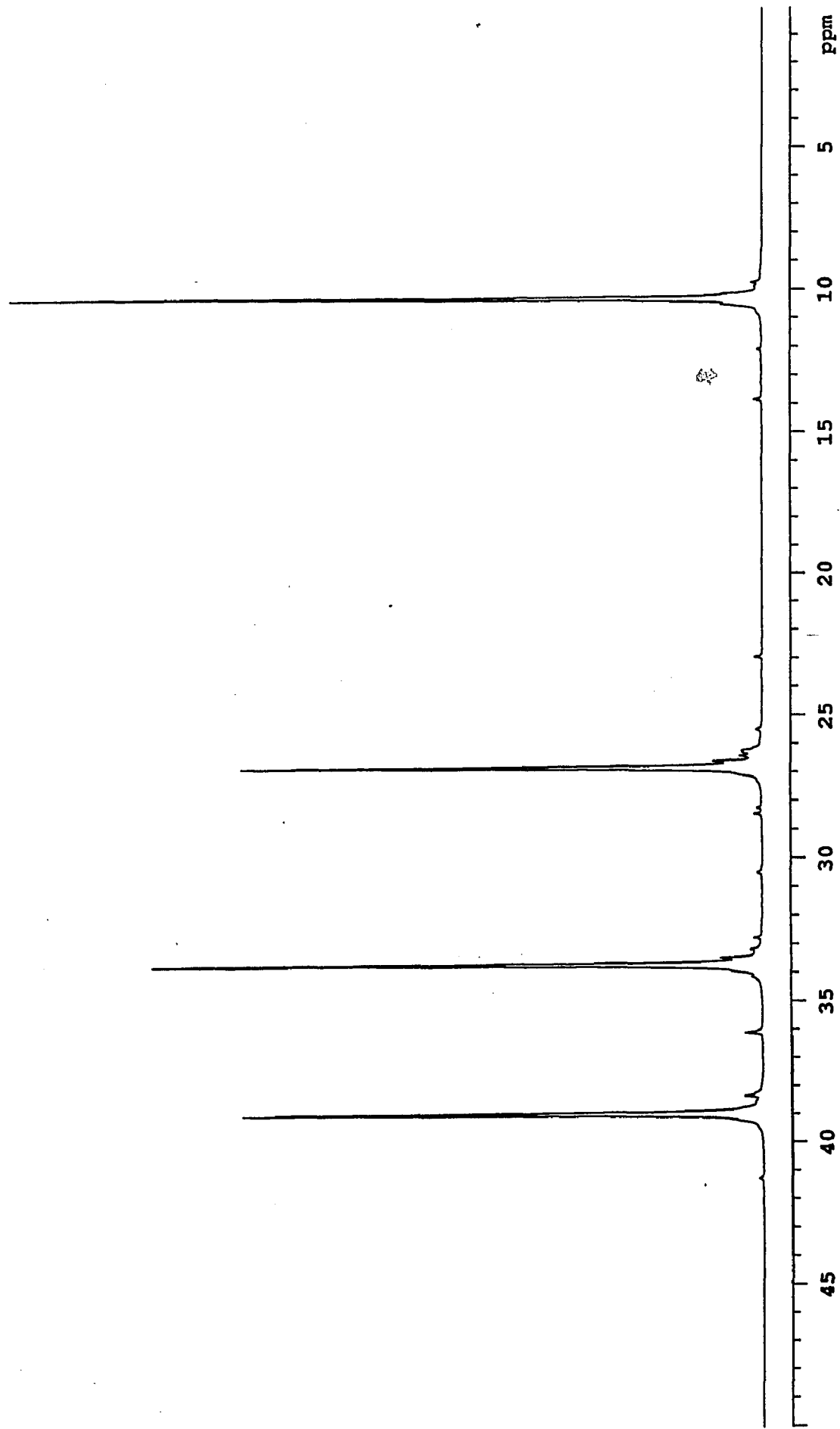


Appendix 12  $^1\text{H}$  NMR of poly(1-butene) synthesized by  
cationic zirconium metallocene catalyst system at 45 °C/60min

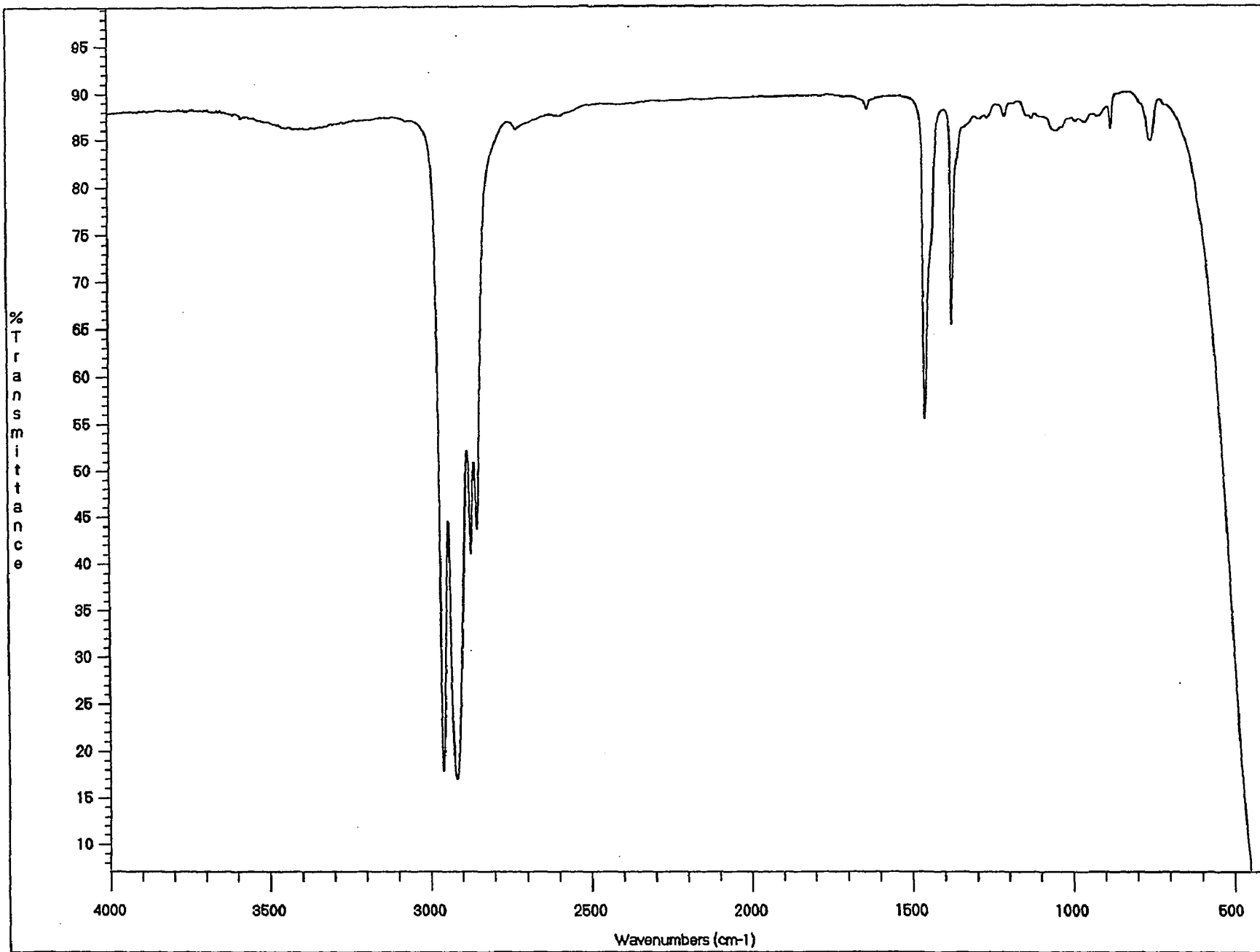


Appendix 13  $^{13}\text{C}$  NMR of poly(1-butene) synthesized by  
cationic zirconium metallocene catalyst system at 25 °C/60min

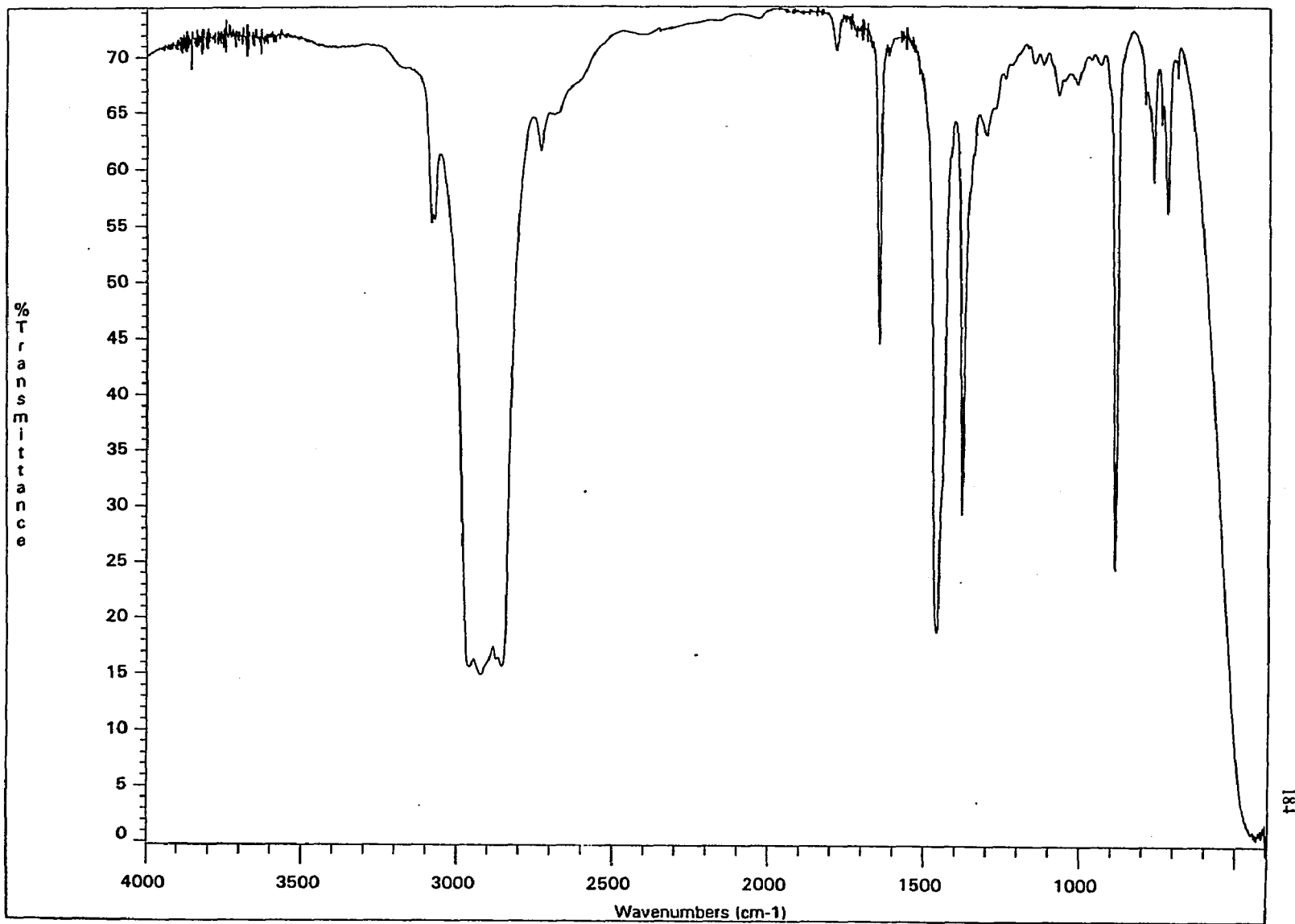




Appendix 14 Infrared spectrum of poly(1-butene)  
synthesized by *rac*-zirconium catalysts system at 80 °C/60min



Appendix 15 Infrared spectrum of poly(ethylene-*co*-1-butene)



### 8.0 References

1. Ziegler, K.; Holzkamp, E.; Breil, H.; Martin, H.  
*Angew. Chem.* **1955**, *67*, 541
2. Ziegler, K. *Angew. Chem.* **1964**, *76*, 545
3. Natta, G.; Corradini, P. *Atti Accad. naz. Lincei Mem. Cl. Sci. Fis. Mat. Nat. Sez. II* **1955**, *5*, 73
4. Natta, G. *Angew. Chem.* **1956**, *68*, 393
5. Natta, G. *ibid.* **1964**, *76*, 553
6. Galli, P.; Haylock, J. C. *Makromol. Chem., Macromol. Symp.* **1992**, *63*, 19-54
7. Odian, G. *Principles of Polymerization*, 3rd ed.; Wiley, New York, 1991; pp 655-658
8. Cossee, P. *Trans. Friday Soc.* **1962**, *58*, 1226
9. Arlman, E. J.; Cossee, P. *J. Catal.* **1964**, *3*, 99
10. Rodriguez, L. A. M.; Van looy, H. M.; Gabant, J. A. *J. Poly. Sci.* **1966**, *Part A4*, 1905
11. Boor, J. *Ziegler-Natta Catalysis and Polymerization*, Academic Press, New York, 1979
12. Odian, G. *Principles of Polymerization*, 3rd ed.; Wiley, New York, 1991; pp 632
13. Cam, D.; Albizzati, E.; Cinquina, P. *Makromol Chem.* **1990**, *191*, 1641
14. Oliva, L.; Longo, P.; Pellecchia, C. *Makromol Chem, Rapid Commun.* **1988**, *9*, 51
15. Zambelli, A.; Ammendola, P.; Grassi, A.; Longo, P.; Proto, A.

- Macromolecules* **1986**, *19*, 2703
16. Ewen, J. A. *J. Am. Chem. Soc.* **1984**, *106*, 6355
17. Couturier, S.; Tainturier, G.; Gautheron, B. *J. Organomet. Chem.* **1980**, *195*, 291
18. Martin, M. L.; Tirouflet, J.; Gautheron, B. *J. Organomet. Chem.* **1975**, *97*, 261
19. Cheng, H. N.; Ewen, J. A. *Makromol. Chem.* **1989**, *190*, 1931
20. Grassi, A.; Zambelli, A.; Resconi, L.; Albizzati, E.; Mazzocchi, R. *Macromolecules* **1988**, *21*, 617
21. Kaminsky, W. *Polymerization and Copolymerization with a Highly Active, Soluble Ziegler-Natta Catalyst*, pp 225-244 in *Transition Metal Catalyzed Polymerization*, R. P. Quirk Ed., Haward Academic, New York, 1983
22. Kaminsky, W.; Bark, A.; Spiehl, R.; Moller-Lindenhoff, N.; Niediba, S. *Isotactic polymerization of Olefins with Homogeneous Zirconium Catalysts*, pp 291-301 in *Transition Metals and Organometallics as Catalysts for Olefin Polymerization*, W. Kaminsky and H. Sinn Eds, Springer-Verlag, Berlin, 1988
23. Rieger, B.; Mu, X.; Mallin, D. T.; Rausch, M. D.; Chien, J. C. W. *Macromolecules* **1990**, *23*, 3559
24. Soga, K.; Shiono, T.; Takemura, S.; Kaminsky, W. *Makromol. Chem. Rapid Commun.* **1987**, *8*, 305
25. Kaminsky, W.; Kulper, K.; Brintzinger, H.; Wild, F. R. W. P. *Angew. Chem. Int. Ed. Engl.* **1985**, *24*, 507
26. Resoconi, L.; Pietmontesi, F.; Franciscono, G.; Abis, L.; Fiorani, T.

- J. Am. Chem. Soc.* **1992**, *114*, 1025
27. Tsutsui, T.; Mizuno, A.; Kashiwa, N. *Polymer* **1989**, *30*, 428
28. Yang, X.; Stern, C. L.; Marks, T. J. *Angew Chem. Int. Ed. Engl.* **1992**, *31*, 1375
29. Eshuis, J. J. W.; Yong, Y. T.; Meetsma, A.; Teuben, J. H. *Organometallics* **1992**, *11*, 362
30. Longo, P.; Grassi, A.; Pellicchia, C.; Zambelli, A. *Macromolecules* **1987**, *20*, 1015
31. Kioka, M.; Mizuno, A.; Tsutsui, T.; Kashiwa, N. in *Catalysis in Polymer Synthesis*, E. J. Vandenberg and J. C. Salamone Eds., ACS Symposium Series 490, Washington DC, 1992, Ch.5
32. Mogstad, A-L.; Waymouth, R. M. *Macromolecules* **1992**, *25*, 2282
33. Dechter, J. J.; Mandelkern, L. *J. Polym. Sci. Phys. Ed.* **1980**, *18*, 1955
34. Ray, G. J.; Spanswick, J.; Knox, J. R.; Serres, C. *Macromolecules* **1981**, *14*, 1323
35. Hsieh, E.; Randall, J. C. *Macromolecules* **1982**, *15*, 353
36. Kaminsky, W.; Schlobohm, M. *Makromol. Chem. Macromol. Symp.* **1986**, *4*, 103
37. Kuroda, N.; Nishikitani, Y.; Matsuura, K.; Mitsuji, M. *Makromol. Chem.* **1987**, *188*, 1897
38. Cheng, H. N. *Polym. Bull.* **1990**, *23*, 589
39. Cheng, H. N. *Macromolecules* **1991**, *24*, 4813
40. Kuroda, N.; Nishinori, Y.; Matsuura, K.; Ikegami, N. *Macromolecules* **1992**, *25*, 2820
41. Randall, J. C.; Rucker, S. P. *Macromolecules* **1994**, *27*, 2120

42. Rossi, A.; Odian, G.; Zhang, J. *Macromolecules* **1995**, *28*, 1739
43. Chien, J. C. W.; Babu, G. N.; Newmark, R. A. *Macromolecules* **1994**, *27*, 3383
44. Welborn, H. C. European Patent Application(Exxon), No. 89302675.7, Publ. No. 0 344 887 A2, December 6, 1989
45. Spaleck, W.; Antberg, M.; Rohrmann, J.; Winter, A.; Bachmann, B.; Kiprof, P.; Behm, J.; Herman, W. A. *Angew. Chem. Int. Ed. Engl.* **1992**, *31*, 1347
46. Silverstein, R. M.; Bassler, G. C.; Morrill, T. C. *Sspectrometric Identification of Organic Compounds*, 5th ed., Wiley, New York, 1991, pp 215, 237-238
47. Wehrli, F. W.; Wirthlin, T. *Interpretation of Carbon-13 NMR Spectra*, Wiley, New York, 1976, pp 41-43
48. Couperus, P. A.; Clague, A. D. H.; Van Dongen, J. P. C. M. *Org. Magn. Reson.* **1976**, *8*, 426
49. Grant, D. M.; Paul, E. G. *J. Am. Chem. Soc.* **1964**, *86*, 2984
50. Asakura, T.; Omaki, K.; Zhu, S.; Chujo, R. *Polymer J.* **1984**, *16*, 717
51. Asakura, T.; Demura, M.; Yamamoto, K.; Chujo, R. *Polymer* **1987**, *28*, 1037
52. Cookson, D. J.; Smith, B. E. *J. Magn. Reson.* **1984**, *57*, 355
53. Prasad, J. V.; Rao, P. V. C.; Grag, V. N. *Eur. Polym. J.* **1991**, *27*, 251
54. Randall, J. C.; Hsieh, E. T. *NMR and Macromolecules* **1984**, pp 131-151
55. Rossi, A.; Rea, S.; Stanat, J.; Wright, L.; Kaufman, K. L.; Frederick, J. W.; Koros, R. M. Exxon Chemical Patene, International Pat. Appl. No. 94/13715, filed US December 17, 1992

Published June 23, 1994

56. Babu, G. N.; Newmark, R. A.; Chien, J. C. W. *Macromolecules* **1994**, *27*, 3383
57. Carman, C. J.; Harrington, R. A.; Wikes, C. E. *Macromolecules* **1977**, *10*, 536
58. Koenig, J. L. *Chemical Microstructure of Polymer Chains*, Wiley, New York, 1980, Ch.3
59. Heiland, K.; Kaminsky, W. *Makromol Chem.* **1992**, *193*, 601
60. Zambelli, A.; Grassi, A. *Makromol. Chem., rapid Commun.* **1991**, *12*, 523
61. An alternate mechanism for formation of trisubstituted double bonds, chain transfer to vinylidene end groups, was proposed in 1-butene homopolymerization. Recent experiments show that transfer to vinylidene end groups is absent. Performing the polymerization of 1-butene in the presence of approximately 25 mol-% of 2-ethyl-1-butene or isobutylene, model compound for vinylidene end groups, did not alter the identity or amounts of double bonds or trisubstituted end groups.
62. Rieger, B.; Reinmuth, A.; Roll, W.; Brintzinger, H. H. *Journal of Molecular Catalysis* **1993**, *82*, 67
63. Chen, Y.; Rausch, M. D.; Chien, J. C. W. *Macromolecules*, **1995**, *28*, 5399
64. Busico, V.; Cipullo, R. *Macromol. Symp.* **1995**, *89*, 277
65. Jungling, S.; Mulhaupt, R.; Stehling, U.; Brintzinger, H. H.; Fisher, D.; Langhauser, F. *J. Polymer Sci. Part A* **1995**, *33*, 1305
66. Busico, V.; Cipullo, R.; Chadwick, J.; Modder, J. F.; Sudmeijer, O.

*Macromolecules* **1994**, *27*, 7538

67. Doi, Y.; Asakura, T. *Macromolecules* **1981**, *14*, 69
68. Asakura, T.; Nakayama, N. *Polymer* **1992**, *33*, 650
69. Kioka, M.; Mizuno, A.; Tsutsui, T.; Kashiwa, N. *ACS Symposium*  
**1991**, *4*, 73
70. Busico, V.; Cipullo, R.; Borriello, A. *Macromol. Rapid. Commun.*  
**1995**, *16*, 269